Context-dependent effects of drought and invasive species on population dynamics

by

Aleah Querns

B.S., North Carolina State University, 2017
M.S., North Carolina State University, 2020

AN ABSTRACT OF A DISSERTATION

submitted in partial fulfillment of the requirements for the degree

DOCTOR OF PHILOSOPHY

Division of Biology
College of Arts and Sciences

KANSAS STATE UNIVERSITY
Manhattan, Kansas

2025

Abstract

Invasive species are a major driver of global ecological change and are expected to intensify under future climate scenarios. Yet, the impacts of invaders and their population growth are not uniform and are often shaped by the environmental and management contexts in which they occur. Understanding how these dynamics vary across contexts is essential for predicting invasion trajectories and designing effective management strategies, particularly in vulnerable ecosystems such as grasslands. In this dissertation, I examine how environmental and biotic context shapes both the impacts and performance of plant species, focusing primarily on invasive and encroaching species in grassland ecosystems. In the first component of my work, I examine how herbivory affects population dynamics in the native African subshrub *Hibiscus meyeri*. Using demographic models, I show that large mammalian herbivores can impede demographic compensation across environmental gradients, primarily due to their influence on the degree of spatial variability in vital rates. In the second component, I use the invasive grass *Bromus inermis* (smooth brome) to test how its effects on native grass demography varies across rainfall levels. I show that the impacts of brome can be context dependent and differ both across the life stage of native grasses and across rainfall levels. In the final component, I focus on woody encroachment by *Juniperus virginiana* (eastern red cedar), a native conifer rapidly encroaching in the Great Plains. Using a demographic model, I demonstrate that the invasion speed of red cedar is shaped by interactions among fire, grazing, and climate. Both frequent fires and cattle presence slow invasion, although these effects vary considerably with climate. Together, these results reveal that both invasion processes and species responses more broadly are highly context dependent. The effects of invaders on native species and their own performance are strongly shaped by environmental and management conditions, and similar processes govern native

species responses to biotic and abiotic stressors. These findings underscore the need to incorporate environmental variability, management history, and species demography into predictions of invasion dynamics and the development of adaptive, context-specific management strategies.

Context-dependent effects of drought and invasive species on population dynamics

by

Aleah Querns

B.S., North Carolina State University, 2017
M.S., North Carolina State University, 2020

A DISSERTATION

submitted in partial fulfillment of the requirements for the degree

DOCTOR OF PHILOSOPHY

Division of Biology
College of Arts and Sciences

KANSAS STATE UNIVERSITY
Manhattan, Kansas

2025

Approved by:

Major Professor
Dr. Allison Louthan

Copyright

Abstract

Invasive species are a major driver of global ecological change and are expected to intensify under future climate scenarios. Yet, the impacts of invaders and their population growth are not uniform and are often shaped by the environmental and management contexts in which they occur. Understanding how these dynamics vary across contexts is essential for predicting invasion trajectories and designing effective management strategies, particularly in vulnerable ecosystems such as grasslands. In this dissertation, I examine how environmental and biotic context shapes both the impacts and performance of plant species, focusing primarily on invasive and encroaching species in grassland ecosystems. In the first component of my work, I examine how herbivory affects population dynamics in the native African subshrub *Hibiscus meyeri*. Using demographic models, I show that large mammalian herbivores can impede demographic compensation across environmental gradients, primarily due to their influence on the degree of spatial variability in vital rates. In the second component, I use the invasive grass *Bromus inermis* (smooth brome) to test how its effects on native grass demography varies across rainfall levels. I show that the impacts of brome can be context dependent and differ both across the life stage of native grasses and across rainfall levels. In the final component, I focus on woody encroachment by *Juniperus virginiana* (eastern red cedar), a native conifer rapidly encroaching in the Great Plains. Using a demographic model, I demonstrate that the invasion speed of red cedar is shaped by interactions among fire, grazing, and climate. Both frequent fires and cattle presence slow invasion, although these effects vary considerably with climate. Together, these results reveal that both invasion processes and species responses more broadly are highly context dependent. The effects of invaders on native species and their own performance are strongly shaped by environmental and management conditions, and similar processes govern native

species responses to biotic and abiotic stressors. These findings underscore the need to incorporate environmental variability, management history, and species demography into predictions of invasion dynamics and the development of adaptive, context-specific management strategies.

Table of Contents

List of Figures

List of Tables

Acknowledgements

I would like to acknowledge my advisor, Allison Louthan, who has supported me through this whole process. Not only has she been invaluable for tossing around wacky ideas, but she somehow also got me to enjoy math.

I would like to give the most heartfelt thank you to my friends, both old and new, with whom I have made the most amazing memories over the years. All my pals from back East, who have supported me from afar. There is truly no better part of my week than watching trashy reality TV with you. All my friends who I met in Kansas; you have made this place feel like home over the years. Sarah and Bess: our cackling and chanting will echo through the halls of Bushnell forever more. With mine being the final dissertation, the ritual is complete.

I would like to thank my family, who have supported me. Sierra, I promise to get you some more candles someday.

I would also like to acknowledge the support of all those who have aided the completion of my dissertation, including my committee members (Zak Ratajczak, Jesse Nippert, and Mike Neubert), the Louthan Labbies (specific shout outs to Dayton Raines and Brian Gentry, who were a huge help in completing the drought shelter project), and the support staff at K-State (especially the accounting office, who have been so kind and patient with me throughout the years). The folks up at the K-State Herbarium were also very kind about teaching me how to use their scanner. The support staff at Konza Prairie Biological Station have also been a huge help; specifically, Patrick O'Neal, who taught me to hitch a trailer, which has somehow become one of the skills I am most proud of.

I would like to thank all the land managers who I have consulted with over the years. Your knowledge of the land where you work has been a huge help for my research.

I would also like to thank my funders, including K-State, GAANN, the Konza Prairie LTER program, the Biology Graduate Student Association, and the Grassland Heritage Foundation.

Finally, I would like to thank my cats, who are freeloading jerks, but also very cute.

Dedication

For my grandparents, who taught me that true joy is in feeling the sun on your face and the dirt between your fingers.

Preface

Chapters 2-3 of this dissertation have been prepared and formatted for submission to peer-reviewed journals. The results of Chapter 4 are provisional, as the analysis is ongoing and the model continues to be refined.

Chapter 1 - Introduction

Invasive species are among the most pervasive drivers of ecological change, capable of altering community composition, disrupting critical ecosystem processes, and threatening native biodiversity worldwide (Sala et al. 2000). These impacts are expected to intensify under future climate change, which may not only expand the suitable ranges for some invaders (McDowell et al. 2014) but also amplify their ecological effects through altered disturbance regimes, increases in relative performance of invasives, and decreases in the effectiveness of management efforts (Hellmann et al. 2008, Liu et al. 2017, LaForgia et al. 2020). Invasive species, which are often broadly tolerant and disperse easily, are thought to be particularly capable of thriving in the face of these shifting climates (Catford and Jones 2019).

Yet, invasion is not a uniform process. The strength of invader impacts and their ability to establish, persist, and spread often depends on both abiotic conditions and interactions with other species (Pyšek et al. 2012, Catford et al. 2022). Environmental drivers such as temperature, precipitation, disturbance, and resource availability can strongly influence both invader performance and their effects on native communities. For example, in some cases nutrient enrichment has been shown to exacerbate the impacts of some invasive species by increasing their performance relative to natives (Uddin and Robinson 2018), while in other cases it may more strongly constrain invader success (Liu et al. 2016). Similarly, changes in precipitation may benefit or have little effect on invaders (Eskelinen and Harrison 2014, Bishop et al. 2024). Conceptual frameworks such as the Stress Gradient Hypothesis (Bertness and Callaway 1994) or the Species Interactions–Abiotic Stress Hypothesis (Louthan et al. 2015) may generalize how the effects of invasive species on native species shift along stress gradients, but they often fall short of explaining the high variability of invader effects across contexts. This is partly because invaders can both respond to and actively modify environmental gradients (MacDougall et al. 2006, Gibbons et al. 2017a). Further complicating matters, the effects of invasive species on native species may vary depending on the life stage of the native species under consideration; for example, allelopathic effects of invaders may be stronger on certain life stages (Bieberich et al. 2018a). This context dependence creates substantial uncertainty both in managing invasive species and restoring native species diversity under different environmental contexts.

Our understanding of how invaders themselves respond to management actions also remains incomplete, particularly with respect to how their responses vary across environmental contexts. Management tools such as prescribed fire, grazing, mowing, or herbicide application can differentially affect invader performance depending on environmental conditions (Clout and Williams 2009). For instance, the effectiveness of prescribed fire at reducing invasive species can be reduced by higher grazing pressures (Briggs et al. 2002) or vary depending on climatic conditions (i.e., heat or precipitation; Hessl 2011). Similarly, climatic conditions can alter the effectiveness of herbicide application, for instance leading to less effective management under dry environments (Ramsey et al. 2005). While we know that management effectiveness can fluctuate across contexts, it is unclear to what degree these variations scale to influence the long-term demographic trajectories of invasive populations. Understanding how these interactions impact the population growth rates of invaders is critical for developing adaptive, context-specific management strategies that remain effective under changing environmental conditions.

Grassland and savannah ecosystems are particularly vulnerable to invasion. They are globally extensive, support high biodiversity and critical ecosystem services, but are also among the most threatened ecosystems globally (Comer et al. 2022). In recent decades, fire suppression, changes in grazing pressure, and changing climates have created conditions that favor native woody species (Archer 1994a), allowing them to encroach into grasslands and displace grass and forb species. Further, humans have introduced multiple non-native grass species to grasslands, either intentionally (i.e., for forage or aesthetic purposes) or unintentionally, many of which are either tricky or impossible to eradicate (Gaskin et al. 2021). These invaders can fundamentally reshape ecosystem structure and function through a range of pathways. Non-native grasses can alter competitive dynamics, outcompete native herbaceous species, and drive feedbacks that increase fire frequency or intensity, often resulting in state changes that are difficult to reverse (Ellis-Felege et al. 2013, Bradley et al. 2018). Similarly, woody encroachers can reduce light availability, alter soil moisture and nutrient dynamics, and suppress herbaceous communities, thereby reducing biodiversity and altering ecosystem processes such as nutrient cycling and hydrology (Briggs et al. 2005, McKinley et al. 2008, Liu et al. 2020).

Taken together, these patterns highlight that invasion in grassland systems are shaped by a complex interplay between species traits, environmental gradients, and management regimes. Invaders and native encroachers not only respond to variation in climate, disturbance, and biotic interactions but can also modify these conditions in ways that reinforce their dominance (Gaertner et al. 2014, Ratajczak et al. 2014, Bradley et al. 2018). Yet, despite this well-recognized complexity, efforts to predict and eradicate invasions in grasslands often fail, in part because we do not fully understand how environmental and biotic context shapes both invader performance and their impacts on native species. Addressing this gap requires integrating demographic processes, environmental variability, and management history across spatial and temporal scales.

In this dissertation, I examine how environmental drivers, biotic context, and management decisions shape both the impacts and performance of plant species, focusing primarily on invasive species. Grassland ecosystems, where invasion and encroachment are strongly influenced by interactions among climate, disturbance, and management, provide a powerful system for testing how these differing contexts shape and invasion outcomes and effects.

I begin by examining how large mammalian herbivory influences population dynamics in the native African shrub *Hibiscus meyeri*. I show that megaherbivores can alter patterns of demographic compensation, which occurs when changes in vital rates along environmental gradients offset one another, buffering population growth against environmental variation. Specifically, herbivory leads to less predictable variation in vital rates across sites, weakening negative correlations between vital rates and thereby limiting compensation. This case illustrates that context dependence in species performance is not unique to invaders but reflects a broader ecological phenomenon in which biotic context modulates population dynamics across environmental gradients.

Building on this foundation, the second component of my dissertation investigates how environmental context mediates the effects of an invasive species on native grass demography. Using field experiments manipulating drought and competition, I show that the invasive grass *Bromus inermis* (smooth brome) can influence native performance in context-dependent ways. Specifically, I found that smooth brome consistently reduced survival of native grass plugs regardless of drought, but its effects on germination were context dependent: high brome competition slightly improved germination under ambient rainfall, yet strongly decreased germination under drought. These findings highlight that restoration outcomes depend not only on invader pressure but also on environmental conditions and the developmental stage at which native species are introduced.

In the third component, I focus on woody encroachment driven by the species *Juniperus virginiana* (eastern redcedar), a native conifer rapidly spreading across the Great Plains. Here, I use a demographic model to examine how fire, grazing, and climate interact to shape the invasion speed of *J. virginiana*. Both frequent fires and cattle presence slow invasion, although these effects vary considerably with climate.

Together, these studies highlight that species performance and invasion dynamics can be context dependent, shaped by both environmental variability and biotic interactions. Incorporating this variability into ecological theory and management is essential for developing adaptive, effective strategies in changing ecosystems.

Chapter 2 - Large mammalian herbivores disrupt demographic compensation along an aridity gradient

2.1 Abstract

Ecologists often assume demographic rates such as survival and reproduction vary in concert along abiotic gradients, but growing evidence suggests that these rates may change in opposition leading to demographic compensation. However, it is unclear how biotic interactions such as herbivory may affect the presence or strength of demographic compensation. Here, we employ a series of strong tests for demographic compensation for a common forb species in the presence and absence of large mammalian herbivores. Namely, we test for demographic compensation in *Hibiscus meyeri* across a rainfall gradient using a large-scale exclosure experiment that includes or excludes large mammalian herbivores of various sizes (i.e., small, meso-, and mega-herbivores). We found that demographic compensation did not occur while all large mammalian herbivores were present. By contrast, demographic compensation occurred when megaherbivores were excluded, and this discrepancy was driven by an excess of negative correlations between vital rates. Understanding how biotic factors interact with abiotic gradients to modify demographic processes is crucial for understanding the drivers of species population dynamics for broader efforts in conservation and management.

2.2 Introduction

Demographic rates of plant species, such as survival, growth, or reproduction, frequently vary across space. This spatial variation in demographic rates has important implications for species distribution patterns, as these rates directly influence population growth rate and, consequently, the overall distribution of a species. Many studies have examined how abiotic factors induce spatial variation in demographic rates, but biotic factors (e.g., herbivory, predation, and competition) also play a significant, though lesser-studied role in influencing demographic rates. Biotic drivers' impacts on demographic rates can be considerable and often vary spatially (Kauffman and Maron 2006, Maron et al. 2014). Furthermore, biotic and abiotic gradients can interact with one another, such as when biotic interactions limit demographic rates, and thus population growth rate, more strongly in less abiotically stressful environments (Dobzhansky 1950, Connell 1972, Louthan et al. 2018). Although biotic factors clearly affect demographic processes, their relative importance in driving spatial variation in population growth rates along abiotic gradients remains uncertain. Here, we explore how herbivory drives spatial variation in population growth rate by examining its role in generating demographic compensation, which occurs when a species' demographic rates are negatively correlated across space, resulting in higher demographic rates at one end of a gradient "compensating" for low demographic rates that reduce population growth rate (Doak and Morris 2010, Villellas et al. 2015).

Previous theory has suggested that demographic rates should be positively correlated across space (Pironon et al. 2017). For example, if plant growth is higher at one end of an abiotic gradient, theory suggests that reproduction will also be higher, as both demographic rates might respond similarly to the same favorable abiotic conditions. However, an emerging body of research suggests that demographic rates are not always positively correlated. This phenomenon can occur when spatial variation arises from multiple underlying abiotic or biotic gradients that affect rates differently, or when demographic rates respond in opposite directions to the same gradient, leading to demographic compensation. For example, survival may be high at one end of a gradient while the probability of fruiting is low, reducing spatial variation in population growth rates. Because demographic compensation can act to prevent population growth rates from falling below replacement across a broader range of environments, it has important implications for species distributions.

Abiotic drivers are often assumed to be the primary force behind demographic compensation, and recent studies have attributed demographic compensation to spatial variation in abiotic drivers such as precipitation (Doak and Morris 2010, García-Camacho et al. 2012, Villellas and García 2018) or mean annual temperature (Sheth and Angert 2018, Daco et al. 2021). Despite the emphasis on abiotic drivers, biotic drivers (e.g., herbivores) affect many demographic rates (Crawley 1989, Maron and Crone 2006), either negatively (Doust and Doust 1988, Vergeer and Kunin 2011) or positively (Trumble et al. 2003, Pratt et al. 2005). Furthermore, herbivore effects often vary spatially (Wetzel et al. 2023), either due to changes in plant and herbivore communities across space (Cyr and Face 1993), or due to responses of plant performance to underlying abiotic gradients (Louthan et al. 2018). Because most studies showing demographic compensation have not quantified the effect of biotic drivers, it remains unclear whether spatial variation in biotic drivers such as herbivory (or spatial variation in their effects on plants) contributes to demographic compensation.

On one hand, biotic drivers such as herbivory could generate demographic compensation in plant species whose demographic rates would otherwise be positively correlated due to shared responses to an environmental gradient (e.g., rainfall; Figure 2.1A, top). For example, if herbivores reduce competition most strongly in high-rainfall, productive areas, and have a stronger positive effect on certain demographic rates (such as probability of growth) than on others (such as probability of fruiting), herbivores may create negative correlations among demographic rates and reduce spatial variation in population growth rate (Figure 2.1A, bottom). On the other hand, biotic drivers like herbivory could also disrupt demographic compensation. In this scenario, in the absence of herbivory, demographic rates may be negatively correlated due to differing responses to the same abiotic driver (Figure 2.1B, top). If herbivore effects are greater in high-rainfall, productive areas (McNaughton et al. 1989, Chase et al. 2000) and strongly reduce multiple demographic rates, herbivores could generate positively correlated demographic rates and a loss of demographic compensation (Figure 2.1B, bottom). Similar effects could arise in the absence of spatial variation in herbivore activity levels; for example, if compensatory responses (as in Maschinski and Whitham 1989) occur or if the sensitivity of population growth rate to herbivory (as in Louthan et al. 2018) varies across space.

In this study, we examined whether large mammalian herbivores generated, disrupted, or had no effect on demographic compensation in *Hibiscus meyeri* (Malvaceae), a representative subshrub in sub-Saharan Africa. We used a long-term herbivore exclusion experiment in which various size guilds of large mammalian herbivores are excluded from plots across a rainfall gradient. We estimated the effects of rainfall level and herbivore exclusion treatment on population growth rate of *H. meyeri*, then tested for demographic compensation in the presence and absence of a suite of large mammalian herbivore guilds. Finally, we quantified the herbivore-induced changes in demographic rates that resulted in effects on demographic compensation

2.3 Methods

2.3.1 Study system

Mpala Conservancy (hereafter, ‘Mpala’) is a 49,000-acre conservancy located near the equator in central Kenya (0°17' N, 37°52' E), composed primarily of semiarid savanna and acacia bushland. Mpala houses a large diversity of large mammalian herbivores. Rainfall is weakly triannual (Goheen et al. 2013). Mpala is situated along a rainfall gradient with mean annual 2008-2012 rainfall ranging from ~440 mm/y in the North to ~640 mm/y in the South (Goheen et al. 2013). Soil characteristics and elevation do not change significantly across the gradient, allowing a fair comparison of rainfall effects on plant populations and communities (Goheen et al. 2013).

The Ungulate Herbivory Under Rainfall Uncertainty experiment (hereafter, ‘UHURU’), established in 2008, includes replicated size-based herbivore exclusion treatments at three rainfall levels spanning the Mpala rainfall gradient (hereafter, “Mesic”, “Intermediate”, and “Arid” sites). While there is substantial intra-annual variation in rainfall, seasonal rainfall is consistently highest at the Mesic site and lowest at the Arid site. At each rainfall level, four treatments (complete large mammalian herbivore exclusion, meso- and megaherbivore exclusion, megaherbivore exclusion, and an open control) are replicated three times in a randomized blocked design. Complete large mammalian herbivore exclusion (LMH plots) excludes all herbivore species taller than 50 cm, allowing access by small herbivores such as hares; mesoherbivore exclusion (MESO plots) excludes all herbivore species taller than 120 cm, allowing access by dik-dik (*Madoqua cavendishi*) and warthog (*Phacochoerus africanus*); megaherbivore exclusion (MEGA plots) excludes only megaherbivores such as elephant (*Loxodonta africana*) and giraffe (*Giraffa camelopardalis*); and control plots are open to all herbivores (Goheen et al. 2013).

2.3.2 Demographic data collection

Hibiscus meyeri, a common water-limited subshrub, occurs at all rainfall levels in UHURU. *Hibiscus meyeri* is consumed by multiple herbivore species and exhibits no known physical or chemical defenses against large mammalian herbivory (Louthan et al. 2018). Within the UHURU experiment, we conducted biannual demographic surveys between June 2011 and February 2015 to quantify herbivore and rainfall effects on *H. meyeri*. Our demographic monitoring methods are described Louthan et al. (2018). Briefly, we searched exhaustively for *H. meyeri* individuals at each rainfall level x herbivore exclusion treatment x block combination in June 2011. We then conducted a biannual census (after the wet season in July-August and after the dry season in January-February) to score plants' survival, measure size (height and basal area, which together correlate well with biomass; Louthan et al. 2018), count the number of fruits, and mark new plants to replace any that died or could not be relocated. Note that these data were collected biannually, rather than annually as in Louthan et al. 2018. Further, fruiting rates are reflective of herbivory (including seed and flower predation), and thus reflect the demographic consequences of herbivory rather than only potential output. We also quantified the number of seedlings produced per fruit (i.e., recruitment) by counting all seedlings in a 2-m radius around reproductive plants following one wet season. Hereafter, we call each of our seven unique six-month time intervals between subsequent censuses a "transition."

2.3.3 Modeling demographic rates and population growth rates

We used these data to estimate the effects of rainfall level, herbivore exclusion treatment, block, and transition identity on *H. meyeri* performance. We first synthesized the data into five metrics of performance for each transition: survival, probability of producing fruits, the logged number of fruits per biomass (given fruits were produced), growth (i.e., size difference between censuses), and variance in growth.

We then tested for the effects of size, block, and transition on each rainfall level and herbivore exclusion treatment-specific performance metric using a model selection approach to generate a demographic rate function. We created demographic rate functions for each rainfall level and herbivore exclusion treatment, where global models included size in initial census as a fixed effect, with transition and block as random effects. Probability of survival and of fruiting were fit using a binomial error term and all other demographic rate functions were fit using a normal error term. To assess which fixed effects best predicted demographic rates, we used AICc to compare all possible subsets of each global model, including random effects in all models (Hurvich and Tsai 1989; Appendix Table A.1). If the model fit was singular, we refit global models with transition and block as fixed effects, then repeated the model selection process.

We used the best fit models for each rainfall level and herbivore treatment-specific demographic rate function to construct 60 herbivore exclusion x rainfall level-specific integral projection model (IPM) kernels (four herbivore exclusion treatments x three rainfall levels). If the best-fit model included block or transition as a random effect, we did not include random effects in demographic rate predictions. If it included block or transition as fixed effects, we predicted demographic rates as the across-block or across-transition average response, averaging first across timepoint, then block. The parameters included in best-fit demographic rate functions are shown in Appendix Table A.2. We represented recruitment as rainfall level-specific values (as in Louthan et al. 2018), because recruitment did not vary across herbivore exclusion treatments, and we assumed that fruits transitioned to the smallest size class in the subsequent time step. We chose to use IPMs rather than traditional matrix models to increase precision of demographic rate estimates (Ramula et al. 2009, Doak et al. 2021). However, given our need to assess correlations among a limited number of demographic rates, we chose to limit the number of mesh points to four, selected to generate three size classes equally spanning the range of sizes observed in our study (biomass <24.09, 24.09-48.18, and 48.18-72.28) in addition to one discrete state (fruits). Hereafter, we refer to our three size classes as small, medium, and large (S, M and L), and refer to growth rates as transitions between size classes (e.g., M-S regression indicates shrinkage of medium plants to the small size class, M-M stasis indicates medium plants remaining in the medium size class; and M-L growth indicates the growth of medium plants to the large size class, and so on).

We used the IPMs to estimate deterministic population growth rate (λ) for each herbivore exclusion treatment x rainfall level combination using standard methods (Morris and Doak 2002). To generate confidence intervals on these estimates that incorporate parameter uncertainty, we sampled from the multivariate normal distribution of the fixed effect parameter estimates of best-fit demographic rate functions and recalculated λ, repeating this process 10,000 times. We used these estimates to generate 95% confidence intervals on population growth rate.

2.3.4. Testing for demographic compensation:

We used these IPM kernels and demographic rates to test for demographic compensation, focusing on 15 size-specific demographic rates: survival of S, M, and L; fruiting rate (probability of fruiting x number of fruits produced given fruiting) of S, M, and L; and transitions among all size classes (i.e., S to S, M, or L; etc.). No plants were observed to grow from S to L size class, so we excluded that rate from our analyses (Appendix Table A.2

This test involved two steps. First, we calculated Life Table Response Experiment (LTRE) contribution values for each demographic rate at each rainfall level x herbivore exclusion treatment. These values, describing the contribution of each rate to differences in population growth rate across rainfall levels within an herbivore exclusion treatment, are estimated as:

$$C_{r,h} = \left(v_{r,h} - v_{\bar{r},h}\right) \times S_{\bar{r},h} \qquad Eq.\ 1$$

Here, $v_{r,h}$ represents the demographic rate *v* at rainfall level *r* and herbivore exclusion treatment h, $v_{\bar{r},h}$ indicates the across-rainfall level mean value of demographic rate *v* at herbivore exclusion treatment h, and $S_{\bar{r},h}$ corresponds to the sensitivity of λ to the across-rainfall level mean value of demographic rate *v* for herbivore exclusion treatment h. Thus, $C_{r,h}$ describes the contribution of a given demographic rate to differences in population growth rate across rainfall levels, calculated separately for each herbivore exclusion treatment.

To obtain LTRE contributions, we first estimated the sensitivity of population growth to changes in the across-rainfall level mean demographic rates (Appendix Table A.3). For each herbivore enclosure treatment, we estimated these sensitivities using a perturbation approach, perturbing an IPM kernel constructed using the across-rainfall level mean values for each demographic rate (Morris and Doak 2002). These sensitivity values were multiplied by the difference between the across-rainfall level mean demographic rate and the rainfall-level specific value of a demographic rate for each herbivore exclusion treatment to obtain the LTRE contribution.

Next, we used the LTRE contributions to test for evidence of demographic compensation within each herbivore exclusion treatment (Appendix Figure A.2). First, we calculated the Pearson product moment correlations between all pairwise combinations of $C_{r,h}$ values for each herbivore exclusion treatment to obtain "observed" proportions of positive and negative correlations between LTRE contributions of demographic rates (Appendix Figure A.2A). We highlight that because our data included data from only three sites, each of these correlations was represented by only three data points. Because such correlations are unstable, we emphasize that our results should be interpreted with caution (Appendix Figure A.3). However, these data come from a multi-year demographic study with replication across rainfall and herbivore exclusion treatments, and therefore likely capture underlying demographic patterns well. After generating observed proportions of positive and negative correlations, following Villellas et al. (2015), we used a randomization approach to generate null distributions for the proportions of positive and negative correlations between LTRE contributions of demographic rates across the rainfall gradient. For each demographic rate, we randomized $C_{r,h}$ values across rainfall levels and recalculated Pearson correlations among randomized contributions (Appendix Figure A.2B). We repeated this process 10,000 times to generate null distributions for the proportions of positive and negative correlations. We then compared the observed proportions of positive ($P_{obs,+}$) and negative ($P_{obs,-}$) correlations for each herbivore exclusion treatment to their respective null distributions. We assumed that having either more negative correlations than expected by chance (i.e., $P_{obs,-}$ was greater than or equal to the 95th percentile of the null distribution of negative correlations) or fewer positive correlations than expected by chance (i.e., $P_{obs,+}$ was less than or equal to the 5th percentile of the null distribution of positive correlations) indicated evidence for demographic compensation (Villellas et al. 2015). We quantified the mechanism of large mammalian herbivore effects on demographic compensation by comparing correlations among pairs of demographic rates in each herbivore exclusion treatment (Appendix Figure A.2C).

2.4 Results

2.4.1 Effects of drivers on demographic rates and population growth rates

Demographic rate functions for survival, growth and probability of fruiting almost always included size (40/48; Appendix Table A.1), whereas functions for number of fruits per biomass usually did not (2/12; Appendix Table A.1). M, and L survival rates increased from the Arid to the Mesic site, whereas S survival rates remained relatively similar across the gradient, and survival rates were similar on average across herbivore exclusion treatments (Appendix Table A.2, Appendix Figure A.1). S, M, and L fruiting rates showed no consistent response to rainfall and were similar on average across herbivore exclusion treatments (Appendix Table A.2, Appendix Figure A.1). Growth rates varied considerably across the rainfall gradient (Appendix Table A.2, Appendix Figure A.1). Stasis of M and L plants increased toward the Mesic site for most herbivore exclusion treatments except for LMH plots, which declined slightly. Stasis of S plants increased toward the Mesic site for all herbivore exclusion treatments except for the control plots, which indicated no change in S stasis across the gradient. The growth of S to M also declined toward the Mesic site, whereas the growth of M to L varied little across the gradient; these patterns were consistent across herbivore exclusion treatments. The growth of S to L was consistently zero across the gradient. The regression of L to M increased toward the Mesic site for LMH plots but declined for the control, MEGA and MESO plots. Conversely, the regression of L to S declined toward the mesic site for MEGA, MESO and the control plots but increased for the LMH plots. The regression of M to S declined toward the Mesic site for LMH, MEGA, MESO, and control plots. Recruitment of fruits declined toward the Mesic site for all herbivore exclusion treatments (Appendix Table A.2, Appendix Figure A.1).

Population growth rate was higher on average in the LMH, MEGA, and MESO plots compared to the control plots; however, overlapping confidence intervals for site-specific estimates indicate that these differences were not significant overall (Table 2.1). The only exception to this finding was at the Mesic site, where population growth was lower within the MEGA treatment compared to the LMH treatment. In all herbivore exclusion treatments, population growth rate was generally higher at the Mesic site compared to the Intermediate and Arid sites, although those differences were only significant within the LMH and control treatments (Table 2.1).

2.4.2 Results of test for demographic compensation

The presence of all large mammalian herbivores often led to weaker correlations between demographic rates (Appendix Figure A.3). As a result, we found strong evidence for demographic compensation only when large mammalian herbivores were excluded (Appendix Table A.4). Namely, we found evidence for demographic compensation generated by more negative correlations than expected by chance in the LMH (Figure 2.2B), MESO (Figure 2.2D), and MEGA (Figure 2.2F) plots, but not the control plots (Figure 2.2H). In particular, the LMH plots exhibited the greatest number of significant negative correlations (21 significant negative correlations; Fig, 3A), followed by the MESO and MEGA plots (10 significant negative correlations; Figure 2.3B-C). Only four pairs of demographic rates in the control plots were significantly negatively correlated (Fig 3D). Negative correlations frequently appeared between either growth or regression vs. stasis within a size class, likely reflecting probabilistic constraints on transitioning to a different size class vs. stasis in the same size class (Figure 2.3). The extent and significance of negative correlations varied by treatment, and the LMH plots in particular had many significant negative correlations between fruiting and regression rates, suggesting that the complete absence of large mammalian herbivores might exacerbate trade-offs in the role of reproduction vs. shrinkage between environments.

The proportion of observed positive correlations was never significantly lower than we would expect by chance for all herbivore exclusion treatments (Figure 2.2A, C, E, & G; Appendix Table A.4). Across all herbivore treatments, we frequently observed significant positive correlations between similar demographic processes, such as between survival, stasis, regression, or fruiting rates of differing size classes (Figure 2.3). Additionally, fruiting rate often exhibited positive correlations with stasis, reflecting a link between increased reproductive output and reduced probability of growth. Positive correlations were more common in the LMH (16 significant positive correlations; Figure 2.3A), MESO (12 significant positive correlations; Figure 2.3B), and MEGA plots (11 significant positive correlations; Figure 2.3C) treatments compared to the control plots (6 significant positive correlations; Figure 2.3D), suggesting that the exclusion of larger herbivores reduces positive correlations between demographic rates.

2.5 Discussion

Herbivores can profoundly affect plant population dynamics through their influence on demographic rates. In our study, we found that large mammalian herbivores modified the correlations among demographic rates. Namely, the presence of all large mammalian herbivores nullified demographic compensation (as in Fig, 1B). Demographic compensation, which occurred only in herbivore exclusion treatments, was driven by negative correlations between LTRE contributions of demographic rates (Figure 2.2). While the absence of any large mammalian herbivore size guild generated demographic compensation, the effect of megaherbivore exclusion alone was strong enough to generate demographic compensation. The following paragraphs place these findings in the context of previous literature and explore their broader implications.

Large mammalian herbivores had strong effects on demographic rates of *H. meyeri*. This result is consistent with previous work, which has shown that large herbivores strongly affect plant population dynamics, though the direction of these effects can vary across space (Maron and Crone 2006, Koerner et al. 2014, 2018). In some cases, herbivores largely affect plants through reductions in growth, with minimal impacts on survival (Van Der Wal et al. 2000, Townsend and Meyer 2002), whereas in others, herbivores can greatly reduce adult (Pisanu et al. 2012) and seedling (Opedal et al. 2021) survival. Similarly, while herbivores sometimes negatively affect reproduction via consumption (Anderson et al. 2001), they can also reduce competition from neighboring plants, thereby increasing the probability of reproduction for the remaining individuals In our study, large mammalian herbivores reduced rates such as fruiting, survival, and the stasis of large plants, and had weak negative effects on population growth rate overall (i.e., population growth rate was on average lower in the control plots compared to other treatments, though these differences were largely non-significant; Table 2.1).

We found that herbivore effects on population dynamics were sufficient to disrupt demographic compensation, highlighting the importance of considering both biotic and abiotic drivers of demographic compensation. Previous work has assumed that spatial variation in abiotic drivers such as temperature and precipitation (Villellas and García 2018, Sheth and Angert 2018, Yang et al. 2022), length of snow-free periods (Doak and Morris 2010), and soil nutrients (Daco et al. 2021) are the primary drivers of demographic compensation. However, studies examining the effects of abiotic drivers often overlook how biotic drivers might influence these results. While previous work on demographic compensation has been conducted in relatively depauperate ecosystems without large herbivores, it may be that this phenomenon was less prevalent when they were still present. Further, smaller herbivores or other biotic interactions may be limiting the extent of demographic compensation, suggesting that excluding biotic factors could lead to an overestimation of its prevalence. Consistent with this suggestion, our work suggests that only partial herbivore exclusion is necessary to allow compensation to emerge; the removal of just one large mammalian herbivore guild (i.e., MEGA, which excluded megaherbivores) was sufficient to generate demographic compensation.

In our study, demographic compensation when large mammalian herbivores were excluded was driven largely by negative correlations between LTRE contributions of demographic rates along the rainfall gradient. Different abiotic conditions can cause plants to exhibit tradeoffs in physiological and life history traits, as traits that are advantageous in some environments may reduce performance in others (Schlichting 1986, Dudley 1996). For example, a plant species that invests heavily in vegetative growth under greater growing-season precipitation may instead invest in rapid and high flowering rates under reduced growing-season precipitation, as this trait may allow escape from drought stress occurring later in the growing season (van Kleunen 2007). Thus, abiotic gradients can elicit demographic compensation through negative correlations, as demographic rates and the sensitivity of population growth rates to different demographic rates may shift along these gradients as plants alter life history strategies across abiotic contexts. Herbivory may be uniquely poised to affect demographic compensation because it can interact with abiotic gradients to affect plant performance and competitive dynamics (Van Der Wal et al. 2000, Callaway et al. 2002, Hambäck and Beckerman 2003). As herbivores remove biomass and trample plants (Heggenes et al. 2017, Pascual et al. 2017), they may directly increase or decrease growth and the probability of reproduction. Further, changes in competitive dynamics across abiotic conditions (e.g., the stress gradient hypothesis) may be disrupted in the presence of herbivores, who strongly modify competitive dynamics (Hambäck and Beckerman 2003). Consistent with this prediction, we found that in the herbivore exclusion treatments, negative correlations frequently occurred between LTRE contributions for demographic rates associated with conservative strategies (shrinkage/stasis) and those linked to non-conservative strategies (growth/fruiting; Figure 2.3, Appendix Figure A.1). These negative correlations became less frequent in the presence of all large mammalian herbivores (i.e., control plots), suggesting that trade-offs between conservative and non-conservative strategies may become less pronounced with greater herbivore presence (Figure 2.3), in turn leading to a disruption of demographic compensation. At the same time, we observed fewer positive correlations between demographic rates in the presence of all large mammalian herbivores, disrupting the expectation that demographic rates responding similarly to abiotic gradients should covary positively. Together, these results indicate that large mammalian herbivores affect the degree of spatial variability in vital rates (Appendix Figure A.3), reducing both negative and positive correlations among demographic rates, the former leading to weaker demographic compensation (consistent with Figure 1B), and the latter reflecting altered responses to abiotic conditions without direct consequences for demographic compensation.

We saw that excluding multiple large mammalian herbivore sizes did not always lead to a greater number of negative correlations between demographic rates (Figure 2.2). Previous work has shown that herbivores of different sizes can have disparate effects on plant population dynamics. For example, in grassland systems, larger herbivores (>30kg) can have stronger effects on plant community composition compared to small herbivores (Bakker et al. 2006). Alternatively, in savanna systems, large vs. small herbivore effects can be context-dependent, with either group exerting a stronger influence depending on the environmental conditions

(Burkepile et al. 2017). We saw that the exclusion of megaherbivores such as elephants and giraffes alone (i.e., the MEGA exclusion plots) was enough to elicit demographic compensation (Figure 2.2F). This result is consistent with previous work, which shows that megaherbivores have considerable impacts on plant productivity and biomass, particularly in savannah ecosystems (Pellegrini et al. 2017, Davies and Asner 2019, Hyvarinen et al. 2021). The combined exclusion of megaherbivores, mesoherbivores such as zebra and gazelle, and of smaller large mammalian herbivores such as dik-dik and warthogs, (i.e., the LMH exclusion plots) led to the greatest number of negative correlations, suggesting that the combined exclusion of these size guilds can have similar, additive effects on demographic compensation. However, when only mega- and mesoherbivores were excluded and smaller herbivores were included (i.e., MESO exclusion plots), we saw the same number of negative correlations as when only megaherbivores were excluded. These findings suggest that the exclusion of one large mammalian herbivore size guild modifies the effect of others, perhaps because of ecological interactions among guilds.

Several caveats apply to our study. First, many contemporary ecosystems lack large mammalian herbivores, particularly mega- and mesoherbivores, due to human interference, limiting the applicability of our findings to other systems. Even in cases where large mammalian herbivores have persisted or been reintroduced, they are often not as abundant as they once were historically, meaning their densities may not be high enough to elicit demographic compensation. Second, the statistical power of our test for demographic compensation is limited by the number of populations (three) included in our study (Appendix Figure A.3). Most other studies of demographic compensation contain at least six populations (Villellas et al. 2015), though we note that these studies do not have replicated herbivore exclusion treatments such as ours. Thus, our results should be thought of as preliminary evidence that large mammals may influence demographic compensation. We suggest that studies measuring plant demographic rate response to herbivores across a broader array of populations consider conducting a test for demographic compensation to test the generality of our findings.

Our study demonstrates that for *H. meyeri*, large mammalian herbivores play a significant role in shaping population dynamics through affecting spatial variability in vital rates and disrupting demographic compensation. When large herbivores were excluded, *H. meyeri* exhibited strong demographic compensation; conversely, when all large herbivore size guilds were present, demographic compensation was disrupted (Figure 1B). However, rather than disrupting demographic compensation by turning negative correlations between rates to positive (as in Figure 1B), large mammalian herbivores disrupt compensation through reducing variability in LTRE contributions (i.e., diminishing differences in how individual demographic rates influenced population growth across the rainfall gradient; Appendix Figure A.3), leading to multiple rates becoming uncorrelated. While this disruption does not significantly alter spatial variation in population growth rate (Appendix Figure A.4), at least at the 20-km range over which we conducted our study, it suggests that large mammalian herbivores primarily exert negative effects on woody plants such as *H. meyeri* not by directly reducing population growth, but rather by eliminating demographic compensation. Our findings emphasize the need to consider both biotic and abiotic drivers when studying demographic compensation. Although large mammalian herbivores non-significantly reduced population growth in our system, herbivores in other contexts may have positive or neutral effects on plant populations by reducing competition (Dyer et al. 2010, Koerner et al. 2018) or inducing overcompensation (Garcia and Eubanks 2019). Ultimately, understanding the complexity of plant-herbivore interactions is key to predicting population dynamics and species distributions in changing landscapes. Incorporating these insights into conservation planning will be vital for ensuring the long-term persistence of diverse plant communities.

2.6 Acknowledgements

We thank Robert M. Pringle for significant contributions to conceptualization, fieldwork, and data collection and Daniel F. Doak for conceptualization, fieldwork, and logistical support. Data collection for this project was funded by the Philanthropic Educational Organization Scholar Award; United Nations Educational, Scientific and Cultural Organization-L'Oréal International Fellowship; Wyoming NASA Space Grant; funds from the Universities of Colorado and Wyoming; National Science Foundation (NSF) Division of Environmental Biology (DEB) 1311394 (with Daniel F. Doak, to A.M.L.); NSF DEB-1355122, DEB-1457691, and IOS-1656527 (to Robert M. Pringle); NSF DEB Early Concept Grants for Exploratory Research Grant 1547679, NSF DEB 1556728, and awards from the University of Wyoming and the University of Wyoming Biodiversity Institute (to J.R.G.); NSF DEB 1149980 (to T.M.P.); NSF DEB 1242355 and NSF DEB 1352781 (to Daniel F. Doak). The UHURU experiment was built with a Natural Sciences and Engineering Council Research Tools and Instruments grant. Analysis was funded by NSF DEB 2025849, Department of Education Graduate Assistance in Areas of National Need P200A210092. This manuscript is contribution number 25-202-J from the Kansas Agricultural Experiment Station.

2.7 Open research statement

Data and code are published and publicly available at DOI: 10.5281/zenodo.15319614

2.8 Tables

Table 2.1. **Population growth rate (λ) of *Hibiscus meyeri* for all herbivore exclusion treatments.** We show deterministic λ predicted by rainfall level- and treatment specific integral projection model kernels, with the 95% confidence intervals (which incorporate parameter uncertainty) in brackets. Abbreviations: Herbivore exclusion treatments are the complete absence of large mammalian herbivores ("LMH"), absence of meso- and mega- herbivores ("MESO"), absence of megaherbivores ("MEGA"), and presence of all large mammalian herbivores ("control").

Herbivore exclusion treatment	**Rainfall level**		
	Arid	*Intermediate*	*Mesic*
LMH	1.12 [1.02, 1.26]	1.02 [0.98, 1.07]	1.58 [1.30, 1.97]
MESO	1.16 [1.08, 1.25]	1.07 [1.01, 1.11]	1.31 [1.17, 1.47]
MEGA	1.10 [1.04, 1.18]	1.03 [0.98, 1.08]	1.12 [1.02, 1.26]
Control	1.03 [0.995, 1.06]	1.02 [0.97, 1.08]	1.34 [1.13, 1.66]

2.9 Figures

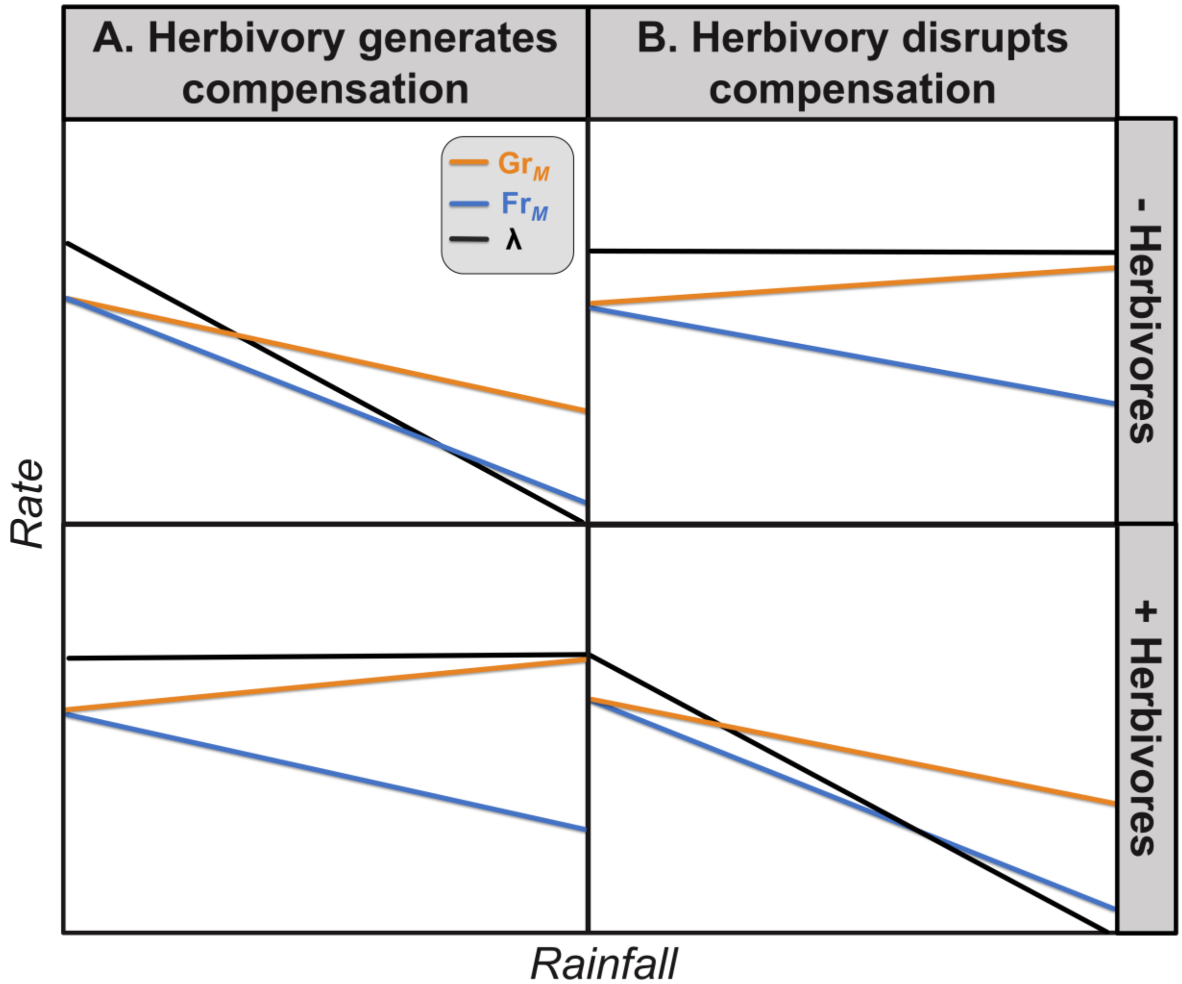

Figure 2.1. Possible effects of herbivory on demographic compensation. In (A), herbivory generates demographic compensation. Without herbivory (- Herbivores), demographic rates such as the growth probability of medium plants (Gr_M, orange line) and the fruiting probability of medium plants (Fr_M, blue line) are positively correlated, resulting in substantial change in population growth rate (λ; black line) with rainfall. With herbivory (+ Herbivores), demographic rates are negatively correlated, resulting in a minimal change in population growth rate with rainfall. Such an effect could arise if herbivores have stronger effects on certain demographic rates (in this case, growth) in certain environments. In (B), herbivory disrupts demographic

compensation. Without herbivory, growth and fruiting probabilities are negatively correlated across a rainfall gradient, resulting in a minimal change in population growth rate with rainfall. With herbivory, growth and fruiting probabilities are positively correlated with one another (i.e., both decrease with increasing rainfall), resulting in a substantial change in population growth rate with rainfall. Such an effect could arise if herbivores have negative effects on multiple demographic rates and these effects differ along environmental gradients.

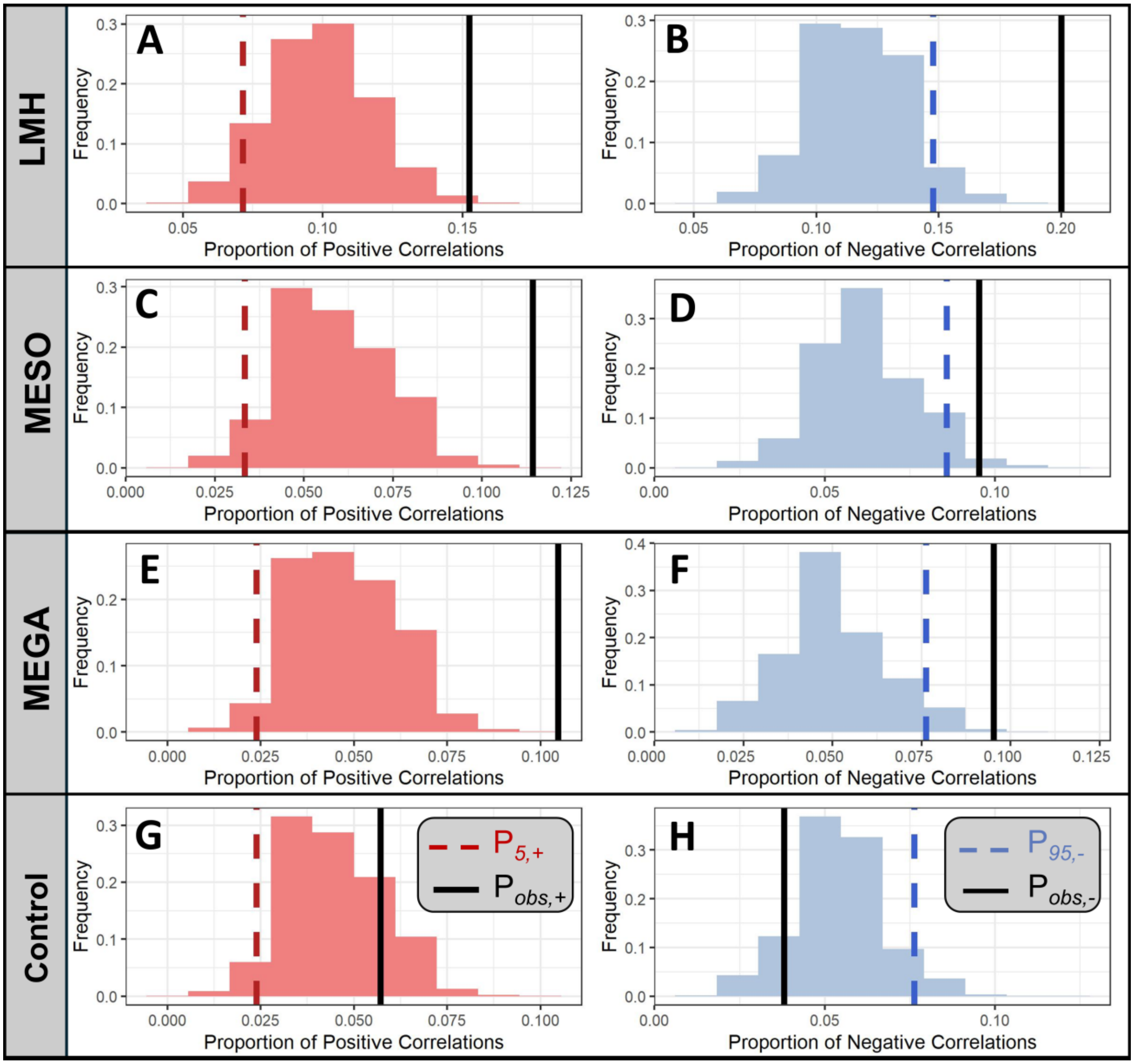

Figure 2.2. Results of tests for demographic compensation. We show null distributions of the proportion of significant positive (A, C, E, G) and negative (B, D, F, H) correlations between Life Table Response experiment contributions for four herbivore exclusion treatments, LMH (A, B), MESO (C, D), MEGA (E, F), and Control (G, H). Null distributions were obtained via randomization following Villelas et al. (2015). In A, C, E and G, red dashed lines indicate the 5th percentile of the null distribution of significant positive correlations ($P_{5,+}$) and solid black lines indicate the observed proportion of significant positive correlations ($P_{obs,+}$) in a given herbivore

exclusion treatment. If $P_{obs,+} <= P_{5,+}$ (A, C, E, G), there is evidence for demographic compensation in that herbivore exclusion treatment because there are fewer positive correlations between demographic rates than expected by chance. In B, D, F and G, blue dashed lines indicate the 95th percentile of the null distribution of significant negative correlations ($P_{95,-}$) and solid black lines indicate the observed proportion of significant negative correlations ($P_{obs,-}$) for a herbivore exclusion treatment. If $P_{obs,-} > P_{95,-}$, there is evidence for demographic compensation in that treatment because there are more negative correlations between demographic rates than expected by chance. Herbivore exclusion treatments are the complete absence of large mammalian herbivores ("LMH"), absence of meso- and mega- herbivores ("MESO"), absence of megaherbivores ("MEGA"), and presence of all large mammalian herbivores ("control").

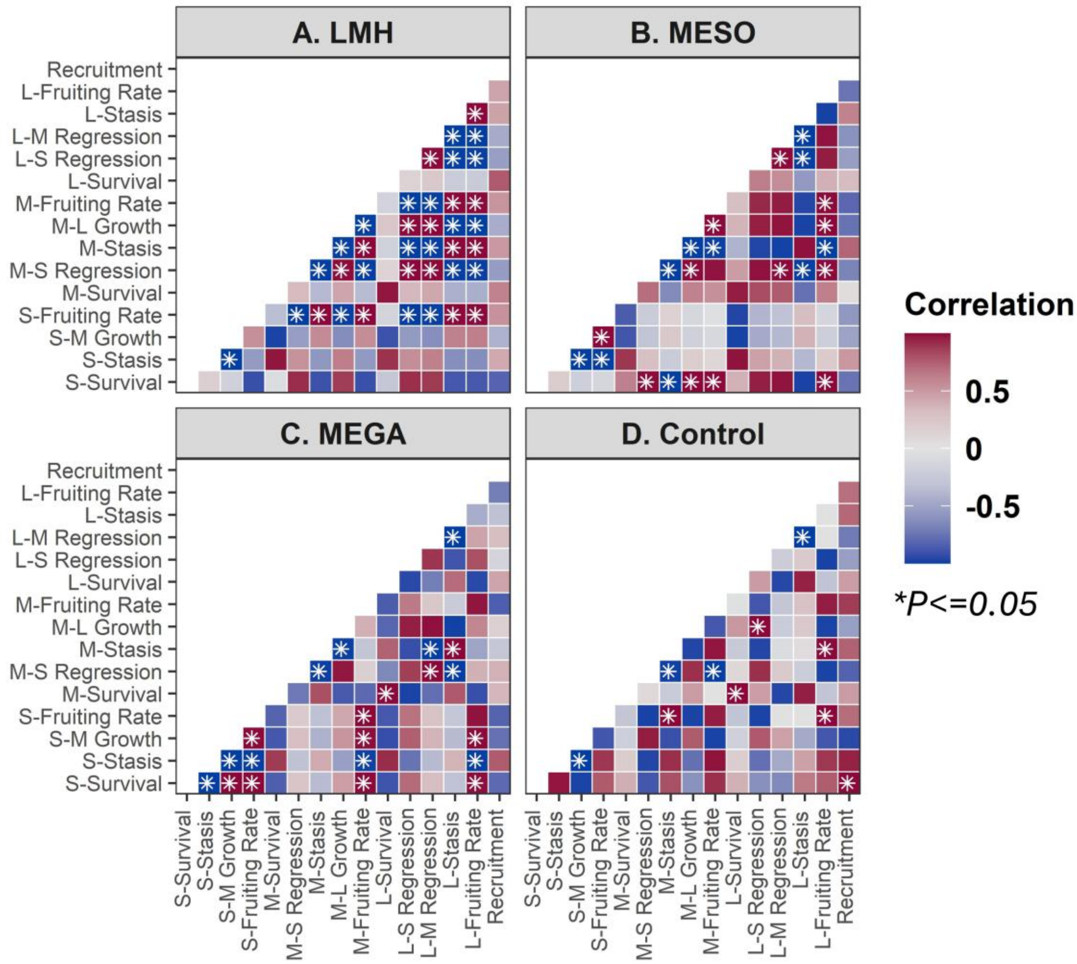

Figure 2.3. Correlations between Life Table Response Experiment (LTRE) contributions of size-specific demographic rates for large mammalian herbivore exclusion treatments. Here, we show across-rainfall gradient Pearson product moment correlations between pairwise combinations of LTRE contributions for demographic rates in four exclosure treatments: (A) the complete exclusion of large mammalian herbivores (“LMH”), (B) the exclusion of meso- and mega- herbivores (“MESO”), which includes smaller herbivores such as dik-dik, (C) the exclusion of megaherbivores (“MEGA”), which includes smaller herbivores and mesoherbivores such as gazelle, and (D) the presence of all large mammalian herbivores (“control”), which includes mesoherbivores, smaller herbivores, and megaherbivores such as elephants. S indicates

small plants, M medium, and L large; thus, for transitions among size classes (stasis, growth, and regression), we show transitions from the first size class to the second (e.g., S-M growth indicates transition probability from small to medium). Color indicates the strength and sign of correlations, and white asterisks (*) indicate significance (P<=0.05). Demographic rates that did not vary across rainfall levels are excluded.

Chapter 3 - Context dependent effects of smooth brome (*Bromus inermis*) on native grass demographic rates

3.1 Abstract

Invasive species reduce native plant diversity and hinder restoration efforts, but their effects on native species often vary across environmental conditions. Such context dependence may arise due to native or invasive species' responses to abiotic conditions, such as drought or disturbance. Understanding these dynamics is critical in grassland systems, where variation in precipitation and disturbance play important roles in shaping community dynamics. We investigated how competitive effects of an invasive species, smooth brome (*Bromus inermis*), on six native bunchgrass species vary with drought in an invaded grassland. We manipulated drought with passive rainout shelters (66% reduction in rainfall) and reduced brome competition via manual removal (30% reduction in above-ground biomass). We quantified brome and drought effects on both plugs and seeds, monitoring their survival and germination over two years. We found that invasive competitors and drought non-significantly reduced plug survival, but the effect of invasive competitors did not differ with drought. By contrast, invasive competitor effects on germination were context dependent, as high brome competition had limited effects on germination under ambient rainfall but decreased germination under drought. Our results suggest that context dependence might be more common for germination rates rather than subsequent life stages, suggesting that more consistent restoration outcomes could be achieved by planting plugs rather than seeding. These results underscore the importance of integrating environmental and competitive conditions with life stage-specific considerations when designing effective restoration strategies.

3.2 Introduction

Invasive species are one of the most substantial threats to biodiversity in the modern era, affecting one-sixth of terrestrial habitats and contributing to 60% of known extinction events (Early et al. 2016a, Roy et al. 2024). Invasive plants in particular, which represent the majority of invasive species, contribute to a 16% decline in species richness across various systems (Mollot et al. 2017) and lead to significant economic loss (Novoa et al. 2021). Invasive plants can affect the performance of native plants through reducing the availability of resources (e.g., water, nutrients, or light) or through allelopathy, both of which directly reduce native plant performance (Jordan et al. 2008). They can also have indirect effects on native plants by changing soil carbon, nitrogen, or water cycling (Evans et al. 2001, Keen 2023, Raheem et al. 2024), altering disturbance regimes (Fusco et al. 2019), or modifying soil microbiota (Gibbons et al. 2017b). Together, these direct and indirect effects can lead to long term negative consequences for biodiversity and ecosystem function.

Effective management of invasive plants requires understanding whether and how their impacts on native species vary with abiotic conditions (i.e., context dependence; Catford et al. 2022). The relative response of invasive vs. native species to abiotic conditions may determine whether or not context dependence is operating. For example, if invasive plant species are more positively impacted by high resource conditions (i.e., high precipitation, nutrients, or CO_2) than native plant species, we might see strong negative effects of invasive species when resources are high (Matzek 2012, Liu et al. 2017), and weaker effects of invasive species when resources are low (Daehler 2003). Context dependence may also occur for some life stages but not others, because some life stages are more sensitive to poor abiotic conditions and/or invasive species' effects than others. For example, certain life stages of native plants may be more negatively affected overall by resource competition with invaders (Barrat-Segretain 2005) or invader allelopathy (Bieberich et al. 2018b). Finally, context dependent effects of invasive species may occur for some native species but not others. For example, fast-growing, resource-acquisitive native species may be more susceptible to invader impacts in resource-poor years, whereas slow growing resource-conservative native species may be more susceptible to invader impacts in high-resource years (LaForgia et al. 2020). Altogether, previous work suggests that the presence and magnitude of context dependence in invasive-native interactions depend on native species' characteristics and may vary across life stages.

In systems where invasive and native species have different tolerances to drought, the effects of drought on invasive species impacts may be predictable. For example, in the Great Plains, native C_4 bunchgrass species are thought to be well-adapted to moderate drought conditions, maintaining higher water use efficiency and productivity under reduced precipitation (Pearcy and Ehleringer 1984, Taylor et al. 2014). In contrast, invasive grasses in the Great Plains are frequently C_3 species, which tend to decline in density under drought (Cully et al. 2003, Cristiano et al. 2012). In this system, because drought reduces invasive species' density, we might expect their impacts on native species to be context dependent. Namely, invasive effects on natives should be higher under ambient rainfall (when invasive densities are high), but weaker under drought conditions (when their densities are reduced; Figure 3.1A. Similar effects could arise if invasive species' water or nutrient uptake strategies differ under ambient rainfall vs. drought. In a system where invasive species can maintain high densities under both ambient rainfall and drought, invasive species effects will be strong under all rainfall conditions (Figure 3.1B), resulting in no context dependence.

Context dependent effects of invasive species on native species could increase the variation in restoration outcomes. In many grassland systems, abiotic conditions during restoration affect subsequent community composition, largely by determining which native species successfully establish (MacDougall et al. 2008). Similar results have been found in other systems, with the community composition of restorations depending strongly on initial abiotic conditions (Stuble et al. 2017, Xing et al. 2025). Such results are usually attributed to differential impacts of drought on native seed germination and seedling survival (Eckhoff et al. 2023, Ren et al. 2024), rather than due to abiotic effects on invasive-native competition (i.e., context dependence). However, there is some evidence that climatic context may alter invader effects: drought in particular affects the relative success of invasive species, in some cases increasing competitive pressure on native species (Ott et al. 2016, Garbowski et al. 2021). Differentiating between these two mechanisms allows us to better predict variation in restoration outcomes; if native species' response to abiotic conditions alone drives variation in restoration outcomes, we can predict variation in restoration outcomes using information on native species alone. If abiotic conditions affect native-invasive interactions, we must quantify both native and invasive species' responses to abiotic conditions.

In this study, we test whether invasive plant species' effects on native plant species are context dependent by conducting a grassland restoration experiment under ambient rainfall and drought conditions. Specifically, we test whether the effect of *Bromus inermis* (hereafter, brome), a widespread invasive C_3 grass in the Great Plains (Salesman and Thomsen 2011, Mackiewicz-Walec et al. 2024), on performance of five native C_4 grasses varies with drought conditions. We used a split-plot design to manipulate drought and brome density. We quantified how the degree of context dependence varies with native species identity across two life stages, as well as for a unified demographic metric of early life success, which includes multiple life stages to approximate fitness. Understanding how the effect of brome on native species' demographic rates changes under drought will clarify how the effects of plant invaders on restoration may shift with increasing drought under climate change.

3.3 Methods

3.3.1 Study site

We worked at the Harold and Olympia Lonsinger Sustainability Research Farm (LF), a 2,300-acre agricultural research site in Alton, Kansas (39.52348, -99.00378). LF receives 613 mm of rainfall annually, primarily in the growing season (Fick and Hijmans 2017), and plant performance in this system is strongly dependent on variability in rainfall (Fay et al. 2011). Common invasive plants at this site include brome, eastern red cedar (*Juniperus virginiana*), and musk thistle (*Carduus nutans*), and common native plants include plains prickly pear (*Opuntia macrorhiza*), little bluestem (*Schizachyrium scoparium*), sideoats grama (*Bouteloua curtipendula*), and blue grama (*Bouteloua gracilis*). Like many of the agricultural lands in the region, LF currently supports livestock production and has historically undergone periods of overgrazing and drought. At LF, we worked in a heavily invaded field with well-drained silt loam soils (Natural Resources Conservation Service, United States Department of Agriculture 2018) where brome was the dominant species, with a mean of 70.1% (SE= 6.0%) above ground percent cover in our 40 3m x 3m experimental plots.

3.3.2 Experimental design

In February 2023, we fenced a 100 x 100-meter area at LF to exclude cattle from the study plots. Within this fenced area, we established 40 regularly spaced 3 m x 3 m plots (Figure 3.2). We randomly assigned plots to one of two rainfall treatments: drought or ambient rainfall treatments. In drought treatment plots, we erected passive rainout shelters in July 2023; shelters were designed to intercept and redirect rainfall away from plots. We modeled our shelters after those used at the Río Mayo Experimental Station (Yahdjian and Sala 2002) and Konza Prairie Biological Station (Broderick et al. 2022). Each shelter consisted of a 3 m x 3 m metal frame, mounted 1 meter above the ground on t-posts. Evenly spaced clear polycarbonate slats intercepted ~66% of rainfall (Broderick et al. 2022), and we angled shelters to channel intercepted water into a drainage system that directed runoff outside the plots. We conducted intermittent maintenance to address damage from seasonal high winds. Ambient rainfall treatments were left undisturbed.

We divided each 3 m x 3 m plot into four 1.5 m x 1.5 m subplots (Figure 3.2). We randomly assigned 2 contiguous subplots to one of two competition treatments (reduced brome density or ambient brome density, hereafter "low competition" and "high competition"; Figure 3.2). In April 2023 (before rainout shelters were erected and before competition treatments were applied), we measured percent cover of brome in each plot x competition treatment by haphazardly placing a 50 cm x 20 cm quadrat three times within each competition treatment and taking the average (placements of quadrat were non-overlapping). In May 2023, we established our competition treatments by manually removing all above-ground vegetation in the low competition treatment subplots, taking care to avoid disturbing the soil. To suppress brome regrowth, we carefully applied glyphosate (Roundup®) to the exposed brome stems. To assess the efficacy of brome removal, we remeasured the percent cover of brome in March 2024 by haphazardly placing a 50 cm x 20 cm quadrat three times in each of the four subplots and computing the average percent cover for each subplot. While brome cover decreased slightly across both treatments during our experiment (likely due to low ambient rainfall), our competition treatments were effective: low competition subplots had a 30% greater reduction brome cover than high competition subplots (Appendix B; Appendix Table 1; Appendix Table B.6; Appendix Figure B.1).

Within each competition treatment, we conducted two types of native plant additions. Namely, in 34 plots (divided equally between drought and ambient rainfall treatments), we randomly assigned one of the two subplots within each competition treatment to a seed addition treatment; the other subplot was assigned to a plug addition treatment (Figure 3.2). For both seed and plug additions, we added five native bunchgrass species (hereafter, focal species) common to the region: big bluestem (*Andropogon gerardii,* hereafter ANGE), sideoats grama (*Bouteloua curtipendula,* BOCU), blue grama (*Bouteloua gracilis,* BOGR), little bluestem (*Schizachyrium scoparium,* SCSC), and Indiangrass (*Sorghastrum nutans,* SONU). In plug addition subplots, we planted 16 live individuals of our focal species, randomly selected from greenhouse-grown plugs of all species, in a 4 x 4 grid pattern, and in seed addition subplots, we sowed seeds of our focal species (see "Plug and Seed Additions" below for details). We left a 30cm buffer around the edge of each subplot (Figure 3.2). The remaining six plots (three drought and three ambient rainfall plots) did not receive any plant additions and were designed to quantify background levels of seed germination; hereafter we call these plots germination control plots. We analyzed the results from plug addition and seed addition separately, such that our study consists of a split-plot factorial design housing two concurrent experiments. Rainfall treatments were applied at the plot level, competition treatments were applied at the subplot level, and we analyzed seed and plug data separately.

3.3.3 Plug and seed additions

For the plug addition subplots, we planted live plants that we grew from seed (Prairie Moon Nursery; Winona, MN) in the Kansas State University greenhouse. To grow plants from seed, in March 2023, we sowed 360 cells per species, at a rate of 10-15 seeds/cell, into 72-cell plug trays. Locations of trays were randomized in the greenhouse. We used a 1:1 mixture of Pro-Mix All Purpose Planting Mix and Miracle-Gro ® Seed Starting Potting Mix. We watered cells biweekly. Two weeks after planting, we thinned germinants to 1 individual/cell. In April 2023, we reduced watering for all trays to once per week. In June 2023 (before rainout shelters were erected but after competition treatments were applied), we planted 1088 of the surviving plugs, randomly assigned plugs to subplots and grid positions. Sample sizes among species differ to reflect the number of surviving plugs of each species. We watered plugs intermittently during the first two weeks following planting to encourage establishment. Plugs that failed to establish due to transplant shock during the first two weeks were replaced with a randomly selected plug from the greenhouse that was not included in the initial planting (all planted plugs were started from seed in March 2023 and thus were of similar ages. In total, this process resulted in the planting of 1088 plugs (135 ANGE, 115 BOCU, 205 BOGR, 332 SCSC, and 301 SONU. In September 2023 and November 2024, we returned to plots to score the survival of each plug. Hereafter, we call survival over the first 4 month period (June 2023 - September 2023) “first growing season survival” and survival over the remaining span of the experiment (September 2023 - November 2024) “annual survival”.

In seed addition subplots, we sowed local variants seeds of our five focal species (Sharp Bros Seed Co.; seeds were collected locally near Healy, KS). Local variants should exhibit locally adapted climate-dependent germination probabilities (Johnson et al. 2015, Gallagher and

Wagenius 2016, Galliart et al. 2019). We conducted seed additions in March 2024, hand broadcasting seeds at rates designed to yield 600 live seeds/ m^2 for each species: 2.052 g/m^2 (ANGE), 2.481 g/m^2 (BOCU), 0.500 g/m^2 (BOGR), 2.052 g/m^2 (little bluestem), and 1.499 g/m^2 (SONU). We repeated the removal of above ground biomass for the low competition seed addition subplots immediately prior to seed addition. In July 2024, we returned to count germinants of each species in the two seed addition subplots (germinant counts were summed across two non-overlapping haphazardly placed 50 cm x 20 cm quadrats). We used identical methods to count germinants in germination control plots.

3.3.4 Data analysis

We conducted all analyses in R (version 4.4.2) using the lme4 package (version 1.1-35.5). We used generalized linear mixed effects models to estimate the effects of competition treatment, rainfall treatment, species identity, and all two-way interactions between these terms on plug survival. For these models, we treated plot identity as a random effect and used a binomial distribution. We used AICc to compare all possible subsets of a global model and present results from the best-fit models in our results (Burnham and Anderson 2002, Lavergne et al. 2008). Note that competition treatment, rainfall treatment, and species identity were crossed factors, and plot identity was implicitly nested within rainfall treatment. We repeated this model selection procedure for both first growing season survival (June 2023-September 2023) and annual survival (September 2023-November 2024). Survival analyses did not include data from germination control plots and seed addition subplots.

We used a similar approach to test for the effects of rainfall and competition treatments on germinant counts. We first corrected for background germination (i.e., from a seed bank) by calculating the species-specific germinant counts for each competition treatment x rainfall treatment combination in our six germination control plots, averaged across the three replicates (hereafter, “background germinant counts”). We then obtained corrected germinant counts by subtracting background germinant counts from the germinant counts in corresponding seed addition subplots. We used a generalized linear model with a negative binomial distribution to estimate effects of competition treatment, rainfall treatment, species identity, and all two-way interactions among the terms on corrected germinant count, treating plot identity as a random effect. We used AICc to compare all subsets of this global model and present the best fit model in the results. We excluded data for ANGE, SCSC, and SONU due to very low corrected germinant counts which impeded model convergence (Appendix Figure B.2).

To estimate the net effect of competition and drought on early life success, we combined data from corrected germination counts, growing season, and annual survival. Namely, for each species, we quantified early life success as the product of competition treatment x rainfall treatment specific germination rates (corrected germinant count/m^2 divided by the number of live seeds/m^2), averaged across plots, plot x competition treatment specific growing season survival, and plot x competition treatment specific annual survival. We estimate the effects of competition and rainfall treatment (note that rainfall treatments differ among plots), on early life success using a model selection approach. We first fit a global model including competition and rainfall treatments, species identity, and all two-way interactions between these terms. We used a generalized linear model with a zero-inflated beta distribution, with plot identity as a random effect. Lastly, we used AICc to compare all subsets of the global model and present the best fit model in the results.

3.4 Results

3.4.1 Plug additions

Both high competition and drought treatments reduced plug survival, but the effects of treatments varied across species and across years. The best-supported model describing first growing season survival included competition, species, and their interaction (Figure 3.3; AICc model weight = 0.53; Appendix Table 2; Appendix Table B.7), but not rainfall treatment, suggesting that competition influenced survival and that the strength of competitive effects varied among species. The absence of a rainfall effect suggests that the effect of brome competition did not vary with abiotic context. Across all species, competition reduced survival: first growing season survival was, on average, 47.3% lower in high competition subplots compared to low competition subplots (SE = 0.252; Figure 3.3). BOCU was most strongly affected by competition, experiencing approximately twice the reduction in survival observed for BOGR, SCSC, and SONU, and nearly three times the reduction observed for ANGE (Appendix Table B.7). Regardless, high competition significantly reduced survival in the first growing season for most species (with the exception of ANGE), as evidenced by non-overlapping 95% confidence intervals for the mean predicted species-specific survival between competition treatments (Figure 3.3). Differences in the strength of brome competition effects across species resulted in changes in the rank ordering of species survival in the low vs. high competition treatment. Namely, in the low competition treatment, first growing season survival was higher for BOCU, BOGR, and SONU (who did not significantly differ form one another, as evidenced by overlapping confidence intervals; 95% CIs= [0.818, 0.969], [0.811, 0.938], [0.785, 0.911] respectively; Figure 3.3) compared to SCSC and ANGE (who did not significantly differ from one another; 95% CIs= [0.519, 0.707] and [0.309, 0.580] respectively). Under high competition, survival was uniformly low across most species (Figure 3.3), with almost all species pairs having overlapping confidence intervals (only SCSC was significantly different from BOGR; SCSC< BOGR; 95% CI for SCSC = [0.059, 0.161]; 95% CI for BOGR = [0.265, 0.488]).

The best-fit model for annual survival (September 2023-November 2024) included competition treatment and rainfall treatment, as well as species identity (Figure 3.4, AICc model weight=0.36; Appendix Table 3; Appendix Table B.8), but no interactions among these effects, suggesting that the effect of brome competition did not vary with abiotic context. While competition was included in the best fit model, with 30.3% lower survival in the presence of competitors (SE=0.595; Figure 3.4A), approximate confidence intervals for the mean predicted survival in each treatment overlapped, suggesting non-significant differences (95% CI for low competition = [0.309, 0.518]; 95% CI for high competition = [0.488, 0.639]). Drought was also included in the best-fit model, with lower annual survival in the drought treatment than in the ambient rainfall treatment (Figure 3.4B; mean reduction of 8.27%, SE= 2.65); again, however, the approximate confidence intervals for mean predicted survival within the treatment overlapped, indicating a lack of significance (95% CI for ambient rainfall= [0.452, 0.651]; 95% CI for drought= [0.323, 0.526]). Across species, survival was highest for BOGR, followed by BOCU, SONU, SCSC, and ANGE (Figure 3.4C). Confidence intervals for many species overlapped, indicating broadly similar survival rates; only the 95% CI of BOGR's survival ([0.552, 0.752]) differed from any other species (SCSC and SONU; 95% CIs = [0.298, 0.518] and [0.326, 0.516], respectively).

3.4.2 Seed additions

The best-fit model for corrected germinant counts included competition treatment, rainfall treatment, and their interaction (AICc model weight=0.15; Appendix Table 4; Appendix

Table B.9), indicating that the effect of competition from brome varied with abiotic context. There was no effect of species in the best-fit model, suggesting that germination rates did not differ across species. Although competition was included in the best fit model, in the ambient rainfall treatment, approximate confidence intervals for mean predicted germinant counts across competition treatments overlapped, suggesting non-significant differences (95% CI for low competition = [0.555, 2.021]; 95% CI for high competition = [0.621, 2.23]). Within the drought treatment, however, competition reduced germination: germinant counts were significantly lower in the high competition treatment compared to low competition treatment (mean reduction of 1.8 germinants/plot, SE=0.61; 95% CI for high competition= [0.289, 1.196]; 95% CI for low competition = [1.326, 4.388]; Figure 3.5).

3.4.3 Early life success

The best-fit model for early life success included competition treatment, rainfall treatment, species, and all two-way interactions among these variables (AICc model weight = 1; Appendix Table 5; Appendix Table B.10), suggesting that rainfall, species and competition influenced early life success. Further, this finding suggests that species differed in their responses to both competition and rainfall, and that the effect of competition from brome was driven by abiotic context. Under ambient rainfall levels, high brome competition significantly reduced early life success for ANGE, BOGR, and SCSC, evidenced by non-overlapping confidence intervals for treatment-specific predicted early life success rates (Figure 3.6). By contrast, for BOCU high brome competition increased early life success under ambient rainfall level (Figure 3.6; 95% CI for BOCU under low competition = [0.0067, 0.007] and high competition = [0.010, 0.014]. Under ambient rainfall, high competition similarly increased early life success for SONU (95% CI under low competition= [0.00015, 0.00044] and high competition= [0.0013, 0.0019]).

The influence of brome competition also depended on abiotic context. For ANGE, BOGR, and SCSC, as outlined in the previous paragraph, competition significantly reduced early life success under ambient conditions; however, these effects changed under drought. For BOGR, the significant negative effect of competition was larger under drought conditions (Figure 3.6; 95% CI under low competition= [0.0198, 0.0216] and high competition= [0.00182, 0.00323]). For ANGE, however, competitor effects weakened under drought, although this difference remained significant (95% CI under low competition= [0.000438, 0.000902] and high competition= [0.0000258, 0.0000968]). For SCSC, rather than having negative effects, competition had significantly positive effects under drought conditions (low competition; 95% CI= [0.00685, 0.0237] compared to high competition (95% CI= [0.000577, 0.00135]). For BOCU and SONU, as outlined in the previous paragraph, competition significantly increased early life success under ambient conditions, but these effects changed under drought. For BOCU, competition significantly decreased early life success under drought (Figure 3.6; 95% CI under low competition = [0.0162, 0.0185]; 95% CI under high competition= [0.00715, 0.0114]). Finally, for SONU, competition continued to increase early life success under drought, though the effect was comparatively weak (Figure 3.6; 95% CI under low competition = [0.000475, 0.00725]; 95% CI under high competition= [0.000751, 0.00152])

3.5 Discussion

Invasive species can have strong negative effects on native species, but the magnitude of these effects can differ substantially with abiotic conditions, or across species or life stages of the native species (Vasquez et al. 2008, Lu et al. 2016, LaForgia et al. 2020). In our study, competition from brome significantly changed the survival of native grass plugs for many species during the first growing season (shortly after being transplanted), but did not significantly affect survival annually (Figure 3.3, Figure 3.4), indicating a lack of context dependent effects of brome competition (Figure 3.1B). In contrast, greater competition from brome reduced germinant counts only within the drought treatment, reflecting context dependent effects of brome competition (Figure 3.5, Figure 3.1A). When considering the net effect of brome on plant performance (i.e., early life success), multiple species experienced context dependent effects of brome competition (Figure 3.6). Namely, abiotic conditions caused either stronger or weaker effects of brome on native plant performance, which manifests into context dependent effects on overall early life success. Overall, these results suggest that the native grasses in our study were strongly affected by brome and that these effects were context dependent (i.e., the magnitude of their effects depends on abiotic conditions). Below we discuss each of these findings within the context of current literature.

We found that the effect of invasive species on native species differed with rainfall treatments for some demographic rates but not others, meaning that context dependent effects might be missed if only one life stage or demographic rate is considered. This finding is particularly important given that effects of competitors on early life success were context dependent in most species. For example, in BOGR and ANGE, the magnitude of competitor effects differs under drought vs. ambient conditions (becoming, in the case of BOGR, stronger under drought, and in the case of ANGE, weaker under drought). Such species-specific responses likely reflect differences in how drought alters the performance of both the invader and the native species. Reduced brome densities under drought (a 9% greater decline in cover from 2023 to 2024, although this difference is not statistically significant; Appendix Table 1; Appendix

Table B.6, Appendix Figure B.1) could have lessened competitive pressure, thereby amplifying the benefits of reduced competition under drought for species like BOGR, which otherwise performed well under ambient conditions. In contrast, ANGE exhibited low early life success under ambient conditions, suggesting that site conditions were suboptimal for its establishment. For this species, any reduction in brome density under drought may provide little benefit, while the additional negative effect of drought on survival could further limit early life success, potentially explaining the weaker competitive effects observed under drought.

We expected to see negative effects of both drought and competition on native grasses. Thus, the positive effect of competitors on early life success under ambient rainfall (in BOCU and SONU, Figure 3.6) was quite surprising. This positive effect seems to be driven by positive effects of competitors on germination rate (Figure 3.5), because competitor effects on survival are largely negative (Figure 3.3, 3.4). We can think of three possible explanations for why competitors would increase germination and why that positive effect only occurs under ambient rainfall. First, brome may facilitate BOCU and SONU by reducing soil surface temperatures and increasing moisture availability for germinants (similar to Wright et al. 2014, Leverett 2017). If aboveground brome biomass is greater under ambient rainfall compared to drought, faciliative effects would be stronger under ambient rainfall. Given that there is higher cover of brome within ambient rainfall treatments (though not significantly higher; Appendix Table B.6, Appendix Figure B.1), this explanation could be affecting germination. Alternatively, this result could reflect the drought conditions in the year our study was conducted. LF received low precipitation and high temperatures for the 5 months prior to the collection of germinant counts, compared to historical averages (“Monthly National Climate Report for June 2024” 2024). Thus, newly germinated native seedlings were likely experiencing significant evapotranspirative water loss across both drought and ambient rainfall treatments. If facilitation occurs under moderate but not extreme drought (consistent with modern formulations of the stress gradient hypothesis; Holmgren & Scheffer, 2010), in ambient rainfall treatments, faciliation would occur, but in drought plots, where seedlings contend with both LF weather and experimentally imposed drought, facilitation would not occur. Finally, these effects may have been driven by seed predation. In the low competition treatment (without brome cover), seeds may have been more visible and accessible to granivorous birds, reducing germinant count (similar to Doust, 2011; Joyce et al., 2024). However, in the drought treatment, the rainout shelter roofs might have deterred seed predation. In this scenario, we would expect highest germinant counts in the drought treatment (where seeds are shielded from predation) and in the low competition treatment (where seedlings face fewer competitors).

We found that the effects of brome on early life success differed across species. Effects of brome were strongest in BOCU and BOGR, but ANGE, SCSC, and SONU experienced weaker impacts of brome. Much of this effect appears to be driven by very low germinant counts for these species (Appendix Figure B.2). While many restoration studies show low native germination rates in invaded systems (Mangla et al. 2011, Kimball et al. 2014), low germination in these species may also be due to abiotic tolerance. Namely, while *Bouteloua spp*. are well-adapted to dry conditions (Albertson and Weaver 1946, Lauenroth et al. 1987, LeCain et al. 2006), ANGE, SCSC, and SONU are commonly found in more mesic tallgrass prairies (Gibson and Hulbert 1987), and are likely perform best under higher moisture availability. Abiotic tolerance appears to underlie the strength and direction of context dependence in competitive effects. The two more dry-adapted species, BOCU and BOGR, exhibited the strongest context-dependent responses to brome: for BOGR, brome reduction had a stronger positive effect under drought compared to ambient rainfall, whereas for BOCU, the effect of brome shifted from positive under ambient rainfall to negative under drought. In contrast, species more characteristic of tallgrass or less drought-prone prairies (ANGE, SCSC, and SONU) showed consistently low early life success across treatments, resulting in more limited context dependence.

One of the key caveats of our study is that we cannot attribute competition treatment effects solely to changes in resource competition between brome and focal species; instead, other mechanisms may also have contributed. For example, non-native grasses frequently reduce the germination and survival of native grasses through allelopathy (Greer et al. 2014, Singh and Daehler 2023), which can either directly inhibit native grass growth or inhibit growth through changes in the soil microbial community. If such effects were operating in our system, then the negative impacts of brome on native performance may have arisen not only from direct competition for light, water, or nutrients, but also from chemical inhibition of recruitment. Alternatively, seed predation may have played a role in outcomes, leading to stronger or weaker context dependent effects on germination depending on the presence of obstacles to birds (i.e., shelters discouraging birds from landing and consuming seeds). These possibilities complicate the interpretation of our results and highlights the importance of considering both resource-based and non-resource-based mechanisms when evaluating invasive species' impacts.

In our study, both drought and brome affected native plant performance, and effects of brome were often context dependent. These results suggest that previous studies showing strong effects of climate in the year of restoration on the trajectory of restoration communities might be due in part to context-dependent effects of invasive species, rather than abiotic tolerances of the native plants alone. We also found that context dependent effects were common in species that have high drought tolerance, and particularly at the germination stage, suggesting that the outcome of restoration projects in invaded systems might be more predictable if land managers use plugs rather than seeds. While broadcasting seed is relatively easy and inexpensive, planting plugs is time-intensive and costly; thus, managers might consider planting plugs specifically for species with greater sensitivity to environmental changes to increase the reliability of management. Overall, our work highlights the importance of evaluating multiple life stages and species in restoration studies; focusing on a single stage or species could misconstrue the importance of context dependence and reduce the reliability of predictions for restoration outcomes.

3.6 Figures

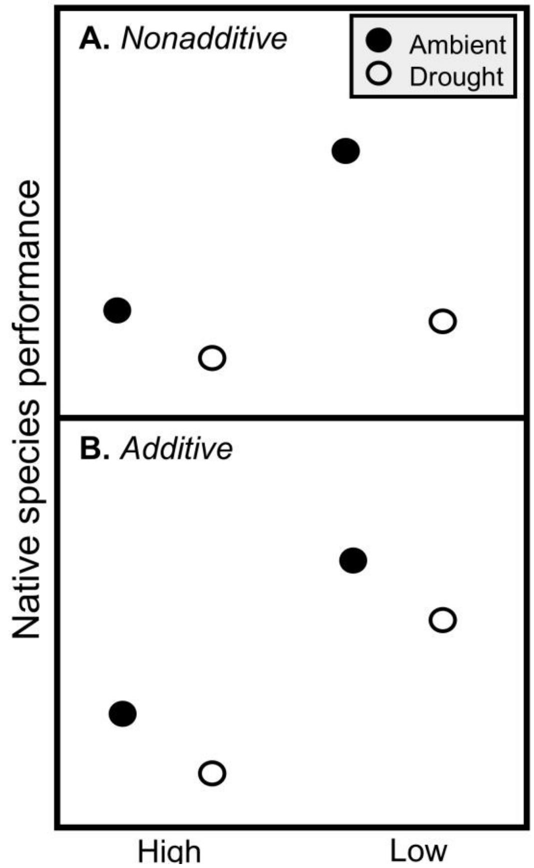

Figure 3.1. Hypotheses explaining the combined effects of drought and competition from invasive species on native species performance. "Low" indicates a treatment were invasive competitors have been reduced; "High" indicates a treatment where invasive competitors are not reduced (present at ambient high densities). In (A), we show context dependent effects of invasive species. Namely, the reduction of invasive species strongly increases performance under ambient conditions, but has much weaker positive effects under drought conditions, where invader densities are already low. In (B) we show no context dependence (i.e, additive effects): drought and the presence of invasive species both reduce native species performance, with no change in invader effects depending on rainfall treatments.

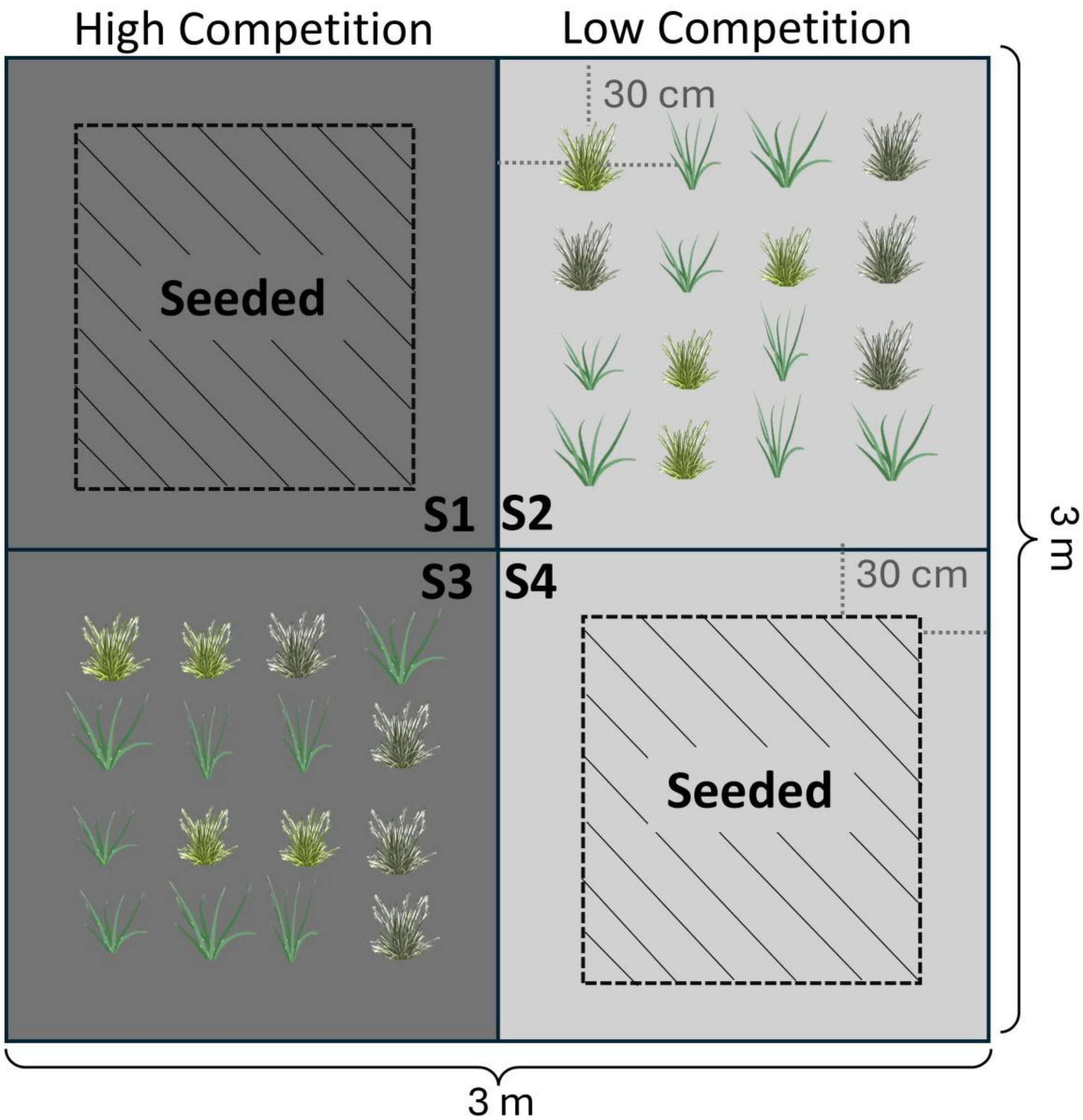

Figure 3.2. Diagram of experimental design. We randomly assigned 34 plots to an ambient rainfall or drought treatment; here we show only one plot. Within each plot, we assigned two contiguous subplots (S1, S2, S3, S4) to one of two competititon treatments, either “Low competition” (light grey), where we removed aboveground brome cover, or “High competition” (dark grey), where we left brome intact. In 34 plots, we randomly assigned subplots within a competition treatment to either seed addition or plug addition, in which we either hand-broadcast seeds or planted 16 evenly spaced plugs of our five focal species: big bluestem (*Andropogon*

gerardii; ANGE), sideoats grama (*Bouteloua curtipendula*; BOCU), blue grama (*Bouteloua gracilis*; BOGR), little bluestem (*Schizachyrium scoparium*; SCSC), and Indiangrass (*Sorghastrum nutans*; SONU). In sum, our study consists of a split-plot factorial design with concurrent sub-experiments, wherein rainfall treatments are applied at the whole-plot level, plant additions and competition treatments are applied at the subplot level, and seed and plug data are analyzed separately.

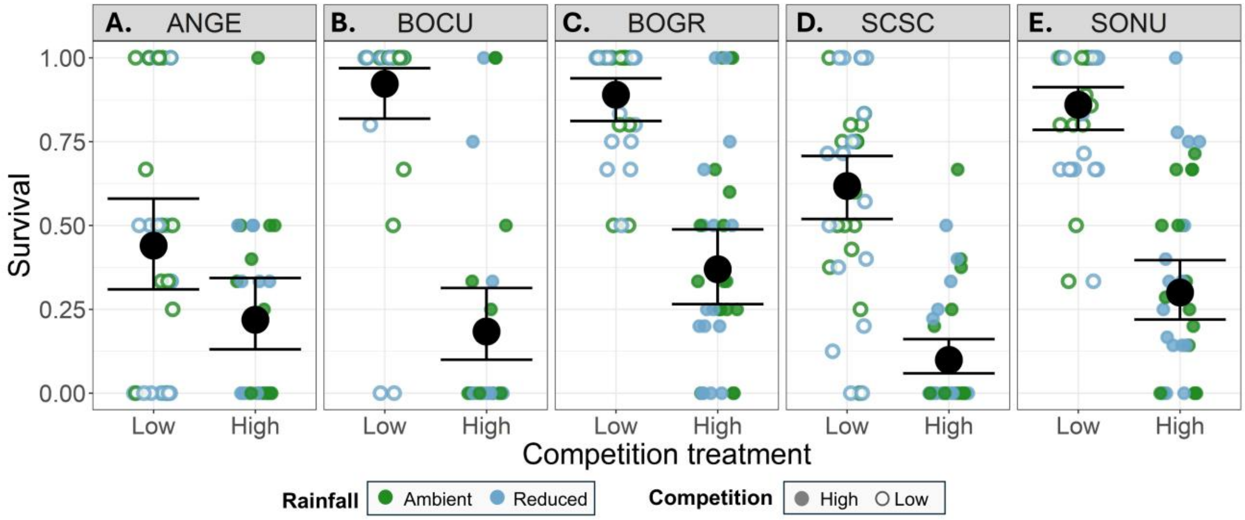

Figure 3.3. First growing season plug survival (June 2023–September 2023). Our best-fit model for survival included competition treatment, species identity, and their interaction; here, we show effects of only terms included in the best-fit model (Appendix Table B.7). Black points represent predictions of the best fit model, with error bars indicating 95% confidence intervals on those predictions. Other points indicate observed plot-level survival rates. Panel headings indicate species: big bluestem (*Andropogon gerardii*, ANGE), sideoats grama (*Bouteloua curtipendula*, BOCU), blue grama (*Bouteloua gracilis*, BOGR), little bluestem (*Schizachyrium scoparium*, SCSC), and Indiangrass (*Sorghastrum nutans*, SONU). Rainfall treatments include: ambient (plots that received ambient rainfall); and drought (plots under rainout shelters that excluded ~66% of ambient rainfall). Competition treatments include: high (no change in brome cover) and low (aboveground brome cover was reduced via cutting and herbicide).

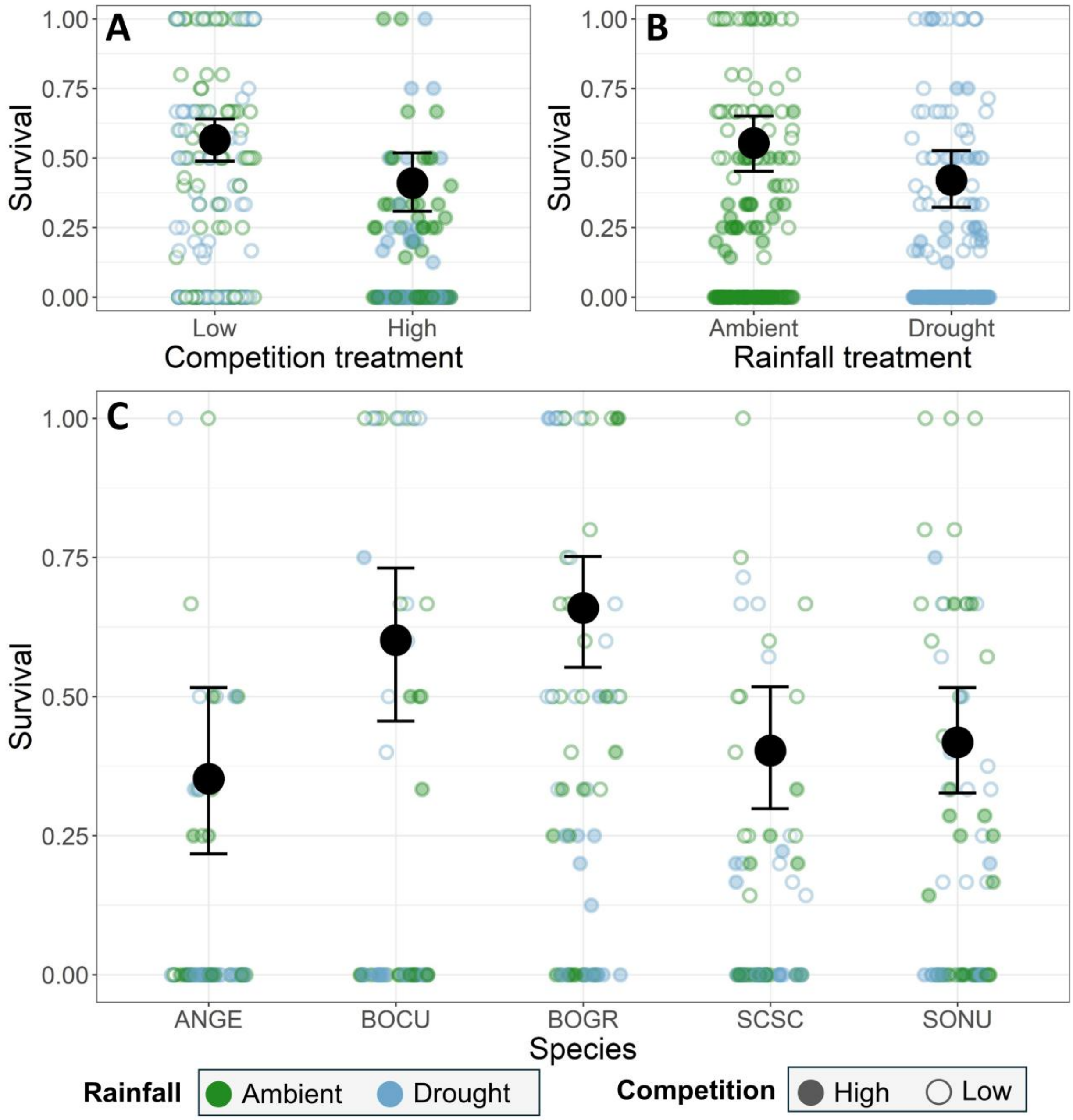

Figure 3.4. Annual plug survival (September 2023–November 2024). Our best-fit model for survival included competition treatment, rainfall treatment, and species; here, we show effects of only terms included in the best-fit model (Appendix Table B.8). Black points represent predictions of the best fit model, with error bars indicating 95% confidence intervals on those predictions. Other points indicate the observed plot-level survival rate. Species include: big

bluestem (*Andropogon gerardii*, ANGE), sideoats grama (*Bouteloua curtipendula*, BOCU), blue grama (*Bouteloua gracilis*, BOGR), little bluestem (*Schizachyrium scoparium*, SCSC), and Indiangrass (*Sorghastrum nutans*, SONU). Rainfall treatments include: ambient (plots that received ambient rainfall); and drought (plots under rainout shelters that excluded ~66% of ambient rainfall). Competition treatments include: high (no change in brome cover) and low (aboveground brome cover was reduced via cutting and herbicide).

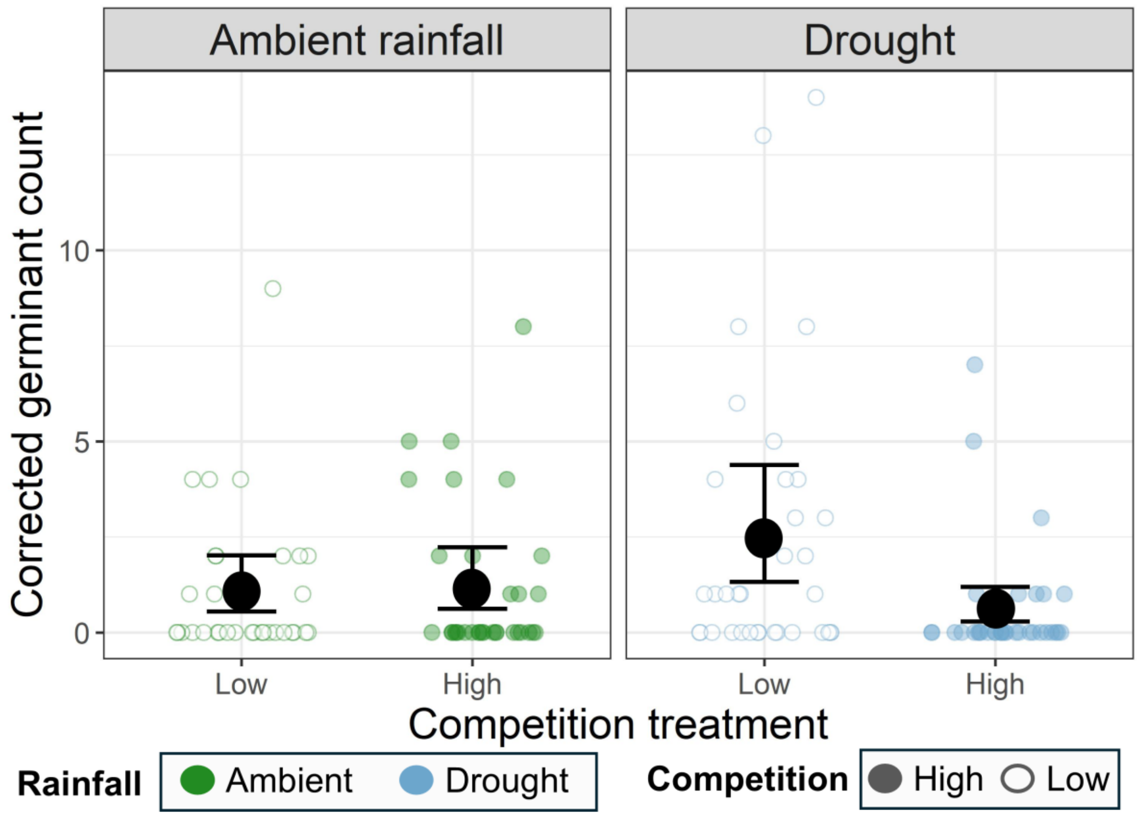

Figure 3.5. Corrected germinant counts (March 2024-July 2024). Our best-fit model for corrected germinant counts included competition treatment, rainfall treatment, and their interaction; here, we show effects of only terms included in the best-fit model (Appendix Table B.9). Black points represent predictions of the best fit model, with error bars indicating 95% confidence intervals on those predictions. Other points indicate observed plot-level corrected germinant counts. Rainfall treatments include: ambient (plots that received ambient rainfall); and drought (plots under rainout shelters that excluded ~66% of ambient rainfall). Competition treatments include: high (no change in brome cover) and low (aboveground brome cover was reduced via cutting and herbicide).

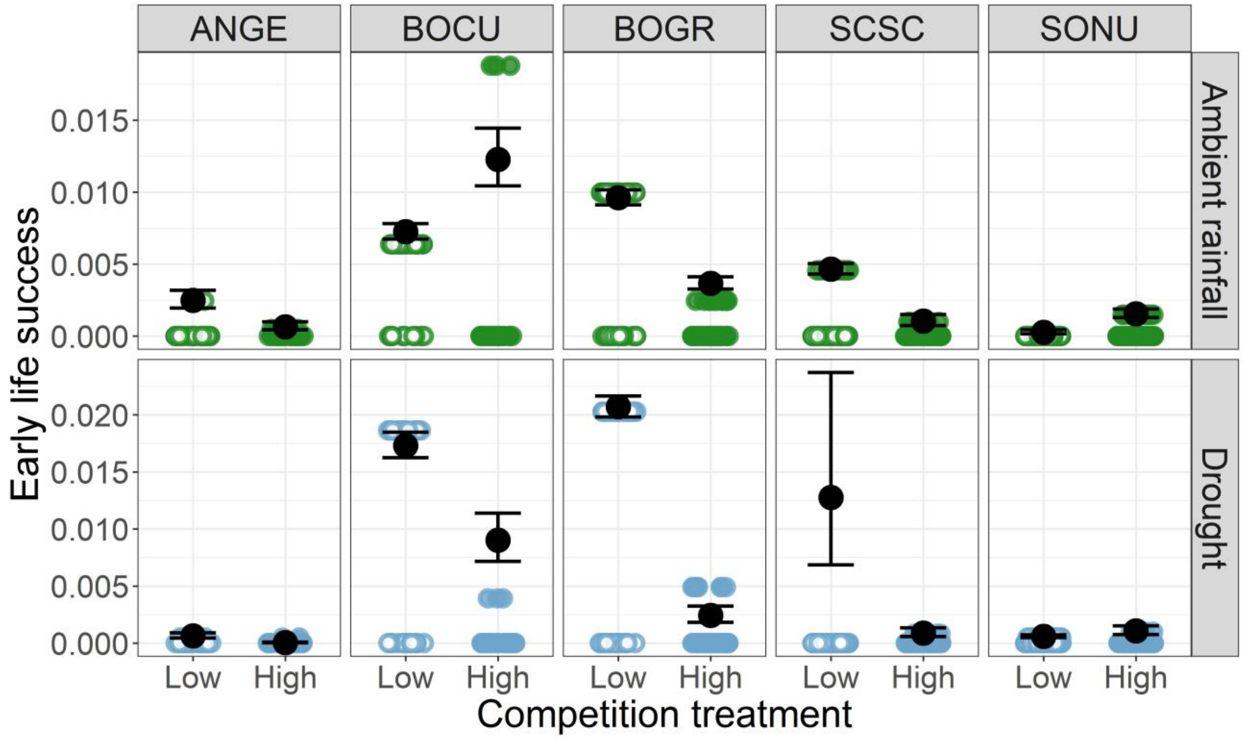

Figure 3.6. Effect of competition, rainfall treatment, and species on early life success. Our best fit model for early life success included competition treatment, rainfall treatment, and their interaction (Appendix Table B.10). Early life success was the product of species- and treatment-specific germination rates and plot, species, and treatment-specific annual survival. Black points represent predictions of the best-fit model, with error bars representing approximate 95% confidence intervals on those predictions. Other points indicate the observed plot-level early life success. Rainfall treatments include: ambient (plots that received ambient rainfall); and drought (plots under rainout shelters that excluded ~66% of ambient rainfall). Competition treatments include: high (no change in brome cover) and low (aboveground brome cover was reduced via cutting and herbicide).

Chapter 4 - Relative and interactive effects of fire, grazing, and climate on eastern red cedar invasion speed

4.1 Abstract

Temperate grasslands are one of the most threatened ecosystems worldwide due to land use changes, climate change, and species invasions. Woody encroachment represents a process of invasion in which (often native) woody species displace grasses and forbs. Eastern red cedar (*Juniperus virginiana*; hereafter, ERC) is an evergreen tree species native to the eastern and central regions of North America which has encroached at a rapid rate in the Great Plains region over the last several decades. While human plantings, changes in dominant megaherbivores, changes in fire regimes, and climate change have all been cited as reasons for woody encroachment, less is known about the relative effect size of each driver, as well as how drivers may interact to affect woody encroachment rate. This project utilizes a demographic model parameterized by field-collected data coupled with realistic dispersal rates to estimate the relative response of ERC invasion speed (i.e., shifts in the location of waves of invasion over time) to changes in fires, grazing, and climate. Because the population model is a function of climate, fire frequency, and grazer presence, we can compare effects of fires, grazers, and climate on woody encroachment rates using a unified modeling framework. Our results suggest that interactions among drivers play a large role in determining the invasion speed. As expected, frequent fires strongly reduced ERC invasion speed. Despite increasing survival during fires, cattle had largely negative effects on invasion speed. Climate shaped demographic responses by altering the strength of fire and grazer effects. These results suggest that effective control of ERC encroachment will require coordinated fire and grazing management strategies that account for climate context. We note that these results are provisional, as the analysis is ongoing and the model continues to be refined.

4.2 Introduction

Species invasions are one of the leading drivers of changes in biodiversity and are expected to have adverse effects on ecosystems worldwide (Sala et al. 2000). Although classical literature on invasion ecology usually focuses on non-native species, it is now recognized that the rapid population growth of some native species may also have detrimental effects on ecosystem function (Nackley et al. 2017). Woody encroachment (Archer 1994b), represents a process of invasion in which native woody species expand into ecosystems previously dominated by grasses. Much like invasions by non-native species, this process involves the rapid spread and establishment of species outside their historical distribution or habitat. Across grasslands worldwide, woody encroachment has become increasingly problematic and, without proper management, threatens to reduce grassland diversity (Horncastle et al. 2005, Frost and Powell 2011) and disrupt biogeochemical cycles (McKinley et al. 2008, Zou et al. 2018).

Woody encroachment in North America has accelerated in the past century due to a variety of anthropogenic effects. For example, widespread fire suppression (Daubenmire 1968), has contributed toward an increased abundance of woody plant species in Great Plains grasslands (Archer 1994b, Briggs et al. 2002, Van Auken 2009). Fires reduce woody cover in grasslands primarily by killing vulnerable juvenile plants that have not achieved a large enough size or bark thickness to protect their vascular tissue (Lawes et al. 2011). In addition, changes in grazing regimes in the Great Plains have likely contributed to woody encroachment. Namely, the region has seen a shift from widely dispersed, bison-dominated grazing to intensive, cattle-dominated grazing. Cattle can promote woody encroachment: because intensive cattle grazing dramatically reduces grass cover, woody seedlings have more light available to establish (Van Auken 2009), and suffer lower mortality during less-intense fires (Briggs et al. 2002). Other studies suggest that cattle grazing could reduce woody encroachment, potentially by reducing woody plant recruitment via trampling (Owensby et al. 1973, Schmidt and Stubbendieck 1993). Finally, climate change (i.e., reduced precipitation and increased temperatures) may affect woody encroachment (Scheiter and Higgins 2009, Tu et al. 2024), though the direction of the effect is unclear. While drought may reduce woody seedling survival (Schmidt and Stubbendieck 1993), it may also reduce fuel load and thus temper the negative effects of fire on woody plants (Kimball et al. 2024).

While the effects of fire suppression, cattle grazing, and climate change on woody encroachment are relatively well understood, the relative effect size of each of these environmental drivers is debated (Fuhlendorf et al. 2008). Factorial experimental manipulations of each of these drivers are unrealistic within a reasonable time scale, and studies showing different levels of woody cover under different management histories do not implicate causality. Neither of these approaches allow us to estimate non-linearities in woody plant response to drivers that could arise due to driver effects on multiple demographic rates. Similarly, we cannot readily compare how specific drivers affect adult and seedling demographic processes, limiting our ability to weigh, for example, the negative impacts of fire on juvenile survival against the positive effects of post-disturbance recruitment opportunities. An understanding of which of these environmental drivers most strongly influence woody encroachment rates (and ideally, the relative effects of each toward different life stages) would allow us to prioritize conservation and management efforts on one particular management action and/or one life stage.

In addition to an understanding of their relative effect size, we also have a poor sense of how these environmental drivers might modulate one another's' effects. Many studies show that controls on woody plant cover are spatially variable (Archer et al. 2017, Fogarty et al. 2022), suggesting that spatial variability in environmental characteristics might modify the effects of other drivers. Similarly, dynamic simulation models suggest that grazing can alter the effects of fire, with weaker grazing impacts under frequent burning (Fuhlendorf et al. 2008). Yet, we still lack studies that quantify how climate modulates these drivers' effects on underlying vital rates, which is particularly important within the context of climate change. This gap limits our ability to predict woody encroachment rates under changing management regimes and within the context of future climate conditions and also limits our ability to understand how combinations of management actions might jointly affect woody encroachment rates. Because woody encroachment represents a process of invasion by native woody species, frameworks developed for understanding invasion dynamics can provide new insight into its mechanisms and rate of spread. Here, we apply a spatially- and demographically- explicit modeling framework (Neubert and Caswell 2000, Caswell et al. 2011) to estimate the invasion speed of an encroaching woody species. This approach allows us to mechanistically link field-measured demographic responses to fire, grazing, and climate with predicted rates of spatial expansion, as well as construct what-if scenarios that reflect alternative management strategies of interest. Our work will provide insight into how environmental drivers and their interactions shape woody encroachment dynamics.

4.3 Methods

4.3.1 Study system

Eastern red cedar (*Juniperus virginiana,* hereafter ERC) is a long-lived coniferous evergreen tree species native to North America (Gilman and Watson 1993). In the last century, it has begun to invade grassland habitat in the Great Plains. This invasion has reduced plant, mammalian and avian diversity and modified hydrological function and biogeochemical cycles (McKinley et al. 2008, Horncastle et al. 2004, Frost and Powell 2011, Zou et al. 2018). ERC does not resprout, meaning that topkill from fires can be effective at reducing densities (Burns et al. 1990). While small trees suffer high mortality from fire, adult trees may experience lower mortality due to fire, especially in cattle-grazed areas with low fuel loads (Briggs et al. 2002).

4.3.2 Fire, climate, and cattle effects on ERC demographic rates

To quantify each drivers' impact on demographic rates, we quantified ERC demographic rates (Figure 4.1) at multiple sites within specific study locations across the Great Plains (Appendix Figure C.1). We selected sites to maximize the variability in climate and fire histories and cattle presence/absence and included only sites that harbored populations of ERC. When possible, we tried to find study locations that included sites with all possible combinations of these drivers; for example, BESS1, BESS2, BESS3, and BESS4 were close together, and thus experienced similar climate conditions, but differed in their fire and cattle grazing histories. We describe these sites in more detail in Appendix Table C.1.

Within each study location, each site served as a replicate that differed in its fire and grazing histories. At each of these 13 sites (distributed across eight study locations), we established 3–9 10 × 10 m plots that were representative of that site's ERC density (the number of plots depended on ERC density). Within each plot, we measured the height and basal diameter of all ERC present. We used these data to estimate survival using a three-step method. First, we quantified the relationship between size (i.e., height, basal diameter) and age. Next, we use that regression to predict the ages of all ERC in the plot. Finally, we quantified fire, cattle, and climate effects on survival using a population modeling approach, where we compared the age structure observed at each site to age structures that would arise for different levels of survival (Udevitz and Ballachey 1998, Doak and Morris 1999). We describe each step in more detail below.

First, we generated a size-age regression model. We obtained tree ages using dendrochronological methods. To develop the size–age regression, we collected increment cores from a haphazardly selected subset of adult trees (>10 cm diameter at breast height) within each study location. Core sampling was conducted at the level of the study location rather than exhaustively within each individual site. In total, we extracted 143 increment cores, with sample sizes varying by study location depending on the availability of suitable adult trees at a study location (27 from KNZ; 31 from BESS; 11 from ALA; 10 from CB; 22 from LS; 10 from MCK; 8 from TAPR; and 25 from NIO). If a tree had more than one stem, we chose to obtain cores from the larger stem. Cores were taken at breast height using Haglöf 5.15 mm increment borers, then dried, mounted, and sanded with increasingly finer grades of sandpaper (80-1500 grit; Stokes and Smiley 1996). Prepared cores were scanned at 2000 dpi and analyzed in CooRecorder 9.4 for ring identification. We also used CDendro (ver. 9.4) and xDateR (Bunn 2008) to build site-specific chronologies (Appendix Figure C.2) and crossdate cores (Stokes and Smiley 1996), reducing the probability of false rings, which are common in ERC (Appendix Figure C.3). False rings were identified with a combination of crossdating procedures and comparison of ring structure (Appendix Table C.2). For juvenile trees (<=10 cm DBH), we harvested 5-10 haphazardly selected individuals at each site, equally arrayed among plots, and examined stem cross sections under a dissection scope to count the number of rings. We assumed that these juvenile trees did not have false rings. In total, we assessed the ages of 205 individual trees across sites (Appendix Table C.2).

To generate our age–size regression, we fitted a series of generalized linear models predicting age from log-transformed diameter and height, using a log-link Gamma error distribution to reduce heteroskedasticity, and using site as a fixed effect. Using AICc, we compared all hierarchical subsets of models containing linear, quadratic, and polynomial terms for height and diameter. Higher-order terms were only considered in models that also included their lower-order counterparts (Appendix Table C.3). The best-supported model included the cubic effects of both height and diameter (Appendix Table C.4) and was a good fit to the data (McFadden's pseudo-R^2=0.997).

Finally, we used a population modeling approach to estimate age-specific survival rates as a function of fire history, climate conditions, and history of cattle presence at each site. This approach involved generating a series of hypothesized relationships of survival to age and environmental drivers, then using each hypothesized relationship to generate a predicted age distribution using a population model paired with site- and year-specific environmental conditions, and then testing the goodness of fit of each hypothesized relationship by comparing the predicted age distribution to the age distribution observed in the field (Doak and Morris 1999). All hypothesized relationships describing survival assume effects of age, annual precipitation and mean annual temperature (from ClimateNA; Wang et al. 2016), age x annual precipitation, age x mean annual temperature, years since a burn has occurred (hereafter, "time since burn", both linear and quadratic effects), cattle presence, the interaction between time since burn x cattle presence, the interaction between time since burn x age, and the interaction between cattle presence and age. We also include a categorical effect of whether or not a site burned in a given year; we note that we are "double counting" time since burn effects in our analysis, and thus our results should be interpreted with caution.

We used Bayesian rejection sampling to estimate which coefficient values best predicted age distributions (i.e., the posterior distributions of the associated parameters). We used minimally informative uniform priors that were bounded according to known ecological relationships. The prior for the age coefficient was restricted to positive values to reflect increasing survival with age in long-lived plants (Harper 1977). Similarly, priors for age x temperature and age x precipitation coefficients were both restricted to positive values to reflect less vulnerability of older trees to changing climates (Trouillier et al. 2019). The priors for the coefficient for the effect of fire was restricted to negative values to reflect reductions in survival due to fire (Briggs et al. 2005). For all other parameter values, priors were drawn from a uniform distribution of positive and negative values. These randomly drawn priors comprised a "candidate parameter set".

For each replicate draw from the priors, we used the resultant survival rates to simulate site-specific age distributions using an integral projection model (IPM; described in the next section) that projected population dynamics from the estimated site-specific germination year of the oldest tree to either 2022, 2023, or 2024 (the site-specific year in which we quantified age structure). Site-specific histories of temperature and precipitation were extracted from annual records (ClimateNA; Wang et al. 2016; calculated as mm rainfall/year and degrees Celsius), and histories of fire and cattle presence were obtained through consulting with land managers. We initiated simulations using the stable size distribution of the IPM kernel corresponding to the site-specific germination year of the oldest tree. These simulations produced a predicted age distribution for that year. Draws from the prior were retained in the posterior distribution if the mean error across all sites fell below arbitrarily predefined thresholds ($\leq$50 for ages 1-10 and $\leq$5 for ages 11-101), for a total of 5000 draws from prior distributions. This approach resulted in a function for survival that included age, fire, climate, and cattle effects (any of which could be estimated near zero, reflecting minimal effect of that driver), with the posterior distribution representing the best estimate for each coefficient in the survival function.

We used both field data and literature data to estimate cone production and germination. To quantify the probability of producing cones (hereafter, fruiting probability), for each tree within our field plots, we used field data; for each measured tree, we scored whether or not the tree had cones. We assessed the effect of temperature and precipitation (calculated as above), age, and all 2-way interactions between these factors, as well as the effects of the presence of cattle and the interaction between cattle and age on the probability of fruiting using a model selection approach. Climate data were site-specific averages from 1970–2000 obtained from WorldClim (Fick and Hijmans 2017). We compared all possible subsets of a global model containing these effects (fit using a generalized linear model with a binomial error distribution; Appendix Table C.5), evaluated model fit using AICc, and used the best-fit model in our subsequent analyses (Appendix Table C.6). We use the literature-derived average cone crop of an adult female ERC as a metric of number of cones (given a plant produced cones; Table 4.1). We used germination rates (from newly-produced cones and the seedbank) and first-year germinant survival rates derived from the literature (Table 4.1).

4.3.3 Modeling invasion

4.3.3.1 Model overview

We used an integrodifference equation model (IDE) to estimate invasion speed and quantify response of invasion speed to environmental drivers (Neubert and Caswell 2000, Neubert et al. 2000). This model includes an IPM and a dispersal kernel. We used the demographic rates described in the previous section to construct an age-structured IPM with multiple stages: trees of age 1 (first year germinants) through age 100, seedbank stage, and two cone classes: “bird cones” (cones which will be dispersed by birds) and “tree cones” (cones that will fall close to the tree). The age-structured part of the kernel had one year mesh points. We used the midpoint rule to approximate kernels and used bounds on the kernel reflective of observed age distributions.

We combined the IPM and the dispersal kernel into an IDE, where population dynamics are described as the combined effects of demography and dispersal across space and time:

$$n(x, t+1) = \int_{-\infty}^{+\infty} A_{n(y,t)} \circ K(x-y)\, n(y,t) dy \quad (1)$$

Here, $n(y,t)$ is the vector of individuals at location y and time t, $A_n(y,t)$ represents an IPM kernel, and $K(x-y)$ is the age-dependent dispersal kernel describing movement from y to x. Only individuals in the "bird cone" stage dispersed. We assumed that dispersal was exponential, using a relationship derived from previous work (Holthuijzen and Sharik 1985a). We used a Laplace transformation to generate a two-sided moment generating function $m(s)$; all other transitions were modeled as local (i.e., the moment generating function was a Dirac delta function). The format of these matrices is described in Appendix Figure C.4.

4.3.3.2 Invasion speed

We estimated invasion speed under multiple climate and management scenarios defined by combinations of fire return interval (2, 10, and 20 years), cattle presence (present or absent), mean annual temperature (cool: 9 °C; moderate: 10°C), and mean annual precipitation (moderate: 1100 mm; wet: 1200 mm). Within each scenario, precipitation, temperature, and cattle presence were held constant, while fire was represented as a periodic disturbance with a defined fire cycle of length p years.

We estimated the asymptotic invasion speed for each scenario following Caswell et al. (2011). In periodic environments, the combined effects of demography and dispersal over the p years of a fire cycle are captured by the periodic kernel $H_{per}(s) = H_1(s)H_2(s) \cdots H_\rho(s)$, where each year-specific kernel $H_i(s)$ is defined as the Hadamard product of the demographic matrix A_i and a matrix of moment-generating functions $M_i(s)$ (i.e., $H_i(s) = M_i(s) \circ A_i$).

The dominant eigenvalue of $H_{per}(s)$, denoted $\rho_{per}(s)$, describes the multiplicative effects of demography and dispersal over the cycle given s, the shape parameter of the Laplace distribution. The asymptotic invasion speed $c^*$is then given by:

$$c^* = \frac{1}{p} \min_{s>0} \left(\frac{1}{s} \log \rho_{per}(s) \right) \tag{2}$$

We evaluated this function over a range of s values (0 to 1/mean dispersal distance from Holthuijzen and Sharik 1985a). We generated confidence intervals on the c^* estimates by sampling from the posterior distributions of the survival function coefficients 500 times and recalculating invasion speed. We estimated the relative response of invasion speed to each driver (fire, climate, cattle presence) by quantifying the change in invasion speed effected by a given driver by iteratively changing one driver at a time, recalculating invasion speed, and calculating the change in invasion speed per unit change in a driver. For example, to quantify response of invasion speed to fire cycle length, we subtracted invasion speed under the shortest observed fire return interval ($c^*_{short\ FRI}$) from invasion speed under the longest observed fire return interval ($c^*_{long\ FRI}$) while holding cattle presence and climate conditions at constant values, to get the change in invasion speed Δc^*; namely, $c^*_{long\ FRI} - c^*_{short\ FRI}$. We then divided $\Delta c^*$by ΔFRI, the difference between the longest and shortest FRI (i.e., long FRI – short FRI), to estimate $\Delta c^*/\Delta FRI$, the change in invasion speed per unit change in FRI. Finally, we divided all $\Delta c^*/\Delta driver$ values by the mean invasion speed across all FRI, climate, and cattle scenarios for a particular draw from the posterior of the survival function coefficients. Dividing by the mean invasion speed in a draw allowed us to express driver effects as relative changes that were comparable across draws. For brevity, we show the overall effects of drivers under moderate climate conditions (1100 mm rainfall and 10 ºC temperatures).

4.3.4 Sensitivity to survival and fruiting

We evaluated the sensitivity of population growth rate to the probability of producing cones and survival via perturbation. Namely, we used the medians of the posterior distributions of parameters for the survival rate equation to parameterize the IPM kernel. Then, for each of our driver scenarios, we perturbed age-specific survival rates or fruiting rates by 5% and recalculated population growth rate, by multiplying the p-1 kernels together, obtaining the dominant eigenvalue from this kernel, and then taking the p-1'th root of this eigenvalue. This approach allowed us to compare the effect of probabilities survival and fruiting on population growth rate under different driver conditions. For brevity, we present here the sensitivity to survival and fruiting under moderate climate conditions (1100 mm rainfall and 10 ºC temperatures).

4.4 Results

4.4.1 Overall effects of drivers on survival and fruiting

The best-fit model for probability of fruiting included the effects of age, precipitation, mean annual temperature, and all 2-way interactions between these factors (Appendix Table C.7). The probability of fruiting for ERC increased with age ($\beta = 0.28 \pm 0.066$, $p < 0.001$), with greater precipitation ($\beta = 7.55 \pm 1.85$, $p < 0.001$, Appendix Table C.7) and with warmer temperatures ($\beta = 3.98 \pm 0.88$, $p < 0.001$, Appendix Table C.7). The positive effect of age on probability of fruiting was weaker under warmer temperatures ($\beta = -0.019 \pm 0.0043$, $p < 0.001$, Appendix Table C.7). However, the positive effect of age on probability of fruiting increased with greater precipitation ($\beta = 0.013 \pm 0.0067$, $p = 0.055$, Appendix Table C.7). Similarly, the positive effect of precipitation on probability of fruiting declined with greater temperatures (β = -

0.68 ± 0.15, p <0.001, Appendix Table C.7). As a result, under moderate climate conditions (10 °C temperature and 1100 mm precipitation), the model predicts lower fruiting probabilities earlier in life, followed by a steep increase in fruiting probability which levels off at 1 around age 35 (Figure 4.2A).

Survival probability of ERC increased with age and was strongly influenced by interactions among age, fire, grazing, and climatic factors (Figure 4.2B). Overall, the prior distributions of survival equation parameters indicated that survival increased with age (median $\beta = 0.097 \pm 0.0011$ SE), being low during early life stages and leveling off at older ages. Survival also increased with precipitation (median $\beta = 1.19 \pm 0.015$ SE), and this positive effect became stronger with age (median $\beta = 0.050 \pm 0.00052$ SE). Higher temperatures reduced survival (median $\beta = -1.54 \pm 0.029$ SE), but this negative effect weakened with increasing age (median $\beta = 0.049 \pm 0.00053$ SE). Fire had a strong negative effect on survival (median $\beta = -15.8 \pm 0.156$ SE), resulting in low predicted survival following a fire. Time since a burn occurred had a negative effect on survival (median $\beta = -0.693 \pm 0.02$ SE), and the quadratic effect of time since burn also had a negative effect on survival (median $\beta = -0.0072 \pm 0.00069$ SE). However, the negative effect of time since burn was weaker for older trees (median $\beta = 0.026 \pm 0.00079$ SE). Grazing effects on survival were context dependent. Although the main effect of grazing was positive (median $\beta = 10.9 \pm 0.15$ SE), grazing decreased survival with increasing time since burn (median $\beta = -0.61 \pm 0.014$ SE). Together, these effects produced an age-dependent survival pattern in which, under moderate climate conditions, younger individuals are on average less likely to survive a fire in the absence of cattle, are more likely to survive a fire in the presence of cattle, and experience positive effects of cattle in the years after a fire which decline with increasing time since burn (Figure 4.2B).

4.4.2 Sensitivity to survival and fruiting

Under ambient climate conditions, sensitivity of population growth (λ) to perturbations in vital rates varied with burn interval and cattle presence (Table 4.2). Across all scenarios, population growth was more sensitive to changes in survival than to changes in fruiting. In the presence of cattle, sensitivity to survival was highest with moderate fire intervals (10-year burn interval; sensitivity = 1.34), followed by infrequent fire intervals (20-year burn interval; sensitivity = 1.31), and lowest with frequent fire (2-year burn interval; sensitivity = 1.16). In the absence of cattle, however, sensitivity to survival declined with increasing fire frequency (Table 4.2). Sensitivity to fruiting was greater on average in the presence of cattle and declined with increasing fire frequency (Table 4.2).

4.4.3 Invasion speed

4.4.3.1 Overall invasion speed across scenarios

Mean invasion speed varied across climate and management scenarios (Figure 4.3). Across all scenarios, invasion speed was significantly higher in the absence of cattle (mean across scenarios = 405, 95% CI: 392–418; Figure 4.3A-D) compared to when cattle were present (mean across scenarios = 301, 95% CI: 289–313; Figure 4.3E-H).

Burn interval also influenced invasion speed, but the strength of burn treatments depended largely on cattle presence. Without cattle, invasion speed tended to be higher with less frequent fires, but 20- (mean across scenarios = 412, 95% CI: 389–434), 10- (mean across scenarios = 413, 95% CI: 390–436), and 2-year burn regimes (mean across scenarios = 390, 95% CI: 368–411; Figure 4.3A-D) did not significantly differ from one another. By contrast, in landscapes with cattle, burn interval was highest for the 20-year burn cycle (mean across scenarios = 355, 95% CI: 333–377), and lower but not significantly different for 10-year burn cycle (mean across scenarios = 314, 95% CI: 292–336). Finally, invasion speed was strongly reduced under 2-year burn cycles (mean across scenarios = 233, 95% CI: 214–251; Figure 4.3E-H).

Climate scenario also played a strong role in determining invasion speed. On average, invasion speeds were reduced under cooler temperatures (mean across scenarios = 347, 95% CI: 334–359; Figure 4.3A-B, E-F) compared to more moderate temperatures (mean across scenarios = 358, 95% CI: 346–371; Figure 4.3C-D, G-H), but these differences were not significant. Invasion speeds were significantly greater under moderate precipitation (mean across scenarios = 368, 95% CI: 355–380; Figure 4.3A,D,E,H) compared to wetter conditions (mean across scenarios = 338, 95% CI: 325–350; Figure 4.3B,C,F,G). Climate also interacted with other drivers, though these effects were largely non-significant. In the absence of cattle, frequent burns reduced invasion speeds more under cooler temperatures compared to warmer temperatures, though this difference was not significant (mean reduction due to frequent burns across scenarios under cooler temperatures= -5.07%, 95% CI: -9.1– -1.04; mean reduction under moderate temperatures = -1.28 %, 95% CI: -5.37-2.8). Similarly, frequent burns reduced invasion speeds slightly more under moderate precipitation compared to high precipitation, but this difference was not significant (mean reduction due to frequent burns across scenarios under moderate rainfall= -3.43%, 95% CI: -7.7– 0.842; mean reduction under higher rainfall = -2.92 %, 95% CI: -6.76-0.913). When cattle were present, frequent burns reduced invasion speeds more under cooler temperatures compared to warmer temperatures (mean reduction due to frequent burns across scenarios under cooler temperatures= -19.3%, 95% CI: -24.1– -14.6; mean reduction under moderate temperatures = -15.9%, 95% CI: -20.4– -11.4), but this difference was not significant. Frequent burns also reduced invasion speeds more under moderate precipitation compared to wetter conditions (mean reduction due to frequent burns across scenarios under moderate rainfall= -18.4%, 95% CI: -23.1– -13.7; mean reduction under higher rainfall = -16.9 %, 95% CI: -21.4– -12.3), and this difference was not significant.

4.4.3.2 Sensitivity of invasion speed to drivers

Under moderate climate conditions (1100 mm rainfall and 10 ºC temperatures), sensitivity of invasion speed to the addition of cattle was largely similar (not significantly different) across burn intervals (Figure 4.4A). The effect of cattle was negative, and negative effect of cattle on invasion speed was slightly stronger under 2-year burns (mean sensitivity across draws=-0.14 , 95% CI: -0.28– -0.032) compared to 10-year burns (mean sensitivity across draws=-0.109 , 95% CI: -0.20– -0.022) and 20-year burns (mean sensitivity across draws=-0.108 , 95% CI: -0.20– -0.019).

The effect of increasing temperatures on invasion speed varied depending on burn interval (Figure 4.4B). Greater temperatures tended to decrease invasion speeds under 10-year burn cycles, both with (mean sensitivity across draws=-0.18, 95% CI: -0.22– -0.13) and without cattle (mean sensitivity across draws=-0.10, 95% CI: -0.16– -0.046; Figure 4.4B); these effects did not differ depending on the presence of cattle. This negative effect held true under 20-year burn cycles as well, both with (mean sensitivity across draws=-0.13, 95% CI: -0.18– -0.069) and without cattle (mean sensitivity across draws=-0.10, 95% CI: -0.16– -0.047; Figure 4.4B), again, not varying depending on the presence of cattle. Under 2-year burn cycles, increasing temperatures did not significantly affect invasion speeds when cattle were present (mean sensitivity across draws=0.027, 95% CI: -0.043– 0.096). However, when cattle were absent, increasing temperatures significantly increased invasion speeds (mean sensitivity across draws=0.14, 95% CI: 0.071– 0.21; Figure 4.4B); due to overlapping confidence intervals, however, sensitivity to increasing temperatures did not differ significantly in the presence or absence of cattle. Overall, the confidence intervals for 10- and 20-year burn cycles overlapped, indicating similar sensitivity to increasing temperatures in these treatments. In contrast, the confidence intervals for 2-year burn cycles did not overlap with other burn cycles, indicating more positive sensitivity to temperature increases under frequent burning.

The effect of increasing precipitation on invasion speed was often weak but depended on burn cycle and cattle presence (Figure 4.4C). Under 2-year burn cycles, increasing precipitation did not affect invasion speeds, neither with (mean sensitivity across draws=0.036, 95% CI: -0.021– 0.093) nor without (mean sensitivity across draws=-0.020, 95% CI: -0.083– 0.044; Figure 4.4C) cattle. Under 10-year burn cycles, precipitation did not affect invasion speeds when cattle were absent (mean sensitivity across draws=0.033, 95% CI: -0.021– 0.087). However, when cattle were present, precipitation had positive effects on invasion speeds (mean sensitivity across draws=0.081, 95% CI: 0.038– 0.13; Figure 4.4C), though these effects did not differ significantly in the presence vs. absence of cattle. Finally, under 20-year burn cycles, precipitation significantly increased invasion speeds both with (mean sensitivity across draws=0.074, 95% CI: 0.022– 0.13) and without cattle (mean sensitivity across draws=0.057, 95% CI: 0.0034– 0.11; Figure 4.4C), and these effects did not differ significantly depending on cattle presence.

Under moderate climate conditions (1100 mm rainfall and 10 ºC temperatures), the effect of having more frequent burns on invasion speed was negative (Figure 4.4D). When cattle were present, having more frequent burns reduced invasion speeds (mean sensitivity across draws=-0.012, 95% CI: -0.017– -0.0066); similarly, having more frequent burns reduced invasion speeds when cattle were absent (mean sensitivity across draws=-0.0057, 95% CI: -0.011– -0.00072; Figure 4.4D). However, sensitivity did not differ significantly depending on the presence or absence of cattle. We caution that these results are preliminary, subject to change with improved modeling frameworks, and land managers should not use our predictions to inform management decisions.

4.5 Discussion

Understanding the processes that drive and constrain woody encroachment is critical for predicting where and how encroachment will occur and for developing effective management strategies. Our model demonstrates that woody encroachment of ERC is shaped by complex, demographically driven interactions among fire, grazing, and climate. As expected, fire frequency was a strong driver of invasion speed, with frequent burning slowing invasion speeds (Figure 4.4D). The presence of cattle contributed to these dynamics, leading to lower invasion speeds overall (Figure 4.4A), though they did not significantly change invasion speeds across different burn intervals. While fire and cattle exerted the most direct and consistent effects on invasion speed, climatic factors such as temperature and precipitation also influenced key demographic rates, modulated the strength of management effects, and contributed to variation in invasion speed outcomes. These findings highlight the importance of considering multiple drivers simultaneously, as their interactions can produce unexpected effects on encroachment.

Fire and cattle emerged as the most consistent drivers of invasion speed (Figure 4.3), producing negative effects regardless of other drivers. Frequent burns slowed invasions primarily by reducing survival, consistent with previous work showing that fire strongly limits the spread of ERC because it lacks the ability to resprout after topkill (Burns et al. 1990). These effects are most pronounced for young individuals, which are especially vulnerable to fire (Briggs et al. 2002) due to their smaller stature and thinner bark (Lawes et al. 2011). After burning, however, we saw that survival increased (Figure 4.2), potentially reflecting increases in recruitment following fires due to greater resource availability (Pausas and Keeley 2014). In contrast, cattle increased survival rates in the presence of burns (Figure 4.2). Higher survival during fires when cattle are present is driven by reduced fuel loads, which can decrease fire intensity (Briggs et al. 2002, 2005). Importantly, despite increasing survival in the presence of burns, the overall effect of cattle on invasion speeds was still negative regardless of fire interval (Figure 4.4A). This finding supports other studies which have found reduced survival of ERC in cattle presence, and may arise because of their ability to trample juvenile trees (Owensby et al. 1973, Schmidt and Stubbendieck 1993). Our results suggest that the reduction in fire intensity caused by grazing is insufficient to offset the broader negative effects of cattle on population dynamics. Together, these results suggest that both fire and grazing independently suppress ERC expansion, and their combined influence leads to slower ERC spread in frequently burned, grazed grasslands.

Climate played an important role in shaping vital rates. The production of cones in other coniferous species is influenced by environmental conditions (Bravo Oviedo et al. 2017, Chen et al. 2022), possibly due to greater resources in years with favorable climates (i.e., higher rainfall levels; Mutke et al. 2005) triggering masting events. ERC crops vary considerably from year to year for individual trees, though it is unclear whether the tree is considered a masting species (Holthuijzen and Sharik 1985b). Regardless, in our model, fruiting probability increased with greater precipitation and warmer temperatures, potentially because these conditions may lead to less resource limitation. Survival was similarly responsive to climate, for instance decreasing with temperature, and these effects were strongest for younger individuals. This pattern is consistent with other studies showing heat-related mortality disproportionately affecting early life stages of trees (Stevens-Rumann et al. 2022, Lalor et al. 2023). The strong negative effect of higher temperatures on survival was mirrored in sensitivity analyses, which showed that warming reduced invasion speeds when burning was infrequent (Figure 4.4B). In contrast, precipitation benefited survival in our model, though the actual effect of precipitation on invasion speeds was comparatively weak. Precipitation only consistently increased invasion speeds under 20-year burn cycles, or under 10-year burn cycles when cattle were present (Figure 4.4C). ERC is known to be highly drought tolerant due to its ability to resist embolism (Volder et al. 2010, Giddens 2021); thus, this weaker response may reflects the species' ability to maintain performance under a wide range of moisture conditions. Together, these results suggest that while precipitation exerts limited influence on ERC invasion speed, warming generally constrains population growth except under conditions of frequent fire where its effects may be offset.

Climate also modulated the strength of management effects on invasion. In both the presence and absence of cattle, burning more frequently slowed invasion (Figure 4.4D); although this effect tended to be stronger under cooler conditions (Figure 4.3), the difference in burn effectiveness across temperature conditions was not statistically significant. Sensitivity analyses further showed that under frequent burns without cattle, increasing temperatures tended to accelerate invasion speeds (Figure 4.4B), suggesting that warming reduces the effectiveness of fire as a control mechanism. These patterns aligns with previous work showing that in grasslands, the efficacy of fires is dependent on the amount of available fuel (Briggs et al. 2005, Krawchuk and Moritz 2011). In hotter environments, where grass productivity may be limited, we might expect fuel loads to be generally lower, so fires are less effective at slowing encroachment. By comparison, greater precipitation had no significant effect on invasion speeds under frequent burns (Fig. 4.4C). Other studies have shown that precipitation may affect fuel conditions: dry periods can increase fire efficacy because drier vegetation is more flammable

(Stavi 2019). Critically, however, dry conditions may also reduce fuel availability if grass productivity declines, thereby limiting how much fire can suppress woody encroachment (Liu et al. 2013). Thus, the lack of a consistent precipitation effect under frequent burns may reflect the variable influence of precipitation on both flammability and fuel availability across sites.

Several limitations of our modeling approach should be considered when interpreting these results. First, model predictions are constrained by the range of site conditions and tree densities represented in our data, which limits the ability to extrapolate to areas with substantially different environmental or demographic contexts. Second, while the model focused on key drivers such as climate, fire, and cattle, other unmeasured factors, such as soil properties, competition from other species, or topography (i.e., the slope/aspect of a site), may also influence invasion dynamics. Second, we modeled invasion speed under constant climate scenarios, whereas in reality, both the mean and variability of climate are expected to shift under climate change, potentially altering the relative importance of different drivers. Third, multiple vital rates were obtained from literature rather than directly from the study system, and these rates likely vary across environmental gradients and population densities. Finally, we emphasize that this analysis represents a work in progress; the model is still being refined, and additional validation is underway, so results should be interpreted as extremely provisional projections rather than as definitive predictions.

Our findings demonstrate that woody encroachment is governed by dynamic and interacting demographic processes that are strongly shaped by fire, grazing, and climate. Frequent fire emerged as the most consistent mechanism in decreasing invasion speeds due to its strong effects on survival. Cattle limited invasion speeds, despite positive effects on survival during burns. Climate further shaped these interactions, with warmer temperatures reducing invasion speeds when fires were infrequent but increasing invasion speeds when fires were frequent and cattle absent. In contrast, precipitation effects on invasion speeds were positive but comparatively weak, reflecting both ERC's high drought tolerance and the variable influence of moisture on fuel accumulation and fire behavior. Collectively, these results indicate that no single factor drives invasion trajectories; rather, ERC expansion is regulated by the combined and context-dependent influences of management and climate. Anticipating and managing future encroachment therefore requires an integrated approach that explicitly considers how changing climate conditions will interact with fire and grazing regimes to shape demographic processes.

4.6 Tables

Table 4.1. Vital rates collected from literature to parameterize population model of ERC. Symbol indicates the abbreviation used for the rate indicated in the life cycle diagram (Figure 4.1).

Vital rate	**Source**	**Value**	**Symbol**
Average cone crop of an adult tree (averaged across high and low fecundity years)	(Holthuijzen and Sharik 1985b)	805,000	C
Proportion of cones which will be dispersed by birds	(Holthuijzen et al. 1987)	0.653	R_{bird}
Proportion of cones which will be dispersed by gravity (near tree)	(Holthuijzen et al. 1987)	0.116	R_{tree}
Germination rate (if bird-dispersed)	(Holthuijzen and Sharik 1985b)	0.413	Gr_{b}
Germination rate (if not bird-dispersed)	(Afanasiev and Cress 1942)	0.1	Gr_{nb}
Rate at which seeds germinate from the seedbank	(Holthuijzen and Sharik 1984)	0.055	Gr_{sb}
Spring-Summer survival of germinants	(Walton 2020)	0.8545	Sr_{seed}

Table 4.2. Sensitivity of population growth rate to survival and fruiting rates under moderate climate conditions (1100 mm rainfall and 10 ºC temperatures). Sensitivity assessed by perturbing a rate by 5% while holding others constant and assessing the proportional change in population growth.

Rate	Cattle Presence/Absence	Burn interval	Sensitivity
Fruiting	With Cattle	20-year	0.054
Fruiting	With Cattle	10-year	0.062
Fruiting	With Cattle	2-year	0.034
Fruiting	Without Cattle	20-year	0.023
Fruiting	Without Cattle	10-year	0.013
Fruiting	Without Cattle	2-year	0.0072
Survival	With Cattle	20-year	1.31
Survival	With Cattle	10-year	1.34
Survival	With Cattle	2-year	1.16
Survival	Without Cattle	20-year	1.06
Survival	Without Cattle	10-year	0.977
Survival	Without Cattle	2-year	0.705

4.7 Figures

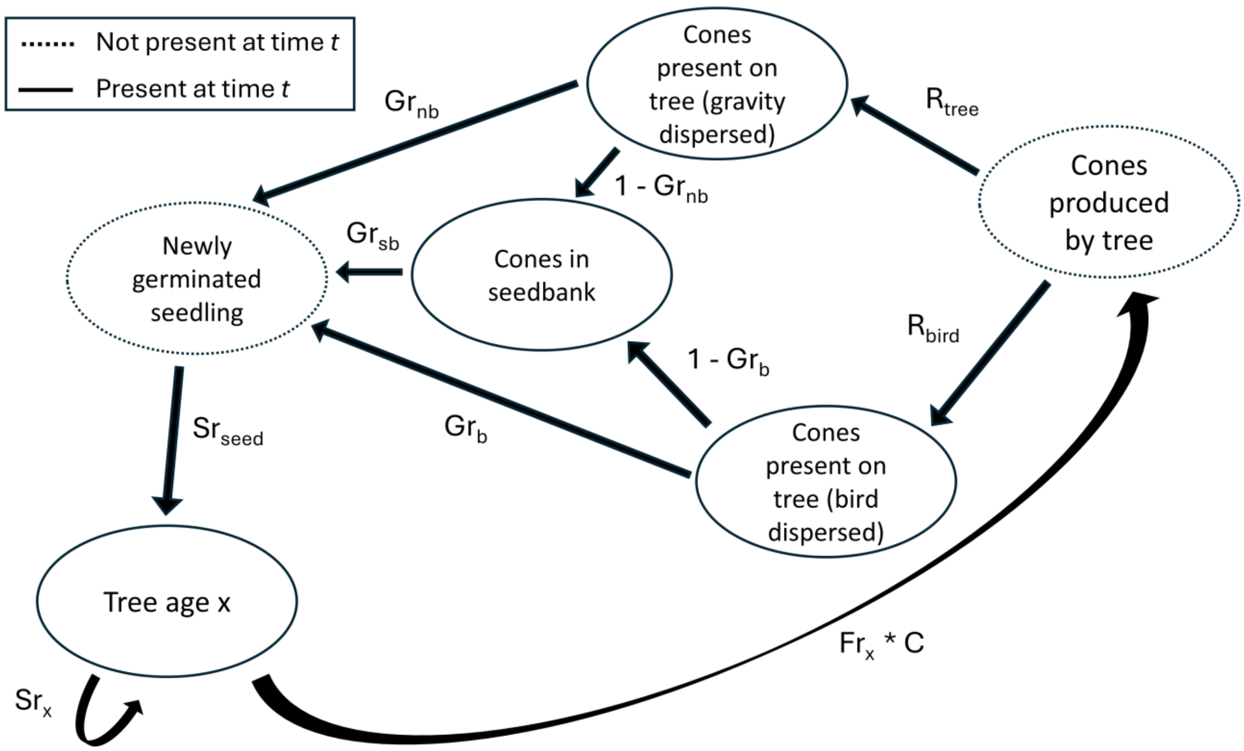

Figure 4.1. Conceptual life cycle of ERC as represented in the invasion speed model. Solid bubbles represent states present during *t*, while dotted bubbles represent transient states not present during *t*. At each timestep *t*, trees of age *x* may survive at age-specific rates (Sr_x) and reproduce at rates (Fr_x), producing cone crops of size *C* (total cones = Fr_x*C). Cones produced by trees (dotted state, not present during *t*) enter either the gravity-dispersed (R_{tree}) or bird-dispersed (R_{bird}) cone pools (solid states, present during *t*) immediately. Cones in these pools may germinate (Gr_{nb} for gravity-dispersed; Gr_b for bird-dispersed), passing through the "newly germinated seedling" state (dotted, not present during *t*) and then survive as seedlings (Sr_{seed}) to recruit into the age-structured tree population by the following timestep. Alternatively, cones may enter the seed bank (present during *t*) with probabilities $1 – Gr_{nb}$ and $1 – G_{rb}$. Seeds in the seed bank germinate at rate Gr_{sb}.

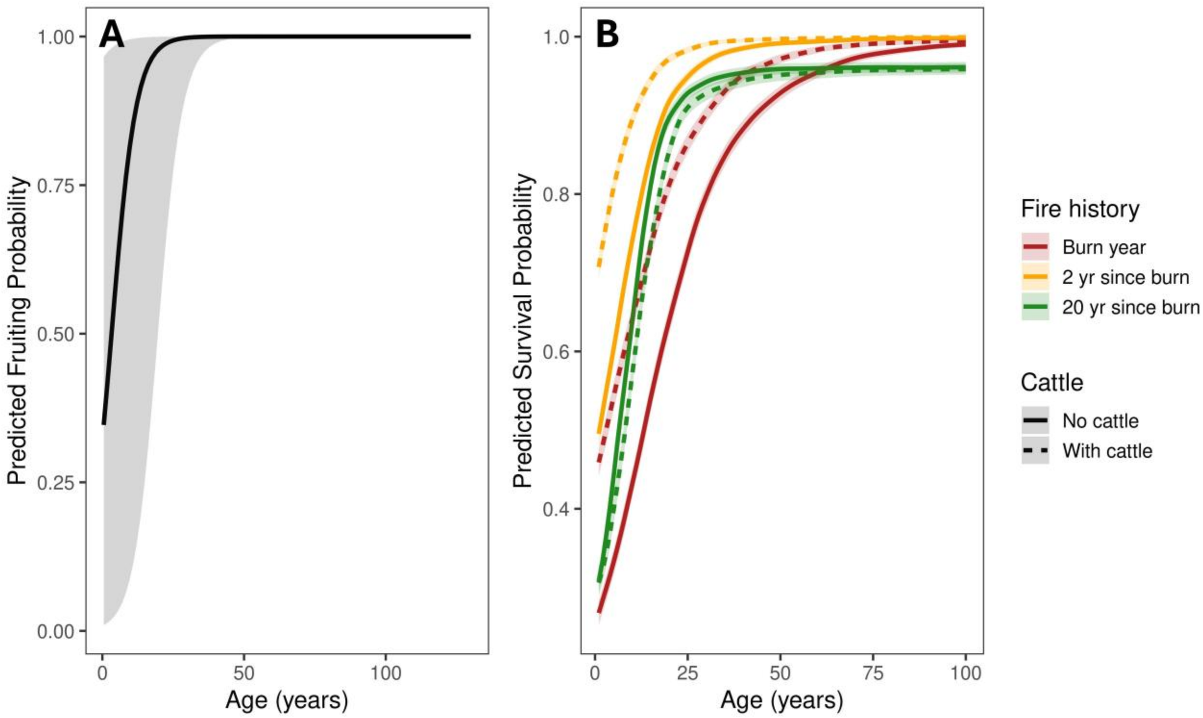

Figure 4.2. Predicted fruiting and survival probability across age under moderate climate conditions (1100 mm rainfall and 10 ºC temperatures). (A) Predicted probability of fruiting as a function of age under moderate climate conditions. Fruiting probabilities were estimated from a binomial generalized linear model fit to empirical fruiting data. Lines indicate mean predicted values and shaded ribbons represent 95% confidence intervals. (B) Predicted survival probability across age, estimated using all posterior draws from the fitted survival model. Line colors indicate fire treatment (with red representing a burn-year, yellow representing 2 years since burn, and green representing 20 years since burn), and line type distinguishes grazing treatments (with vs. without cattle as dashed and solid respectively). Shaded ribbons represent 95% confidence intervals.

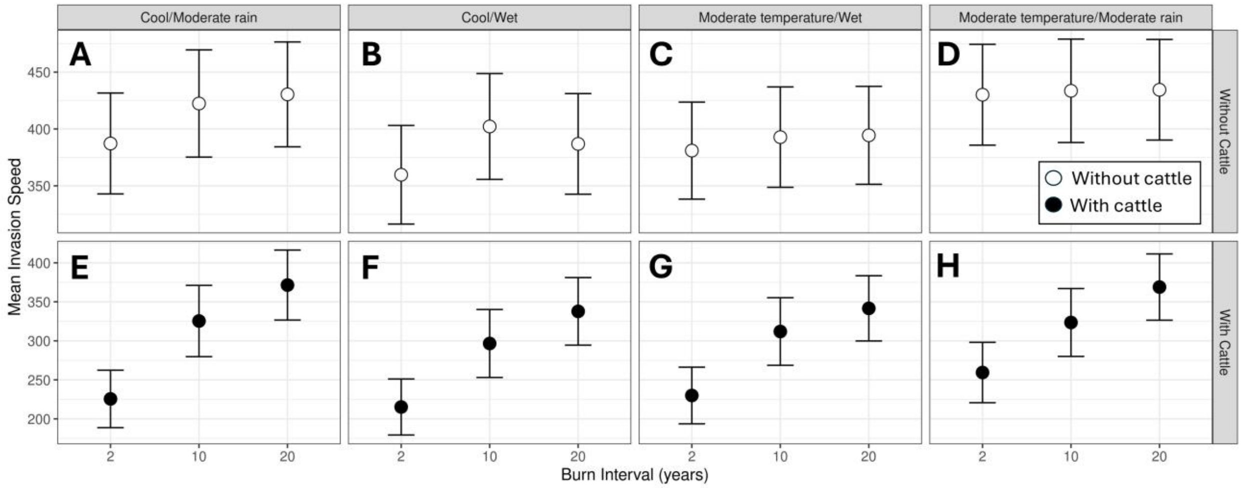

Figure 4.3. Median invasion speed ($\bar{c}_p$) across burn interval, temperature, and rainfall scenarios with and without cattle grazing. Invasion speeds were estimated using posterior draws from the fitted survival equation to propagate uncertainty in survival rates. Bars represent median predicted invasion speeds across simulations, and error bars 95% confidence intervals. Panels show the four climate scenarios (columns) crossed with grazing treatments (rows): A–D illustrate invasion dynamics in the absence of cattle, and E–H in the presence of cattle. Burn interval treatments (2, 10, and 20 years) are displayed on the x-axis.

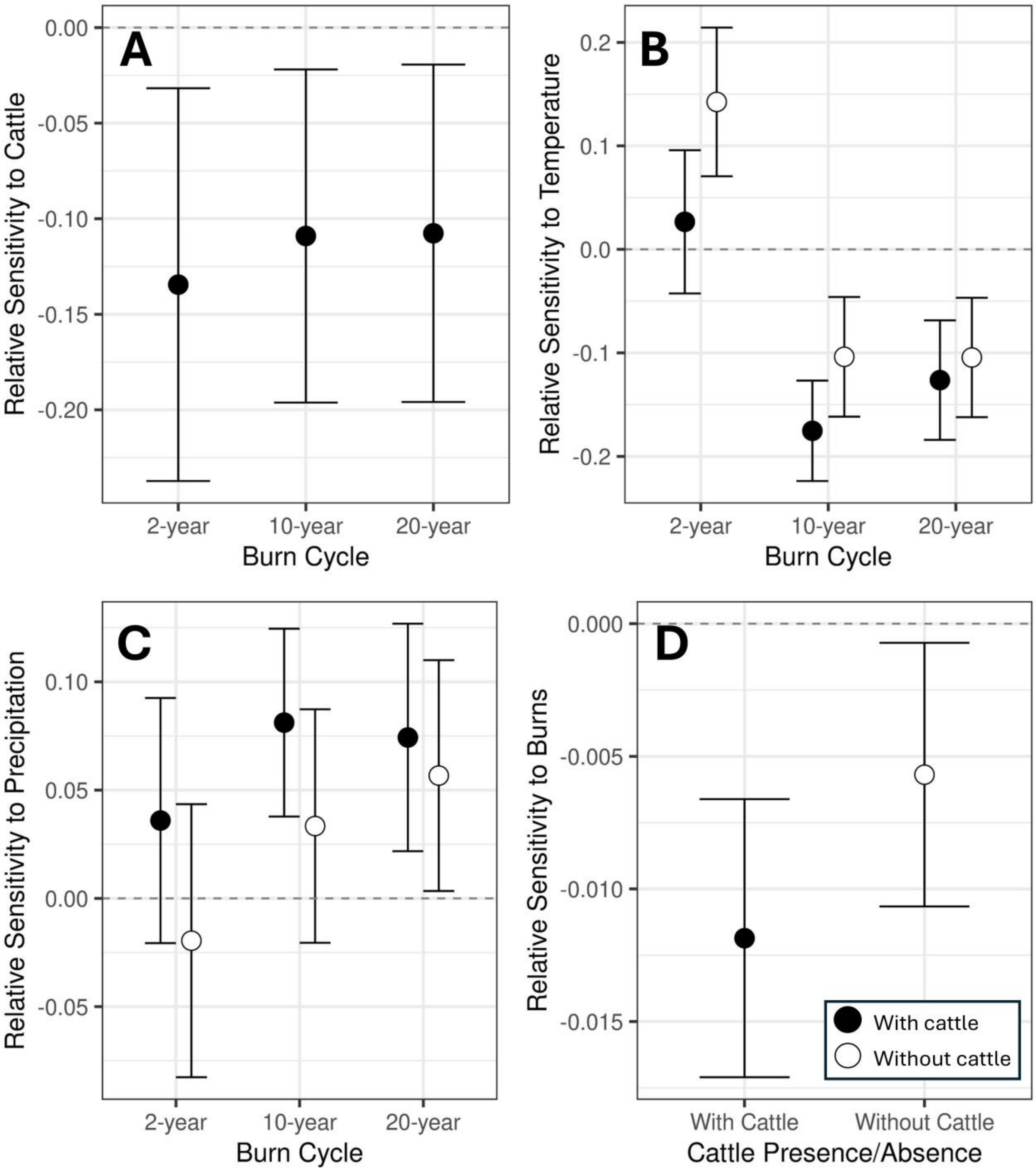

Figure 4.4. Sensitivity of invasion speed ($\bar{c}_p$) to changes in drivers. Panels show the mean sensitivity of $\bar{c}_p$ to changes in (A) cattle presence, (B) temperature, (C) precipitation, and (D) burn interval. Sensitivities were calculated using parameter draws from the posterior distribution of survival, with all other drivers held constant. For each posterior iteration, sensitivity was

estimated as the proportional change in $\bar{c}_p$ over the range of each driver (e.g., presence vs. absence of cattle, 10–9 °C temperature, 1200–1100 mm for precipitation, and 20–2 year burn intervals for fire). Points indicate mean sensitivity across iterations, and error bars represent 95% CIs. Positive values indicate that increasing the driver increases $\bar{c}_p$ (faster spread), whereas negative values indicate slower spread. Dashed horizontal lines at zero denote no effect. Sensitivities are shown under moderate climate conditions (1100 mm rainfall and 10 °C temperature); if assessing the sensitivity to one climatic variable, the other was held at its moderate value.

Chapter 5 - Conclusions

Invasive species are one of the leading causes of biodiversity loss globally and under future climate scenarios, their influence is expected to intensify, driving profound and irreversible changes in ecosystem structure and function (Mainka and Howard 2010, Early et al. 2016b, Catford and Jones 2019, Hald-Mortensen 2023). However, the ecological impacts of invasive species are far from uniform; instead, they are highly context-dependent, with outcomes varying across a range of abiotic factors (e.g., temperature, precipitation, nutrient levels) as well as across biotic contexts, including the degree of competition with native species (Shannon-Firestone and Firestone 2015, Sapsford et al. 2020, Catford et al. 2022). Moreover, the demographic performance of invasive species (including their growth, reproduction, and survival) can vary widely across sites, being influenced by both climate conditions, biotic interactions, and the effectiveness of different management strategies (Buckley et al. 2003, Biswas et al. 2015). This variability makes it challenging to reliably predict how invasive species will spread and what impacts they will have in future climates.

In Chapter 2, I used data from a large-scale herbivore exclusion experiment along a rainfall gradient in central Kenya to test how large mammalian herbivores influence demographic compensation in *Hibiscus meyeri*. Demographic compensation occurs when vital rates vary in opposing directions across space, such that increases in some rates offset declines in others, buffering changes in population growth across a species' range (Villellas et al. 2015). Using integral projection models built from multi-year demographic data, I quantified how herbivory influenced vital rates along an environmental gradient, and how correlations between vital rates changed with varying levels of herbivore exclusion. I found that demographic compensation driven by negative correlations among demographic rates was absent when all large herbivores were present, but emerged when megaherbivores were excluded. This shift was driven by herbivore-induced changes in the variability of vital rates across sites, which decreased the total number of significant correlations between vital rates. These findings demonstrate that large herbivores can play a powerful role in shaping the demographic mechanisms underlying population stability across environmental gradients. More broadly, this work suggests that commonly observed patterns such as demographic compensation (Doak and Morris 2010, Yang et al. 2022) may have been less prevalent when megafaunal communities were intact.

In Chapter 3, I examined how the effects of invasive competitors on demographic rates of native C_4 bunchgrasses in the Great Plains are influenced by abiotic context. Using a factorial design combining rainfall manipulation and *Bromus inermis* removal, I measured seed germination and plug survival across multiple native species to evaluate whether invader effects were context dependent. Both drought and high brome competition reduced native plug survival, but their effects were largely additive rather than interactive. By contrast, invader impacts on germination were context dependent: brome presence had no effect on germination under ambient rainfall but reduced germination under drought, indicating that invader effects can shift with abiotic context. These findings indicate that context dependence may be strongest during early life stages, such as at the germinant stage. This pattern aligns with previous research showing greater variability in performance among younger life stages of plants due to vulnerability to stress (Eriksson and Ehrlén 2008, Gross and Mackay 2014). Collectively, this work demonstrates that restoration outcomes depend not only on invader density but also on climatic conditions and life stage, underscoring the importance of restoration strategies that explicitly integrate both competitive and environmental contexts.

In Chapter 4, I utilized a demographic model to estimate how fire, grazing, and climate interact to influence the invasion speed of *Juniperus virginiana* across the Great Plains. Using a combination of field-derived and literature-derived demographic rates, I developed a spatially-explicit demographic model which predicts invasion speed under varying fire regimes, cattle presence, and climatic conditions. Model results revealed interactions among drivers: frequent fires consistently slowed invasion, and the negative effects of cattle increased this effect on invasion speed. Moreover, the efficacy of fire management depended on climate: cooler, wetter conditions amplified the slowing effect of fire, whereas warmer or drier conditions reduced it. This pattern aligns with fire ecology theory, which predicts that in already-dry ecosystems like grasslands, fire intensity will be limited in more arid environments due to decreased fuel availability (Krawchuk and Moritz 2011). Together, these findings demonstrate that no single management intervention can effectively constrain woody encroachment across all contexts. Instead, coordinated fire and grazing management strategies that explicitly account for climatic variability are needed to curb invasion rates and sustain grassland ecosystems.

Together, the chapters of this dissertation advance our understanding of invasion ecology by demonstrating that the demographic processes underlying invasion and encroachment are inherently context dependent and shaped by interactions among climate, biotic pressures, and management regimes. By integrating experimental, observational, and modeling approaches across multiple systems, this work illustrates that the outcomes of invasion are not fixed but emerge from the dynamic interplay between environmental conditions and species' demographic responses. In an increasingly globalized world where species introductions and range shifts are all but inevitable (van Kleunen et al. 2015, Early et al. 2016b, Pyšek et al. 2020), these findings underscore the importance of moving beyond static, one-size-fits-all management frameworks toward adaptive strategies that account for variability across space, time, and life stage. Effective management in this era will require acknowledging that invasions cannot always be prevented, but their impacts can be mitigated through flexible, evidence-based approaches that respond to ecological context.

References

Afanasiev, M. M., and M. Cress. 1942. Producing seedlings of eastern red cedar (Juniperus virginiana L.). Oklahoma Agricultural and Mechanical College, Agricultural Experiment Station, Stillwater, Okla.

Albertson, F. W., and J. E. Weaver. 1946. Reduction of Ungrazed Mixed Prairie to Short Grass as a Result of Drought and Dust. Ecological Monographs 16:449–463.

Anderson, R. C., E. A. Corbett, M. R. Anderson, G. A. Corbett, and T. M. Kelley. 2001. High White-Tailed Deer Density Has Negative Impact on Tallgrass Prairie Forbs. The Journal of the Torrey Botanical Society 128:381–392.

Archer, S. 1994a. Woody plant encroachment in southwestern grasslands and savannas: rates, patterns, and proximate causes. Pages 13–68 Ecological implications of livestock herbivory in the West. Society for Range Management, Denver, CO.

Archer, S. 1994b. Woody plant encroachment in southwestern grasslands and savannas: rates, patterns, and proximate causes. Pages 13–68 Ecological implications of livestock herbivory in the West. Society for Range Management, Denver, CO.

Archer, S. R., E. M. Andersen, K. I. Predick, S. Schwinning, R. J. Steidl, and S. R. Woods. 2017. Woody Plant Encroachment: Causes and Consequences. Pages 25–84 *in* D. D. Briske, editor. Rangeland Systems: Processes, Management and Challenges. Springer International Publishing, Cham.

Bakker, E. S., M. E. Ritchie, H. Olff, D. G. Milchunas, and J. M. H. Knops. 2006. Herbivore impact on grassland plant diversity depends on habitat productivity and herbivore size. Ecology Letters 9:780–788.

Barrat-Segretain, M.-H. 2005. Competition between Invasive and Indigenous Species: Impact of Spatial Pattern and Developmental Stage. Plant Ecology 180:153–160.

Beguería, S., S. M. Vicente Serrano, and M. Angulo-Martínez. 2010. A Multiscalar Global Drought Dataset: The SPEIbase: A New Gridded Product for the Analysis of Drought Variability and Impacts.

Bertness, M. D., and R. Callaway. 1994. Positive interactions in communities. Trends in Ecology & Evolution 9:191–193.

Bieberich, J., M. Lauerer, M. Drachsler, J. Heinrichs, S. Müller, and H. Feldhaar. 2018a. Species- and developmental stage-specific effects of allelopathy and competition of invasive Impatiens glandulifera on co-occurring plants. PLOS ONE 13:e0205843.

Bieberich, J., M. Lauerer, M. Drachsler, J. Heinrichs, S. Müller, and H. Feldhaar. 2018b. Species- and developmental stage-specific effects of allelopathy and competition of invasive Impatiens glandulifera on co-occurring plants. PLOS ONE 13:e0205843.

Bishop, T. B. B., A. Barnes, B. C. Nusink, and S. B. St. Clair. 2024. Earlier fall precipitation increases the competitive advantage of non-native plant communities in a desert ecosystem. Biological Invasions 26:719–731.

Biswas, S. R., P. M. Kotanen, D. Kambo, and H. H. Wagner. 2015. Context-dependent patterns, determinants and demographic consequences of herbivory in an invasive species. Biological Invasions 17:165–178.

Bradley, B. A., C. A. Curtis, E. J. Fusco, J. T. Abatzoglou, J. K. Balch, S. Dadashi, and M.-N. Tuanmu. 2018. Cheatgrass (Bromus tectorum) distribution in the intermountain Western United States and its relationship to fire frequency, seasonality, and ignitions. Biological Invasions 20:1493–1506.

Bravo Oviedo, F., D. A. Maguire, and S. C. González Martínez. 2017. Factors affecting cone production in Pinus pinaster Ait.: lack of growth-reproduction trade-offs but significant effects of climate and tree and stand characteristics.

Briggs, J. M., G. A. Hoch, and L. C. Johnson. 2002. Assessing the Rate, Mechanisms, and Consequences of the Conversion of Tallgrass Prairie to Juniperus virginiana Forest. Ecosystems 5:578–586.

Briggs, J. M., A. K. Knapp, J. M. Blair, J. L. Heisler, G. A. Hoch, M. S. Lett, and J. K. McCarron. 2005. An Ecosystem in Transition: Causes and Consequences of the Conversion of Mesic Grassland to Shrubland. BioScience 55:243–254.

Broderick, C. M., K. Wilkins, M. D. Smith, and J. M. Blair. 2022. Climate legacies determine grassland responses to future rainfall regimes. Global Change Biology 28:2639–2656.

Buckley, Y. M., D. T. Briese, and M. Rees. 2003. Demography and management of the invasive plant species Hypericum perforatum. II. Construction and use of an individual-based model to predict population dynamics and the effects of management strategies. Journal of Applied Ecology 40:494–507.

Bunn, A. G. 2008. A dendrochronology program library in R (dplR). Dendrochronologia 26:115–124.

Burkepile, D. E., R. W. S. Fynn, D. I. Thompson, N. P. Lemoine, S. E. Koerner, S. Eby, N. Hagenah, K. R. Wilcox, S. L. Collins, K. P. Kirkman, A. K. Knapp, and M. D. Smith. 2017. Herbivore size matters for productivity–richness relationships in African savannas. Journal of Ecology 105:674–686.

Burnham, K. P., and D. R. Anderson. 2002. Model Selection and Multimodel Inference: A Practical Information-Theoretic Approach. Springer-Verlag.

Burns, R. M., B. H. Honkala, and T. Coordinators. 1990. Silvics of North America: Volume 1. Conifers. United States Department of Agriculture (USDA), Forest Service, Agriculture Handbook 654.

Callaway, R. M., R. W. Brooker, P. Choler, Z. Kikvidze, C. J. Lortie, R. Michalet, L. Paolini, F. I. Pugnaire, B. Newingham, E. T. Aschehoug, C. Armas, D. Kikodze, and B. J. Cook. 2002. Positive interactions among alpine plants increase with stress. Nature 417:844–848.

Caswell, H., M. G. Neubert, and C. M. Hunter. 2011. Demography and dispersal: invasion speeds and sensitivity analysis in periodic and stochastic environments. Theoretical Ecology 4:407–421.

Catford, J. A., and L. P. Jones. 2019. Grassland invasion in a changing climate. Pages 149–171 *in* D. J. Gibson and J. A. Newman, editors. Grasslands and Climate Change. First edition. Cambridge University Press.

Catford, J. A., J. R. U. Wilson, P. Pyšek, P. E. Hulme, and R. P. Duncan. 2022. Addressing context dependence in ecology. Trends in Ecology & Evolution 37:158–170.

Chase, J. M., M. A. Leibold, A. L. Downing, and J. B. Shurin. 2000. The Effects of Productivity, Herbivory, and Plant Species Turnover in Grassland Food Webs. Ecology 81:2485–2497.

Chen, X., J. L. Willis, and K. A. Bowman. 2022. Assessing the influence of climate on cone production of longleaf pine forests. Trees, Forests and People 9:100297.

Clout, M. N., and P. A. Williams. 2009. Invasive Species Management: A Handbook of Principles and Techniques. Oxford University Press.

Comer, P. J., J. C. Hak, and E. Seddon. 2022. Documenting at-risk status of terrestrial ecosystems in temperate and tropical North America. Conservation Science and Practice 4:e603.

Connell, J. H. 1972. Community Interactions on Marine Rocky Intertidal Shores. Annual Review of Ecology and Systematics 3:169–192.

Crawley, M. J. 1989. Insect Herbivores and Plant Population Dynamics. The Annual Review of Entomology 34:531–564.

Cristiano, P. M., G. Posse, C. M. Di Bella, and T. Boca. 2012. Influence of contrasting availabilities of water and nutrients on the radiation use efficiency in C3 and C4 grasses. Austral Ecology 37:323–329.

Cully, A. C., J. F. Cully Jr., and R. D. Hiebert. 2003. Invasion of Exotic Plant Species in Tallgrass Prairie Fragments. Conservation Biology 17:990–998.

Cyr, H., and M. L. Face. 1993. Magnitude and patterns of herbivory in aquatic and terrestrial ecosystems. Nature 361:148–150.

Daco, L., G. Colling, and D. Matthies. 2021. Altitude and latitude have different effects on population characteristics of the widespread plant *Anthyllis vulneraria*. Oecologia 197:537–549.

Daehler, C. C. 2003. Performance Comparisons of Co-Occurring Native and Alien Invasive Plants: Implications for Conservation and Restoration. Annual Review of Ecology, Evolution, and Systematics 34:183–211.

Daubenmire, R. 1968. Ecology of Fire in Grasslands. Advances in Ecological Research 5:209–266.

Davies, A. B., and G. P. Asner. 2019. Elephants limit aboveground carbon gains in African savannas. Global Change Biology 25:1368–1382.

Doak, D. F., and W. Morris. 1999. Detecting Population-Level Consequences of Ongoing Environmental Change Without Long-Term Monitoring. Ecology 80:1537–1551.

Doak, D. F., and W. F. Morris. 2010. Demographic compensation and tipping points in climate-induced range shifts. Nature 467:959–962.

Doak, D. F., E. Waddle, R. E. Langendorf, A. M. Louthan, N. Isabelle Chardon, R. R. Dibner, D. A. Keinath, E. Lombardi, C. Steenbock, R. K. Shriver, C. Linares, M. Begoña Garcia, W. C. Funk, S. W. Fitzpatrick, W. F. Morris, and M. L. DeMarche. 2021. A critical comparison of integral projection and matrix projection models for demographic analysis. Ecological Monographs 91:e01447.

Dobzhansky, T. 1950. Evolution in the Tropics. American Scientist 38:209–221.

Doust, J. L., and L. L. Doust. 1988. Plant Reproductive Ecology: Patterns and Strategies. Oxford University Press.

Doust, S. J. 2011. Seed Removal and Predation as Factors Affecting Seed Availability of Tree Species in Degraded Habitats and Restoration Plantings in Rainforest Areas of Queensland, Australia. Restoration Ecology 19:617–626.

Dudley, S. A. 1996. The Response to Differing Selection on Plant Physiological Traits: Evidence for Local Adaptation. Evolution 50:103–110.

Dyer, L. A., D. K. Letourneau, G. V. Chavarria, and D. S. Amoretti. 2010. Herbivores on a dominant understory shrub increase local plant diversity in rain forest communities. Ecology 91:3707–3718.

Early, R., B. A. Bradley, J. S. Dukes, J. J. Lawler, J. D. Olden, D. M. Blumenthal, P. Gonzalez, E. D. Grosholz, I. Ibañez, L. P. Miller, C. J. B. Sorte, and A. J. Tatem. 2016a. Global threats from invasive alien species in the twenty-first century and national response capacities. Nature Communications 7:12485.

Early, R., B. A. Bradley, J. S. Dukes, J. J. Lawler, J. D. Olden, D. M. Blumenthal, P. Gonzalez, E. D. Grosholz, I. Ibañez, L. P. Miller, C. J. B. Sorte, and A. J. Tatem. 2016b. Global threats from invasive alien species in the twenty-first century and national response capacities. Nature Communications 7:12485.

Eckhoff, K. D., D. A. Scott, G. Manning, and S. G. Baer. 2023. Persistent decadal differences in plant communities assembled under contrasting climate conditions. Ecological Applications 33:e2823.

Ellis-Felege, S. N., C. S. Dixon, and S. D. Wilson. 2013. Impacts and management of invasive cool-season grasses in the Northern Great Plains: Challenges and opportunities for wildlife. Wildlife Society Bulletin 37:510–516.

Eriksson, O., and J. Ehrlén. 2008. Seedling recruitment and population ecology. Pages 239–254 *in* M. A. Leck, R. L. Simpson, and V. T. Parker, editors. Seedling Ecology and Evolution. Cambridge University Press, Cambridge.

Eskelinen, A., and S. Harrison. 2014. Exotic plant invasions under enhanced rainfall are constrained by soil nutrients and competition. Ecology 95:682–692.

Evans, R. D., R. Rimer, L. Sperry, and J. Belnap. 2001. Exotic plant invasion alters nitrogen dynamics in an arid grassland. Ecological Applications 11:1301–1310.

Fay, P. A., J. M. Blair, M. D. Smith, J. B. Nippert, J. D. Carlisle, and A. K. Knapp. 2011. Relative effects of precipitation variability and warming on tallgrass prairie ecosystem function. Biogeosciences 8:3053–3068.

Fick, S. E., and R. J. Hijmans. 2017. WorldClim 2: new 1-km spatial resolution climate surfaces for global land areas. International Journal of Climatology 37:4302–4315.

Fogarty, D. T., R. B. Peterson, and D. Twidwell. 2022. Spatial patterns of woody plant encroachment in a temperate grassland. Landscape Ecology 37:2835–2846.

Frost, J. S., and L. A. Powell. 2011. Cedar Infestation Impacts Avian Communities along the Niobrara River Valley, Nebraska. Restoration Ecology 19:529–536.

Fuhlendorf, S. D., S. A. Archer, F. Smeins, D. M. Engle, and C. A. Taylor. 2008. The Combined Influence of Grazing, Fire, and Herbaceous Productivity on Tree–Grass Interactions. Pages 219–238 *in* O. W. Van Auken, editor. Western North American Juniperus Communities: A Dynamic Vegetation Type. Springer, New York, NY.

Fusco, E. J., J. T. Finn, J. K. Balch, R. C. Nagy, and B. A. Bradley. 2019. Invasive grasses increase fire occurrence and frequency across US ecoregions. Proceedings of the National Academy of Sciences 116:23594–23599.

Gaertner, M., R. Biggs, M. Te Beest, C. Hui, J. Molofsky, and D. M. Richardson. 2014. Invasive plants as drivers of regime shifts: identifying high-priority invaders that alter feedback relationships. Diversity and Distributions 20:733–744.

Gallagher, M. K., and S. Wagenius. 2016. Seed source impacts germination and early establishment of dominant grasses in prairie restorations. Journal of Applied Ecology 53:251–263.

Galliart, M., N. Bello, M. Knapp, J. Poland, P. St Amand, S. Baer, B. Maricle, A. B. Smith, and L. Johnson. 2019. Local adaptation, genetic divergence, and experimental selection in a foundation grass across the US Great Plains' climate gradient. Global Change Biology 25:850–868.

Garbowski, M., D. B. Johnston, D. V. Baker, and C. S. Brown. 2021. Invasive annual grass interacts with drought to influence plant communities and soil moisture in dryland restoration. Ecosphere 12:e03417.

Garcia, L. C., and M. D. Eubanks. 2019. Overcompensation for insect herbivory: a review and meta-analysis of the evidence. Ecology 100:e02585.

García-Camacho, R., M. J. Albert, and A. Escudero. 2012. Small-scale demographic compensation in a high-mountain endemic: the low edge stands still. Plant Ecology & Diversity 5:37–44.

Gaskin, J. F., E. Espeland, C. D. Johnson, D. L. Larson, J. M. Mangold, R. A. McGee, C. Milner, S. Paudel, D. E. Pearson, L. B. Perkins, C. W. Prosser, J. B. Runyon, S. E. Sing, Z. A. Sylvain, A. J. Symstad, and D. R. Tekiela. 2021. Managing invasive plants on Great Plains grasslands: A discussion of current challenges. Rangeland Ecology & Management 78:235–249.

Gibbons, S. M., Y. Lekberg, D. L. Mummey, N. Sangwan, P. W. Ramsey, and J. A. Gilbert. 2017a. Invasive Plants Rapidly Reshape Soil Properties in a Grassland Ecosystem. mSystems 2:e00178-16.

Gibbons, S. M., Y. Lekberg, D. L. Mummey, N. Sangwan, P. W. Ramsey, and J. A. Gilbert. 2017b. Invasive Plants Rapidly Reshape Soil Properties in a Grassland Ecosystem. mSystems 2:10.1128/msystems.00178-16.

Gibson, D. J., and L. C. Hulbert. 1987. Effects of Fire, Topography and Year-to-Year Climatic Variation on Species Composition in Tallgrass Prairie. Vegetatio 72:175–185.

Giddens, J. 2021. THE EFFECTS OF PRECIPITATION, TREE SIZE, AND STAND DENSITY ON WATER USE AND DROUGHT TOLERANCE OF EASTERN REDCEDAR IN OKLAHOMA, USA. University of Oklahoma Graduate Thesis.

Gilman, E. F., and D. G. Watson. 1993, November. *Juniperus virginiana* Eastern Redcedar USFS Factsheet. US Forest Service.

Goheen, J. R., T. M. Palmer, G. K. Charles, K. M. Helgen, S. N. Kinyua, J. E. Maclean, B. L. Turner, H. S. Young, and R. M. Pringle. 2013. Piecewise Disassembly of a Large-Herbivore Community across a Rainfall Gradient: The UHURU Experiment. PLOS ONE 8:e55192.

Greer, M. J., G. W. T. Wilson, K. R. Hickman, and S. M. Wilson. 2014. Experimental evidence that invasive grasses use allelopathic biochemicals as a potential mechanism for invasion: chemical warfare in nature. Plant and Soil 385:165–179.

Gross, C. L., and D. Mackay. 2014. Two decades of demography reveals that seed and seedling transitions limit population persistence in a translocated shrub. Annals of Botany 114:85–96.

Hald-Mortensen, C. 2023, September 19. The Main Drivers of Biodiversity Loss: A Brief Overview. SSRN Scholarly Paper, Social Science Research Network, Rochester, NY.

Hambäck, P. A., and A. P. Beckerman. 2003. Herbivory and plant resource competition: a review of two interacting interactions. Oikos 101:26–37.

Harper, J. L. 1977. Population biology of plants. Fourth edition. London ; New York : Academic Press.

Heggenes, J., A. Odland, T. Chevalier, J. Ahlberg, A. Berg, H. Larsson, and D. K. Bjerketvedt. 2017. Herbivore grazing—or trampling? Trampling effects by a large ungulate in cold high-latitude ecosystems. Ecology and Evolution 7:6423–6431.

Hellmann, J. J., J. E. Byers, B. G. Bierwagen, and J. S. Dukes. 2008. Five Potential Consequences of Climate Change for Invasive Species. Conservation Biology 22:534–543.

Hessl, A. E. 2011. Pathways for climate change effects on fire: Models, data, and uncertainties. Progress in Physical Geography: Earth and Environment 35:393–407.

Holmgren, M., and M. Scheffer. 2010. Strong facilitation in mild environments: the stress gradient hypothesis revisited. Journal of Ecology 98:1269–1275.

Holthuijzen, A. M. A., and T. L. Sharik. 1984. Seed Longevity and Mechanisms of Regeneration of Eastern Red Cedar (Juniperus virginiana L.). Bulletin of the Torrey Botanical Club 111:153–158.

Holthuijzen, A. M. A., and T. L. Sharik. 1985a. The Red Cedar (*Juniperus virginiana* L.) Seed Shadow along a Fenceline. The American Midland Naturalist 113:200–202.

Holthuijzen, A. M. A., and T. L. Sharik. 1985b. The avian seed dispersal system of eastern red cedar (*Juniperus virginiana*). Canadian Journal of Botany 63:1508–1515.

Holthuijzen, A. M. A., T. L. Sharik, and J. D. Fraser. 1987. Dispersal of eastern red cedar (*Juniperus virginiana*) into pastures: an overview. Canadian Journal of Botany 65:1092–1095.

Horncastle, V. J., E. C. Hellgren, P. M. Mayer, A. C. Ganguli, D. M. Engle, and D. M. Leslie. 2005. Implications of Invasion by Juniperus virginiana on Small Mammals in the Southern Great Plains. Journal of Mammalogy 86:1144–1155.

Horncastle, V. J., E. C. Hellgreni, P. M. Mayer, D. M. Engle, and J. David M. Leslie. 2004. Differential consumption of eastern red cedar *(Juniperus virginiana)* by avian and mammalian guilds: implications for tree invasion. The American Midland Naturalist 152:255–268.

Hurvich, C. M., and C.-L. Tsai. 1989. Regression and time series model selection in small samples. Biometrika 76:297–307.

Hyvarinen, O., M. Te Beest, E. le Roux, G. Kerley, E. de Groot, R. Vinita, and J. P. G. M. Cromsigt. 2021. Megaherbivore impacts on ecosystem and Earth system functioning: the current state of the science. Ecography 44:1579–1594.

Johnson, L. C., J. T. Olsen, H. Tetreault, A. DeLaCruz, J. Bryant, T. J. Morgan, M. Knapp, N. M. Bello, S. G. Baer, and B. R. Maricle. 2015. Intraspecific variation of a dominant grass and local adaptation in reciprocal garden communities along a US Great Plains' precipitation gradient: implications for grassland restoration with climate change. Evolutionary Applications 8:705–723.

Jordan, N. R., D. L. Larson, and S. C. Huerd. 2008. Soil modification by invasive plants: effects on native and invasive species of mixed-grass prairies. Biological Invasions 10:177–190.

Joyce, F. H., B. M. Ramos, R. A. Zahawi, and K. D. Holl. 2024. Vertebrate seed predation can limit recruitment of later-successional species in tropical forest restoration. Biotropica 56:e13381.

Kauffman, M., and J. Maron. 2006. Consumers Limit the Abundance and Dynamics of a Perennial Shrub with a Seed Bank. The American naturalist 168:454–70.

Keen, R. M. 2023. Ecohydrological implications of clonal shrub encroachment in tallgrass prairie.

Kimball, S., M. E. Lulow, K. A. Mooney, and Q. M. Sorenson. 2014. Establishment and Management of Native Functional Groups in Restoration. Restoration Ecology 22:81–88.

Kimball, S., J. Rath, J. E. Coffey, M. R. Perea-Vega, M. Walsh, N. M. Fiore, P. M. Ta, K. T. Schmidt, M. L. Goulden, and S. D. Allison. 2024. Long-term drought promotes invasive species by reducing wildfire severity. Ecology 105:e4265.

van Kleunen, M. 2007. Adaptive genetic differentiation in life-history traits between populations of *Mimulus guttatus* with annual and perennial life-cycles. Evolutionary Ecology 21:185–199.

van Kleunen, M., W. Dawson, F. Essl, J. Pergl, M. Winter, E. Weber, H. Kreft, P. Weigelt, J. Kartesz, M. Nishino, L. A. Antonova, J. F. Barcelona, F. J. Cabezas, D. Cárdenas, J. Cárdenas-Toro, N. Castaño, E. Chacón, C. Chatelain, A. L. Ebel, E. Figueiredo, N. Fuentes, Q. J. Groom, L. Henderson, Inderjit, A. Kupriyanov, S. Masciadri, J. Meerman, O. Morozova, D. Moser, D. L. Nickrent, A. Patzelt, P. B. Pelser, M. P. Baptiste, M. Poopath, M. Schulze, H. Seebens, W. Shu, J. Thomas, M. Velayos, J. J. Wieringa, and P. Pyšek. 2015. Global exchange and accumulation of non-native plants. Nature 525:100–103.

Koerner, S. E., D. E. Burkepile, R. W. S. Fynn, C. E. Burns, S. Eby, N. Govender, N. Hagenah, K. J. Matchett, D. I. Thompson, K. R. Wilcox, S. L. Collins, K. P. Kirkman, A. K. Knapp, and M. D. Smith. 2014. Plant community response to loss of large herbivores differs between North American and South African savanna grasslands. Ecology 95:808–816.

Koerner, S. E., M. D. Smith, D. E. Burkepile, N. P. Hanan, M. L. Avolio, S. L. Collins, A. K. Knapp, N. P. Lemoine, E. J. Forrestel, S. Eby, D. I. Thompson, G. A. Aguado-Santacruz,

J. P. Anderson, T. M. Anderson, A. Angassa, S. Bagchi, E. S. Bakker, G. Bastin, L. E. Baur, K. H. Beard, E. A. Beever, P. J. Bohlen, E. H. Boughton, D. Canestro, A. Cesa, E. Chaneton, J. Cheng, C. M. D'Antonio, C. Deleglise, F. Dembélé, J. Dorrough, D. J. Eldridge, B. Fernandez-Going, S. Fernández-Lugo, L. H. Fraser, B. Freedman, G. García-Salgado, J. R. Goheen, L. Guo, S. Husheer, M. Karembé, J. M. H. Knops, T. Kraaij, A. Kulmatiski, M.-M. Kytöviita, F. Lezama, G. Loucougaray, A. Loydi, D. G. Milchunas, S. J. Milton, J. W. Morgan, C. Moxham, K. C. Nehring, H. Olff, T. M. Palmer, S. Rebollo, C. Riginos, A. C. Risch, M. Rueda, M. Sankaran, T. Sasaki, K. A. Schoenecker, N. L. Schultz, M. Schütz, A. Schwabe, F. Siebert, C. Smit, K. A. Stahlheber, C. Storm, D. J. Strong, J. Su, Y. V. Tiruvaimozhi, C. Tyler, J. Val, M. L. Vandegehuchte, K. E. Veblen, L. T. Vermeire, D. Ward, J. Wu, T. P. Young, Q. Yu, and T. J. Zelikova. 2018. Change in dominance determines herbivore effects on plant biodiversity. Nature Ecology & Evolution 2:1925–1932.

Krawchuk, M. A., and M. A. Moritz. 2011. Constraints on global fire activity vary across a resource gradient. Ecology 92:121–132.

LaForgia, M. L., S. P. Harrison, and A. M. Latimer. 2020. Invasive species interact with climatic variability to reduce success of natives. Ecology 101:e03022.

Lalor, A. R., D. J. Law, D. D. Breshears, D. A. Falk, J. P. Field, R. A. Loehman, F. J. Triepke, and G. A. Barron-Gafford. 2023. Mortality thresholds of juvenile trees to drought and heatwaves: implications for forest regeneration across a landscape gradient. Frontiers in Forests and Global Change 6.

Lauenroth, W. K., O. E. Sala, D. G. Milchunas, and R. W. Lathrop. 1987. Root Dynamics of Bouteloua gracilis During Short-Term Recovery from Drought. Functional Ecology 1:117–124.

Lavergne, C., M.-J. Martinez, and C. Trottier. 2008. Empirical model selection in generalized linear mixed effects models. Computational Statistics 23:99–109.

Lawes, M. J., H. Adie, J. Russell-Smith, B. Murphy, and J. J. Midgley. 2011. How do small savanna trees avoid stem mortality by fire? The roles of stem diameter, height and bark thickness. Ecosphere 2:art42.

LeCain, D. R., J. A. Morgan, D. G. Milchunas, A. R. Mosier, J. A. Nelson, and D. P. Smith. 2006. Root Biomass of Individual Species, and Root Size Characteristics After Five Years of CO2 Enrichment on Native Shortgrass Steppe. Plant and Soil 279:219–228.

Leverett, L. D. 2017. Germination phenology determines the propensity for facilitation and competition. Ecology 98:2437–2446.

Liu, L., H. Quan, B.-C. Dong, X.-Q. Bu, L. Li, F.-D. Liu, G.-C. Lei, and H.-L. Li. 2016. Nutrient enrichment alters impacts of Hydrocotyle vulgaris invasion on native plant communities. Scientific Reports 6:39468.

Liu, Y., A. M. O. Oduor, Z. Zhang, A. Manea, I. M. Tooth, M. R. Leishman, X. Xu, and M. van Kleunen. 2017. Do invasive alien plants benefit more from global environmental change than native plants? Global Change Biology 23:3363–3370.

Liu, Y., J. Prestemon, S. Goodrick, T. Holmes, J. Stanturf, J. Vose, and G. Sun. 2013. Future Wildfire Trends, Impacts, and Mitigation Options in the Southern United States. Pages 85–126 Climate Change Adaptation and Mitigation Management Options. CRC Press.

Liu, Y.-H., J.-H. Cheng, B. Schmid, L.-S. Tang, and J.-D. Sheng. 2020. Woody plant encroachment may decrease plant carbon storage in grasslands under future drier conditions. Journal of Plant Ecology 13:213–223.

Louthan, A. M., D. F. Doak, and A. L. Angert. 2015. Where and When do Species Interactions Set Range Limits? Trends in Ecology & Evolution 30:780–792.

Louthan, A. M., D. F. Doak, J. R. Goheen, T. M. Palmer, and R. M. Pringle. 2014. Mechanisms of plant–plant interactions: concealment from herbivores is more important than abiotic-stress mediation in an African savannah. Proceedings of the Royal Society B: Biological Sciences 281:20132647.

Louthan, A. M., R. M. Pringle, J. R. Goheen, T. M. Palmer, W. F. Morris, and D. F. Doak. 2018. Aridity weakens population-level effects of multiple species interactions on *Hibiscus meyeri*. Proceedings of the National Academy of Sciences 115:543–548.

Lu, X., E. Siemann, M. He, H. Wei, X. Shao, and J. Ding. 2016. Warming benefits a native species competing with an invasive congener in the presence of a biocontrol beetle. New Phytologist 211:1371–1381.

MacDougall, A. s., J. Boucher, R. Turkington, and G. e. Bradfield. 2006. Patterns of plant invasion along an environmental stress gradient. Journal of Vegetation Science 17:47–56.

MacDougall, A. S., S. D. Wilson, and J. D. Bakker. 2008. Climatic variability alters the outcome of long-term community assembly. Journal of Ecology 96:346–354.

Mackiewicz-Walec, E., P. J. Żarczyński, S. J. Krzebietke, and K. Żarczyńska. 2024. Smooth Brome (Bromus inermis L.)—A Versatile Grass: A Review. Agriculture 14:854.

Mainka, S. A., and G. W. Howard. 2010. Climate change and invasive species: double jeopardy. Integrative Zoology 5:102–111.

Mangla, S., R. L. Sheley, J. J. James, and S. R. Radosevich. 2011. Role of competition in restoring resource poor arid systems dominated by invasive grasses. Journal of Arid Environments 75:487–493.

Maron, J. L., K. C. Baer, and A. L. Angert. 2014. Disentangling the drivers of context-dependent plant–animal interactions. Journal of Ecology 102:1485–1496.

Maron, J. L., and E. Crone. 2006. Herbivory: effects on plant abundance, distribution and population growth. Proceedings of the Royal Society B: Biological Sciences 273:2575–2584.

Maschinski, J., and T. G. Whitham. 1989. The Continuum of Plant Responses to Herbivory: The Influence of Plant Association, Nutrient Availability, and Timing. The American Naturalist 134:1–19.

Matzek, V. 2012. Trait Values, Not Trait Plasticity, Best Explain Invasive Species' Performance in a Changing Environment. PLoS ONE 7.

McDowell, W. G., A. J. Benson, and J. E. Byers. 2014. Climate controls the distribution of a widespread invasive species: implications for future range expansion. Freshwater Biology 59:847–857.

McKinley, D. C., M. D. Norris, J. M. Blair, and L. C. Johnson. 2008. Altered Ecosystem Processes as a Consequence of *Juniperus virginiana L.* Encroachment into North American Tallgrass Prairie. Pages 170–187 *in* O. W. Van Auken, editor. Western North American Juniperus Communities: A Dynamic Vegetation Type. Springer, New York, NY.

McNaughton, S. J., M. Oesterheld, D. A. Frank, and K. J. Williams. 1989. Ecosystem-level patterns of primary productivity and herbivory in terrestrial habitats. Nature 341:142–144.

Mollot, G., J. H. Pantel, and T. N. Romanuk. 2017. Chapter Two - The Effects of Invasive Species on the Decline in Species Richness: A Global Meta-Analysis. Pages 61–83 *in* D. A. Bohan, A. J. Dumbrell, and F. Massol, editors. Advances in Ecological Research. Academic Press.

Monthly National Climate Report for June 2024. 2024, July 1. . https://www.ncei.noaa.gov/access/monitoring/monthly-report/national/202406#ytd-highlights.

Morris, W. F., and D. F. Doak. 2002. Quantitative Conservation Biology: Theory and Practice of Population Viability Analysis. Sinauer Associates, Sunderland, MA.

Mutke, S., J. Gordo, and L. Gil. 2005. Variability of Mediterranean Stone pine cone production: Yield loss as response to climate change. Agricultural and Forest Meteorology 132:263–272.

Nackley, L. L., A. G. West, A. L. Skowno, and W. J. Bond. 2017. The Nebulous Ecology of Native Invasions. Trends in Ecology & Evolution 32:814–824.

Natural Resources Conservation Service, United States Department of Agriculture. 2018, October 5. Web Soil Survey. https://www.nrcs.usda.gov/resources/data-and-reports/web-soil-survey.

Neubert, M. G., and H. Caswell. 2000. Demography and Dispersal: Calculation and Sensitivity Analysis of Invasion Speed for Structured Populations. Ecology 81:1613–1628.

Neubert, M. G., M. Kot, and M. A. Lewis. 2000. Invasion speeds in fluctuating environments. Proceedings of the Royal Society of London. Series B: Biological Sciences 267:1603–1610.

Novoa, A., D. Moodley, J. A. Catford, M. Golivets, J. Bufford, F. Essl, B. Lenzner, Z. Pattison, and P. Pyšek. 2021. Global costs of plant invasions must not be underestimated. NeoBiota 69:75–78.

Opedal, Ø. H., K. O. Nystuen, D. Hagen, H. Holien, M. V. Sørensen, S. I. Lang, S. Lindmo, G. R. Strimbeck, and B. J. Graae. 2021. Herbivores reduce seedling recruitment in alpine plant communities. Nordic Journal of Botany 39.

Ott, J. P., J. L. Butler, Y. Rong, and L. Xu. 2016. Greater bud outgrowth of *Bromus inermis* than *Pascopyrum smithii* under multiple environmental conditions. Journal of Plant Ecology:rtw045.

Owensby, C. E., K. R. Blan, B. J. Eaton, and O. G. Russ. 1973. Evaluation of Eastern Redcedar Infestations in the Northern Kansas Flint Hills. Journal of Range Management 26:256.

Pascual, J., J. Alberti, P. Daleo, and O. Iribarne. 2017. Herbivory and trampling by small mammals modify soil properties and plant assemblages. Journal of Vegetation Science 28:1028–1035.

Pausas, J. G., and J. E. Keeley. 2014. Evolutionary ecology of resprouting and seeding in fire-prone ecosystems. New Phytologist 204:55–65.

Pearcy, R. W., and J. Ehleringer. 1984. Comparative ecophysiology of C3 and C4 plants. Plant, Cell & Environment 7:1–13.

Pellegrini, A. F. A., R. M. Pringle, N. Govender, and Lars. O. Hedin. 2017. Woody plant biomass and carbon exchange depend on elephant-fire interactions across a productivity gradient in African savanna. Journal of Ecology 105:111–121.

Pironon, S., G. Papuga, J. Villellas, A. L. Angert, M. B. García, and J. D. Thompson. 2017. Geographic variation in genetic and demographic performance: new insights from an old biogeographical paradigm. Biological Reviews 92:1877–1909.

Pisanu, S., E. Farris, R. Filigheddu, and M. B. García. 2012. Demographic effects of large, introduced herbivores on a long-lived endemic plant. Plant Ecology 213:1543–1553.

Pratt, P. D., M. B. Rayamajhi, T. K. Van, T. D. Center, and P. W. Tipping. 2005. Herbivory alters resource allocation and compensation in the invasive tree *Melaleuca quinquenervia*. Ecological Entomology 30:316–326.

Pyšek, P., P. E. Hulme, D. Simberloff, S. Bacher, T. M. Blackburn, J. T. Carlton, W. Dawson, F. Essl, L. C. Foxcroft, P. Genovesi, J. M. Jeschke, I. Kühn, A. M. Liebhold, N. E. Mandrak, L. A. Meyerson, A. Pauchard, J. Pergl, H. E. Roy, H. Seebens, M. van Kleunen, M. Vilà, M. J. Wingfield, and D. M. Richardson. 2020. Scientists' warning on invasive alien species. Biological Reviews 95:1511–1534.

Pyšek, P., V. Jarošík, P. E. Hulme, J. Pergl, M. Hejda, U. Schaffner, and M. Vilà. 2012. A global assessment of invasive plant impacts on resident species, communities and ecosystems: the interaction of impact measures, invading species' traits and environment. Global Change Biology 18:1725–1737.

Raheem, A., P. Yohanna, G. Li, N. J. Noh, B. Iqbal, J. Tang, D. Du, T. A. Alahmadi, M. J. Ansari, A. Zhan, and Y. Son. 2024. Unraveling the ecological threads: How invasive alien plants influence soil carbon dynamics. Journal of Environmental Management 356:120556.

Ramsey, R. J. L., G. R. Stephenson, and J. C. Hall. 2005. A review of the effects of humidity, humectants, and surfactant composition on the absorption and efficacy of highly water-soluble herbicides. Pesticide Biochemistry and Physiology 82:162–175.

Ramula, S., M. Rees, and Y. M. Buckley. 2009. Integral projection models perform better for small demographic data sets than matrix population models: a case study of two perennial herbs. Journal of Applied Ecology 46:1048–1053.

Ratajczak, Z., J. B. Nippert, J. M. Briggs, and J. M. Blair. 2014. Fire dynamics distinguish grasslands, shrublands and woodlands as alternative attractors in the Central Great Plains of North America. Journal of Ecology 102:1374–1385.

Ren, Z., S. G. Baer, L. C. Johnson, M. B. Galliart, and D. J. Gibson. 2024. Effects of Manipulated Rainfall and Intraspecific Variation Within Dominant Species on Community Assembly: Insights From a Long-Term Grassland Restoration Experiment. Ecology and Evolution 14:e70571.

Roy, H. E., A. Pauchard, P. Stoett, T. Renard Truong, S. Bacher, B. S. Galil, P. E. Hulme, T. Ikeda, K. Sankaran, M. A. McGeoch, L. A. Meyerson, M. A. Nuñez, A. Ordonez, S. J. Rahlao, E. Schwindt, H. Seebens, A. W. Sheppard, and V. Vandvik. 2024. IPBES Invasive Alien Species Assessment: Summary for Policymakers. Zenodo.

Sala, O. E., F. S. Chapin, J. J. Armesto, J. Bloomfield, R. Dirzo, E. Huber-Sanwald, L. F. Huenneke, R. B. Jackson, A. Kinzig, R. Leemans, D. M. Lodge, H. A. Mooney, M. Oesterheld, N. L. Poff, M. T. Sykes, B. H. Walker, M. Walker, and D. H. Wall. 2000. Global Biodiversity Scenarios for the Year 2100. Science 287:1770–1774.

Salesman, J. B., and M. Thomsen. 2011. Smooth Brome (Bromus inermis) in Tallgrass Prairies: A Review of Control Methods and Future Research Directions. Ecological Restoration 29:374–381.

Sapsford, S. J., A. J. Brandt, K. T. Davis, G. Peralta, I. A. Dickie, R. D. Gibson II, J. L. Green, P. E. Hulme, M. A. Nuñez, K. H. Orwin, A. Pauchard, D. A. Wardle, and D. A. Peltzer. 2020. Towards a framework for understanding the context dependence of impacts of non-native tree species. Functional Ecology 34:944–955.

Scheiter, S., and S. I. Higgins. 2009. Impacts of climate change on the vegetation of Africa: an adaptive dynamic vegetation modelling approach. Global Change Biology 15:2224–2246.

Schlichting, C. D. 1986. The Evolution of Phenotypic Plasticity in Plants. Annual Review of Ecology and Systematics 17:667–693.

Schmidt, T. L., and J. Stubbendieck. 1993. Factors Influencing Eastern Redcedar Seedling Survival on Rangeland. Journal of Range Management 46:448–451.

Shannon-Firestone, S., and J. Firestone. 2015. Allelopathic potential of invasive species is determined by plant and soil community context. Plant Ecology 216:491–502.

Sheth, S. N., and A. L. Angert. 2018. Demographic compensation does not rescue populations at a trailing range edge. Proceedings of the National Academy of Sciences 115:2413–2418.

Singh, M., and C. C. Daehler. 2023. Meta-analytic evidence that allelopathy may increase the success and impact of invasive grasses. PeerJ 11:e14858.

Stavi, I. 2019. Wildfires in Grasslands and Shrublands: A Review of Impacts on Vegetation, Soil, Hydrology, and Geomorphology. Water 11:1042.

Stevens-Rumann, C. S., S. J. Prichard, E. Whitman, M.-A. Parisien, and A. J. H. Meddens. 2022. Considering regeneration failure in the context of changing climate and disturbance regimes in western North America. Canadian Journal of Forest Research 52:1281–1302.

Stokes, M. A., and T. L. Smiley. 1996. An Introduction to Tree-ring Dating. University of Arizona Press.

Stuble, K. L., S. E. Fick, and T. P. Young. 2017. Every restoration is unique: testing year effects and site effects as drivers of initial restoration trajectories. Journal of Applied Ecology 54:1051–1057.

Taylor, S. H., B. S. Ripley, T. Martin, L.-A. De-Wet, F. I. Woodward, and C. P. Osborne. 2014. Physiological advantages of C4 grasses in the field: a comparative experiment demonstrating the importance of drought. Global Change Biology 20:1992–2003.

Townsend, D. S., and A. D. Meyer. 2002. Rapid Recovery of Witch Hazel (*Hamamelis virginiana L.*) by Sprouting, Following Release from White-tailed Deer (*Odocoileus virginianus Zimm.*) Browsing. Natural Areas Journal 22:290–295.

Trouillier, M., M. van der Maaten-Theunissen, T. Scharnweber, D. Würth, A. Burger, M. Schnittler, and M. Wilmking. 2019. Size matters—a comparison of three methods to assess age- and size-dependent climate sensitivity of trees. Trees 33:183–192.

Trumble, J., D. Kolodny-Hirsch, and I. Ting. 2003. Plant Compensation for Arthropod Herbivory. Annual Review of Entomology 38:93–119.

Tu, Y., Z. Yao, J. Guo, L. Yang, Y. Zhu, X. Yang, Z. Shi, and T. Indree. 2024. Predicting the potential risk of *Caragana* shrub encroachment in the Eurasian steppe under anthropogenic climate change. Science of The Total Environment 944:173925.

Uddin, M. N., and R. W. Robinson. 2018. Can nutrient enrichment influence the invasion of Phragmites australis? The Science of the Total Environment 613–614:1449–1459.

Udevitz, M. S., and B. E. Ballachey. 1998. Estimating Survival Rates with Age-Structure Data. The Journal of Wildlife Management 62:779–792.

Van Auken, O. W. 2009. Causes and consequences of woody plant encroachment into western North American grasslands. Journal of Environmental Management 90:2931–2942.

Van Der Wal, R., M. Egas, A. Van Der Veen, and J. Bakker. 2000. Effects of resource competition and herbivory on plant performance along a natural productivity gradient. Journal of Ecology 88:317–330.

Vasquez, E., R. Sheley, and T. Svejcar. 2008. Nitrogen Enhances the Competitive Ability of Cheatgrass (Bromus tectorum) Relative to Native Grasses. Invasive Plant Science and Management 1:287–295.

Vergeer, P., and W. E. Kunin. 2011. Life history variation in *Arabidopsis lyrata* across its range: effects of climate, population size and herbivory. Oikos 120:979–990.

Villellas, J., D. F. Doak, M. B. García, and W. F. Morris. 2015. Demographic compensation among populations: what is it, how does it arise and what are its implications? Ecology Letters 18:1139–1152.

Villellas, J., and M. B. García. 2018. Life-history trade-offs vary with resource availability across the geographic range of a widespread plant. Plant Biology 20:483–489.

Volder, A., M. G. Tjoelker, and D. D. Briske. 2010. Contrasting physiological responsiveness of establishing trees and a C4 grass to rainfall events, intensified summer drought, and warming in oak savanna. Global Change Biology 16:3349–3362.

Walton, A. 2020. The Impact of Nurse Plants and Microclimate on Spatial and Temporal Trends of Juniperus virginiana L. Seedlings in an Oklahoma Grassland. University of Oklahoma Graduate Thesis.

Wang, T., A. Hamann, D. Spittlehouse, and C. Carroll. 2016. Locally Downscaled and Spatially Customizable Climate Data for Historical and Future Periods for North America. PLOS ONE 11:e0156720.

Wetzel, W. C., B. D. Inouye, P. G. Hahn, S. R. Whitehead, and N. Underwood. 2023. Variability in Plant–Herbivore Interactions. Annual Review of Ecology, Evolution, and Systematics 54:451–474.

Wright, A., S. A. Schnitzer, and P. B. Reich. 2014. Living close to your neighbors: the importance of both competition and facilitation in plant communities. Ecology 95:2213–2223.

Xing, X., Q. Qi, S. Tong, Y. An, H. Ni, Y. Xin, M. Zhang, D. Zhang, and W. Du. 2025. Community changes in a restored tussock sedge wetland over 15 years: Expansion and competition. Global Ecology and Conservation 57:e03356.

Yahdjian, L., and O. E. Sala. 2002. A rainout shelter design for intercepting different amounts of rainfall. Oecologia 133:95–101.

Yang, X., A. L. Angert, P. A. Zuidema, F. He, S. Huang, S. Li, S.-L. Li, N. I. Chardon, and J. Zhang. 2022. The role of demographic compensation in stabilising marginal tree populations in North America. Ecology Letters 25:1676–1689.

Zou, C. B., D. Twidwell, C. H. Bielski, D. T. Fogarty, A. R. Mittelstet, P. J. Starks, R. E. Will, Y. Zhong, and B. S. Acharya. 2018. Impact of Eastern Redcedar Proliferation on Water Resources in the Great Plains USA—Current State of Knowledge. Water 10:1768.

Appendix A - Chapter 2 Appendices

Appendix Table A.1. Best-fit models for demographic rates of *Hibiscus meyeri.* We show fixed and random effect coefficients included for generalized linear models (probability of survival, probability of fruiting; binomial error term) and linear models (growth, variance in growth, log-transformed number of fruits). Demographic rate models were fit for each site (Arid, Intermediate, or Mesic) and herbivore exclusion treatment (LMH, complete large mammalian herbivore exclusion; MEGA, megaherbivore exclusion; MESO, mega- and mesoherbivore exclusion; and control, no large mammalian herbivore exclusion). Biomass in the initial timestep was treated as a potential fixed effect in the global model. Block and transition were treated as potential random intercepts; if the inclusion of either resulted in singularity for the global model, the global model was refit with block and transition as fixed effects. Thus, models may or may not be mixed effect models depending on whether random effects were included in the final model. Dashes indicate coefficients not present in the best-fit model. "F" indicates a coefficient was present in the best-fit model as a fixed effect, and "R" indicates a coefficient was present in the best-fit model as a random effect. If there are no indicated fixed or random effects, the model was intercept-only.

Model Specification			Parameter to Include		
Demographic Rate	**Site**	**Treatment**	***Biomass***	***Block***	***Timepoint***
Survival	Arid	Control	F	-	-
Survival	Intermediate	Control	-	-	-
Survival	Mesic	Control	-	R	R
Survival	Arid	LMH	F	R	R
Survival	Intermediate	LMH	F	-	-
Survival	Mesic	LMH	-	-	-
Survival	Arid	MEGA	F	R	R
Survival	Intermediate	MEGA	-	R	R
Survival	Mesic	MEGA	-	R	R
Survival	Arid	MESO	F	R	R
Survival	Intermediate	MESO	-	R	R
Survival	Mesic	MESO	-	R	R
Growth	Arid	Control	F	R	R

Growth	Intermediate	Control	F	-	-
Growth	Mesic	Control	F	R	R
Growth	Arid	LMH	F	R	R
Growth	Intermediate	LMH	F	-	-
Growth	Mesic	LMH	F	R	R
Growth	Arid	MEGA	F	R	R
Growth	Intermediate	MEGA	F	-	-
Growth	Mesic	MEGA	F	-	-
Growth	Arid	MESO	F	R	R
Growth	Intermediate	MESO	F	-	-
Growth	Mesic	MESO	F	R	R
Variance in Growth	Arid	Control	F	R	R
Variance in Growth	Intermediate	Control	F	R	R
Variance in Growth	Mesic	Control	F	R	R
Variance in Growth	Arid	LMH	-	R	R
Variance in Growth	Intermediate	LMH	F	R	R
Variance in Growth	Mesic	LMH	F	-	-
Variance in Growth	Arid	MEGA	F	R	R
Variance in Growth	Intermediate	MEGA	F	R	R
Variance in Growth	Mesic	MEGA	F	-	-
Variance in Growth	Arid	MESO	F	R	R
Variance in Growth	Intermediate	MESO	F	-	-
Variance in Growth	Mesic	MESO	F	R	R
Probability of Fruiting	Arid	Control	F	-	-
Probability of Fruiting	Intermediate	Control	F	-	-
Probability of Fruiting	Mesic	Control	F	R	R
Probability of Fruiting	Arid	LMH	F	R	R
Probability of Fruiting	Intermediate	LMH	F	R	R
Probability of Fruiting	Mesic	LMH	F	R	R
Probability of Fruiting	Arid	MEGA	F	-	-
Probability of Fruiting	Intermediate	MEGA	F	R	R
Probability of Fruiting	Mesic	MEGA	F	R	R
Probability of Fruiting	Arid	MESO	F	R	R
Probability of Fruiting	Intermediate	MESO	F	R	R
Probability of Fruiting	Mesic	MESO	F	R	R
log(Number of Fruits/Biomass)	Arid	Control	-	-	-
log(Number of Fruits/Biomass)	Intermediate	Control	F	-	-
log(Number of Fruits/Biomass)	Mesic	Control	-	R	R
log(Number of Fruits/Biomass)	Arid	LMH	-	R	R
log(Number of Fruits/Biomass)	Intermediate	LMH	-	R	R
log(Number of Fruits/Biomass)	Mesic	LMH	-	R	R

log(Number of Fruits/Biomass)	Arid	MEGA	-	R	R
log(Number of Fruits/Biomass)	Intermediate	MEGA	-	-	-
log(Number of Fruits/Biomass)	Mesic	MEGA	-	R	R
log(Number of Fruits/Biomass)	Arid	MESO	-	-	-
log(Number of Fruits/Biomass)	Intermediate	MESO	F	-	-
log(Number of Fruits/Biomass)	Mesic	MESO	-	-	-

Appendix Table A.2. Demographic rate values for each herbivore exclusion treatment (Control, LMH, MEGA, and MESO) at each rainfall level (Arid, Intermediate, and Mesic). Herbivore exclusion treatments either include all large mammalian herbivores (Control), exclude all large mammalian herbivores (LMH), exclude megaherbivores only (MEGA), or exclude both meso- and megaherbivores while including smaller mammalian herbivores (MESO). All demographic rates are size-class specific, where size classes are small (S), medium (M), or large (L), with the exception of recruitment, which describes the recruitment of seedlings from fruits. For transitions among size classes (stasis, growth, and regression), we show transitions from the first size class to the second (e.g., S-M growth indicates transition probability from small size class to medium size class).

	Control			**LMH**			**MEGA**			**MESO**		
Demographic Rate	***Arid***	***Intermediate***	***Mesic***	***Arid***	***Intermediate***	***Mesic***	***Arid***	***Intermediate***	***Mesic***	***Arid***	***Intermediate***	***Mesic***
S-Survival	9.42E-01	9.42E-01	9.45E-01	9.48E-01	9.68E-01	9.34E-01	9.79E-01	9.69E-01	9.63E-01	9.68E-01	9.87E-01	9.61E-01
M-Survival	8.11E-01	9.42E-01	9.45E-01	8.32E-01	9.16E-01	9.34E-01	9.20E-01	9.69E-01	9.63E-01	9.25E-01	9.87E-01	9.61E-01
L-Survival	5.31E-01	9.42E-01	9.45E-01	5.75E-01	7.97E-01	9.34E-01	7.42E-01	9.69E-01	9.63E-01	8.31E-01	9.87E-01	9.61E-01
S-Fruiting	4.30E-01	3.18E-01	4.63E-01	9.15E-01	2.96E-01	9.18E-01	5.79E-01	3.47E-01	1.48E-01	8.83E-01	4.54E-01	3.93E-01
M-Fruiting	4.11E+00	1.85E+00	6.14E+00	5.90E+00	3.94E+00	5.87E+00	6.32E+00	4.80E+00	3.30E+00	5.74E+00	7.61E+00	4.63E+00
L-Fruiting	8.92E+00	1.80E+00	1.09E+01	1.18E+01	7.62E+00	1.14E+01	1.15E+01	8.27E+00	6.91E+00	1.19E+01	1.97E+01	8.76E+00
S-Stasis	1.00E+00	1.00E+00	1.00E+00	9.95E-01	1.00E+00	1.00E+00	9.98E-01	9.99E-01	1.00E+00	9.91E-01	9.99E-01	1.00E+00
M-S Regression	1.68E-02	2.82E-02	8.85E-03	5.79E-04	5.76E-03	4.96E-04	1.88E-02	2.32E-03	1.59E-02	7.28E-03	2.19E-02	3.75E-03
L-S Regression	8.91E-09	3.29E-06	1.21E-09	6.33E-20	3.75E-09	3.23E-15	1.75E-06	1.13E-11	6.06E-07	8.57E-09	9.91E-06	9.95E-11
S-M Growth	1.58E-04	2.37E-04	1.13E-05	5.16E-03	3.64E-05	3.67E-04	1.81E-03	7.39E-04	1.01E-04	8.74E-03	5.37E-04	1.38E-04

M-Stasis	9.83 E-01	9.62E-01	9.91 E-01	9.98 E-01	9.90E-01	9.98 E-01	9.60 E-01	9.94E-01	9.70 E-01	9.80 E-01	9.40E-01	9.95 E-01
L-M Regression	1.66 E-01	1.15E-01	9.08 E-02	3.00 E-03	4.03E-02	6.56 E-03	7.92 E-02	1.70E-02	6.42 E-02	4.52 E-02	8.35E-02	4.10 E-02
S-L Growth	0.00 E+00	0.00E+00	0.00 E+00	0.00 E+00	0.00E+00	0.00 E+00	0.00 E+00	0.00E+00	0.00 E+00	0.00 E+00	0.00E+00	0.00 E+00
M-L Growth	1.95 E-04	9.34E-03	2.84 E-04	1.09 E-03	4.13E-03	1.42 E-03	2.14 E-02	3.98E-03	1.46 E-02	1.25 E-02	3.86E-02	1.21 E-03
L-Stasis	8.34 E-01	8.85E-01	9.09 E-01	9.97 E-01	9.60E-01	9.93 E-01	9.21 E-01	9.83E-01	9.36 E-01	9.55 E-01	9.16E-01	9.59 E-01
Recruitment	2.12 E-01	1.71E-01	1.21 E+00	2.12 E-01	1.71E-01	1.21 E+00	2.12 E-01	1.71E-01	1.21 E+00	2.12 E-01	1.71E-01	1.21 E+00

Appendix Table A.3. Sensitivity of population growth rate to demographic rates. We show sensitivity of the across-rainfall level mean integral projection model kernel to underlying demographic rates, estimated via perturbation. Herbivore exclusion treatments include the complete absence of large mammalian herbivores ("LMH"), absence of meso- and mega-herbivores (MESO), absence of megaherbivores (MEGA), and presence of all large mammalian herbivores ("control"). Size-classes include small (S), medium (M), and large (L). For transitions among size classes (stasis, growth, and regression), we show transitions from the first size class to the second (e.g., S-M growth indicates transition probability from small size class to medium size class). Nas indicate rates with a value of zero, meaning that transition was not observed during our study.

	Herbivore Exclusion Treatment			
Demographic rate	*Control*	*LMH*	*MEGA*	*MESO*
S-Survival	1.02	1.03	0.98	0.97
M-Survival	4.20E-03	3.13E-02	4.57E-02	8.94E-02
L-Survival	3.70E-05	1.81E-04	2.67E-03	7.59E-03
S-Fruiting	0.38	0.32	0.38	0.32
M-Fruiting	1.92E-04	1.49E-03	1.50E-03	3.14E-03
L-Fruiting	1.21E-06	5.18E-06	5.99E-05	1.39E-04
S-Stasis	0.81	0.75	0.81	0.74
M-S Regression	4.06E-04	3.49E-03	3.21E-03	7.30E-03
L-S Regression	2.56E-06	1.42E-05	1.28E-04	3.24E-04
S-M Growth	5.83	4.24	8.79	6.62
M-Stasis	3.02E-03	2.01E-02	3.62E-02	6.63E-02
L-M Regression	1.85E-05	6.87E-05	1.39E-03	2.90E-03
S-L Growth	NA	NA	NA	NA
M-L Growth	3.37E-03	2.46E-02	4.56E-02	1.17E-01
L-Stasis	2.14E-05	8.58E-05	1.86E-03	5.26E-03
Recruitment	0.29	0.44	0.27	0.38

Appendix Table A.4. **Results of tests for demographic compensation in all herbivore exclusion treatments.** We assume that a deficit of positive or an excess of negative correlations indicates support for demographic compensation for a given herbivore exclusion treatment. Namely, if the observed proportion of positive correlations ($P_{obs,+}$) is less than the 5th percentile of the null distribution of positive correlations ($P_{5,+}$), that would indicate demographic compensation. Similarly, if the observed proportion of negative correlations ($P_{obs,-}$) is greater than or equal to the upper 95th percentile of the null distributions of negative correlations ($P_{95,-}$), that would indicate demographic compensation. Note that for herbivore exclusion treatments, "LMH" excludes meso-, mega-, and smaller herbivores such as dik-dik; "MESO" excludes mega- and mesoherbivores and includes smaller herbivores such as dik-dik; "MEGA" excludes megaherbivores and includes mesoherbivores and smaller herbivores such as dik-dik; and the "Control" includes all three herbivore guilds.

	Deficit of positive correlations			*Excess of negative correlations*		
Herbivore exclusion treatment	$P_{obs,+}$	$P_{5,+}$	Evidence for compensation?	$P_{obs,-}$	$P_{95,-}$	Evidence for compensation?
LMH	0.153	0.071	No	0.200	0.148	Yes
MESO	0.114	0.033	No	0.095	0.086	Yes
MEGA	0.105	0.024	No	0.095	0.076	Yes
Control	0.057	0.024	No	0.038	0.076	No

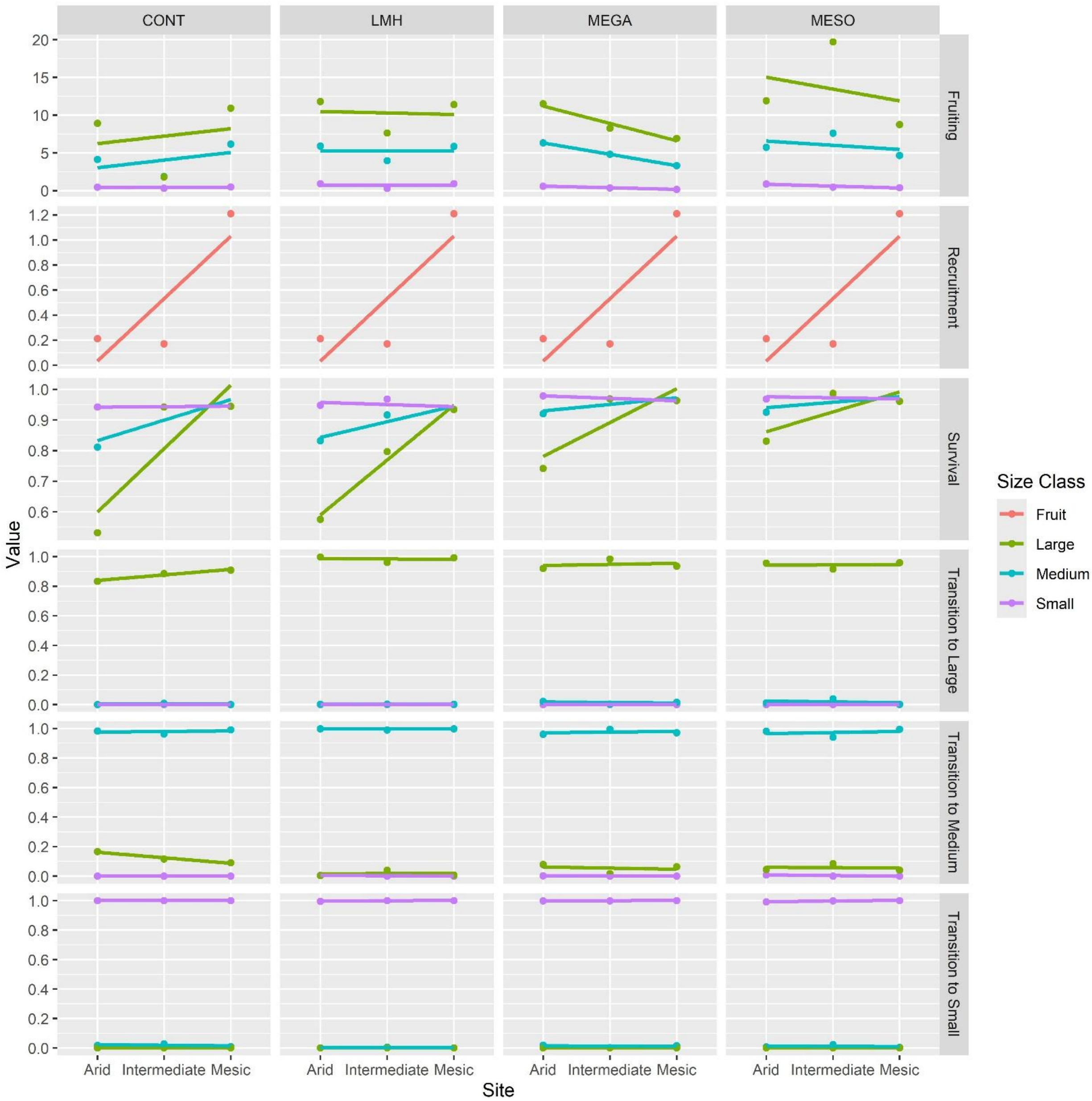

Appendix Figure A.1. Graph of demographic rates of small (S), medium (M), and large (L) plants, as well as recruitment, across Arid, Intermediate and Mesic rainfall levels for all herbivore exclusion treatments. Exclusion treatments are Control (all large mammalian herbivores included), LMH (all large mammalian herbivores excluded), MEGA (megaherbivores excluded) and MESO (meso- and megaherbivores exclude).

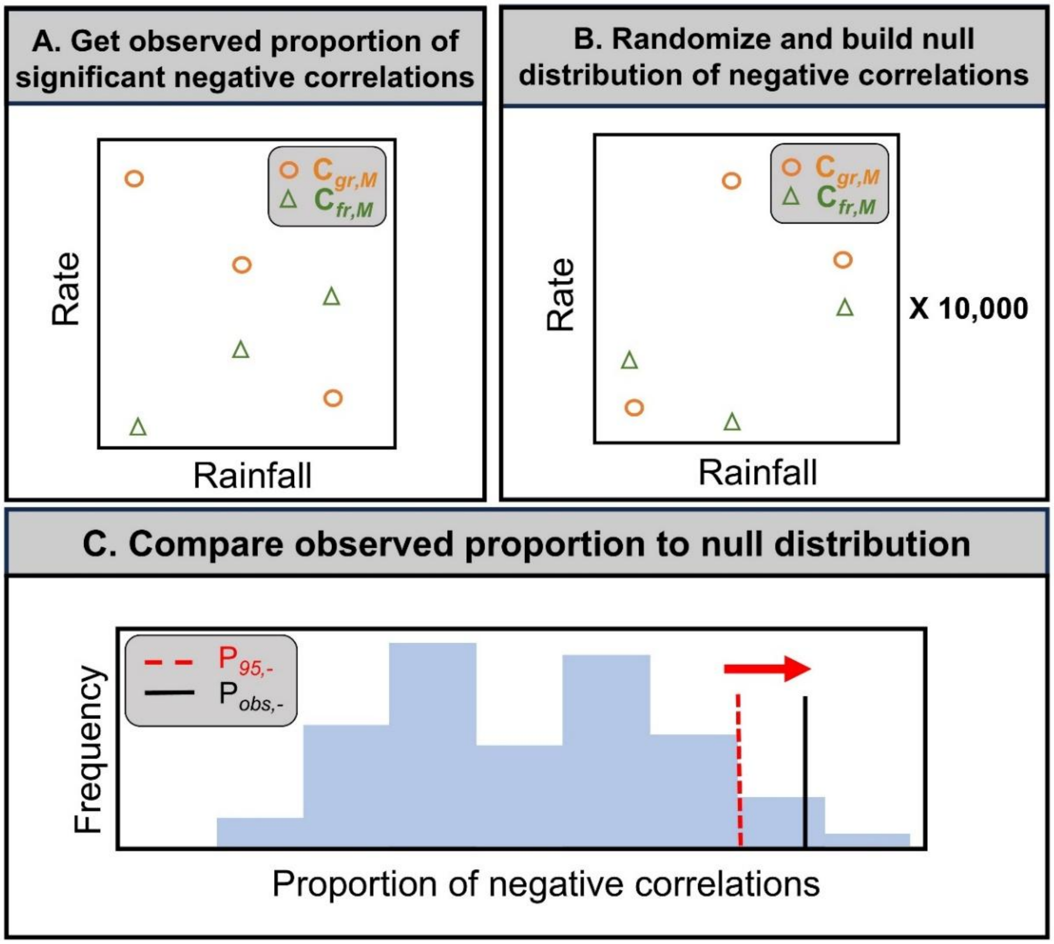

Appendix Figure A.2. Steps describing test for demographic compensation in a given herbivore exclusion treatment. In A, we test for significant negative correlations between life table response experiment (LTRE) contributions *C* for all pairwise combinations of demographic rates. Here, as an example we show a significant negative correlation between $C_{gr,M}$ (i.e., LTRE contributions for the growth of medium plants) and $C_{fr,M}$ (LTRE contributions for the fruit number of medium plants. We then calculate $P_{obs,-}$, the observed proportion of negative correlations (i.e., the proportion of demographic rate pairings whose *C* values are significantly negatively correlated at P<=0.05). In B, we show methods for constructing a null distribution for the129roportionn of negative correlations. We randomize all demographic rates' contributions across the rainfall gradient 10,000 times, each time calculating the proportion of demographic rate pairings that are significantly negatively correlated. These 10,000 proportions yield a null distribution for the proportion of significant negative correlations. We show growth and fruit number of medium plants as an example to illustrate the randomization process for one pair of demographic rates. In C, we compare $P_{obs,-}$ to the null distribution (shown in blue); strong evidence for demographic compensation occurs when the observed proportion of negative correlations ($P_{obs,-}$) is greater than or equal to the 95th percentile of the null distribution for proportion of negative correlations ($P_{95,-}$). We conduct a similar analysis to test whether the observed proportion of positive correlations is significantly less than we would expect by chance ($\leq 5^{th}$ percentile of the null distribution for the proportion of significant positive correlations).

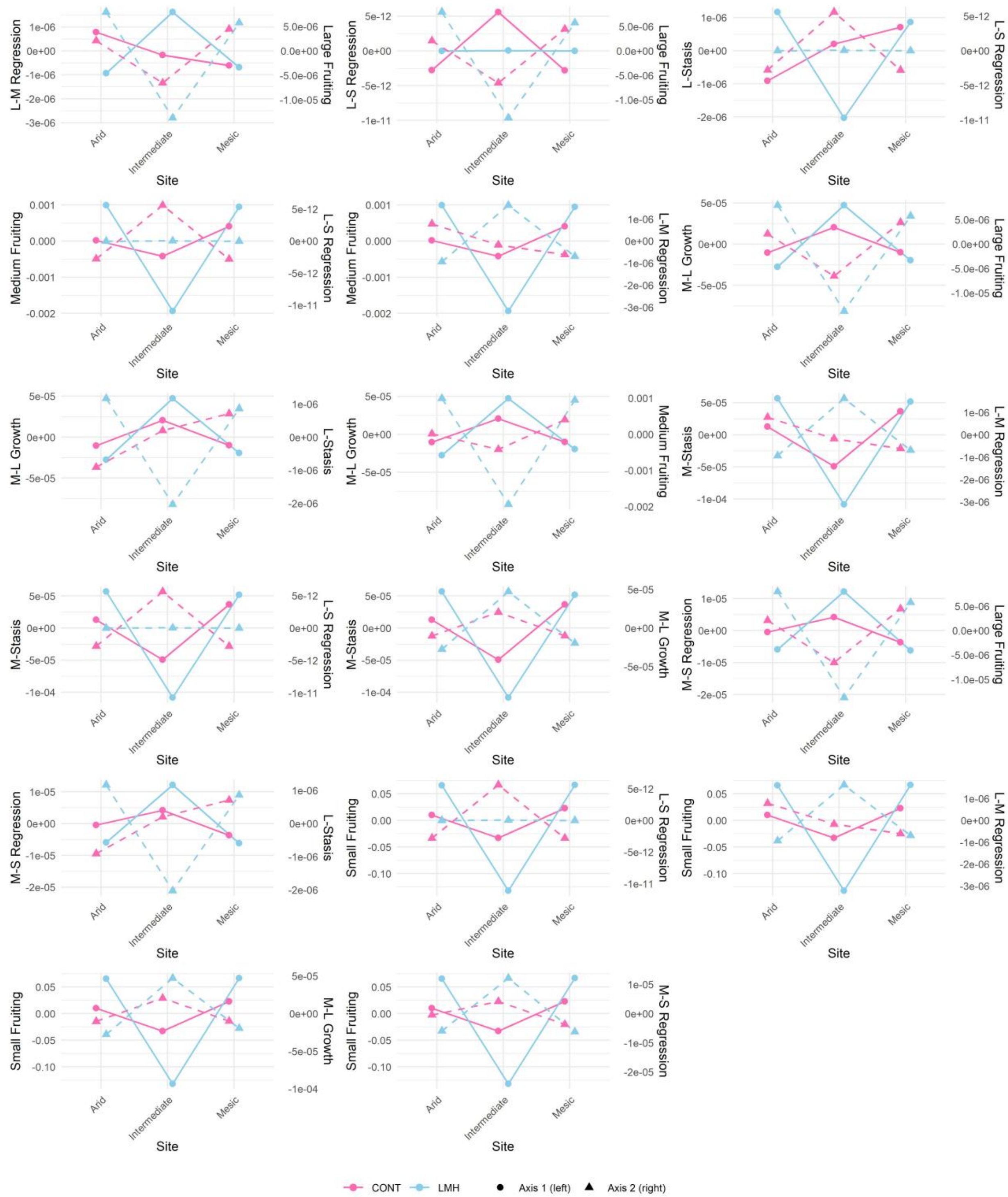

Appendix Figure A.3. Site-specific LTRE (life table response experiment) values for pairs of vital rates that were significantly negatively correlated under the LMH treatment (blue; complete exclusion of large mammalian herbivores) and uncorrelated in the CONT

treatment (pink; all herbivores included). Each point represents the LTRE value for a single vital rate at a given site, with circle points corresponding to the left y-axis (y_1) and triangle points corresponding to the right y-axis (y_2). Lines connect points of the same vital rate/herbivore treatment across sites (solid = y_1, dashed = y_2). These panels illustrate how patterns of site-specific vital rate covariation differ between treatments, which in turn affects the ability of *H. meyeri* to exhibit demographic compensation.

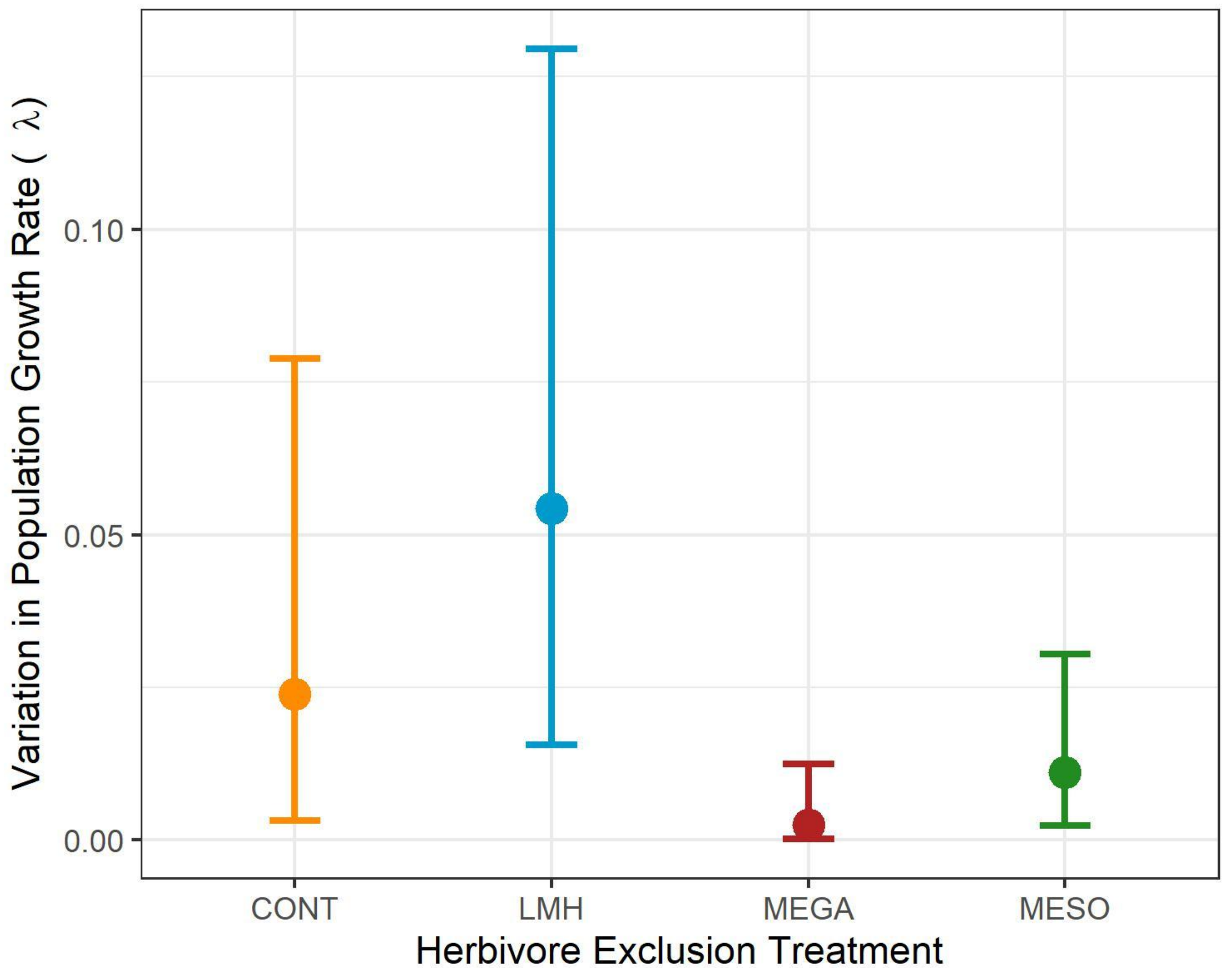

Appendix Figure A.4. Spatial variation in population growth rate (λ) for herbivore exclusion treatments. To test whether demographic compensation resulted in significant decreases in spatial variation in population growth rate, we asked whether herbivore exclusion treatments that showed demographic compensation exhibited significantly lower spatial variation in population growth rate than those that did not. Namely, we calculated the variance in population growth rate across rainfall levels within each treatment for each of 10,000 sets of model coefficients that represented parameter uncertainty (similar to our approach in "Modeling demographic rates and population growth rates"), then compared the mean and 95% confidence intervals of the variance in population growth rate across herbivore exclusion treatments. Here, we show the across-rainfall level variance in log-transformed λ. Herbivore exclusion treatments are the presence of all large mammalian herbivores (“Control”), the complete absence of large mammalian herbivores (“LMH”), the absence of megaherbivores (“MEGA”, and the absence of meso- and mega- herbivores (“MESO”); of these four treatments, MESO, MEGA and control expressed evidence for demographic compensation. Error bars indicate 95% confidence intervals (CIs) of log-transformed spatial variation, where CIs incorporate parameter uncertainty in demographic rate functions.

Appendix B - Chapter 3 Appendices

Testing for Efficacy of Competition Treatments

We used a model selection approach to test for effects of competition treatment, rainfall treatment, and their interaction on the percent change in brome cover (averaged across quadrats) from year 1 to year 2. We used plot as a random effect. This time period included April 2023 — March 2024, with percent cover measured before the March 2024 removal of aboveground vegetation in seed addition subplots. We did not measure brome cover in plug addition subplots in year 2, because these subplots experienced some soil disturbance from planting. We compared all possible subsets of this global model and present results from the best-fit model according to AICc (Burnham & Anderson, 2002). The best-fitting model describing the change in brome cover included competition treatment (model weight=0.6; Appendix Table B.1; Appendix Table B.6). Brome cover was more reduced in the low competition treatment (mean = -48%, SE= 5.58) vs. the high competition treatment (mean = -17.4, SE=4.41) and similar in the reduced rainfall treatment vs. the ambient rainfall treatment (Appendix Table B.6, Appendix Figure B.1). Thus, we found that our competition treatments were effective at reducing brome cover, but the effect size of the competition treatment did not differ significantly with rainfall treatment.

Appendix Table B.1. Dredge results for model of smooth brome percent cover change (2023-2024) in seed addition subplots. The global model included competition treatment (Comp), rainfall treatment (Dr), and their interaction, with plot identity as a random effect. Percent cover change was calculated from April 2023 to March 2024. All subsets of the global model were ranked using AICc. The table reports, for each candidate model, the degrees of freedom (df), the log likelihood (logLik), the small-sample corrected Akaike Information Criterion (AICc), the difference between each model's AICc and that of the top-ranked model (delta), and the Akaike weight (weight), which reflects the relative support for that model.

Intercept	*Comp*	*Dr*	*Comp:Dr*	*df*	*logLik*	*AICc*	*delta*	*weight*
-48.03	30.64	NA	NA	4	-372.16	762.34	0	6.05E-01
-43.84	30.64	-8.38	NA	5	-368.60	763.76	1.43	2.96E-01
-44.53	32.02	-6.99	-2.77	6	-365.53	765.98	3.64	9.81E-02
-32.71	NA	NA	NA	3	-392.66	796.51	34.18	2.29E-08
-28.52	NA	-8.38	NA	4	-389.10	797.89	35.56	1.15E-08

Appendix Table B.2. Dredge results for model of first growing season plug survival (June 2023-September 2023). The global model included competition treatment (Comp), rainfall treatment (Dr), species identity (Spp), and all two-way interactions among these predictors, with plot identity included as a random effect and a binomial error distribution. Data from germination controls and seed-addition subplots were excluded. All subsets of the global model were ranked using AICc. The table reports, for each candidate model, the degrees of freedom (df), the log likelihood (logLik), the small-sample corrected Akaike Information Criterion (AICc), the difference between each model's AICc and that of the top-ranked model (delta), and the Akaike weight (weight), which reflects the relative support for that model.

Intercept	*Comp*	*Dr*	*Spp*	*Comp:Dr*	*Comp:Spp*	*Dr:Spp*	*df*	*logLik*	*AICc*	*delta*	*weight*
-0.24	-1.03	NA	+	NA	+	NA	11	-551.12	1124.49	0.00	5.26E-01
-0.12	-1.03	-0.25	+	NA	+	NA	12	-550.72	1125.72	1.24	2.84E-01
-0.04	-1.18	-0.41	+	0.32	+	NA	13	-550.19	1126.72	2.23	1.73E-01
0.00	-1.05	-0.49	+	NA	+	+	16	-549.99	1132.49	8.00	9.62E-03
0.08	-1.22	-0.65	+	0.37	+	+	17	-549.34	1133.26	8.77	6.56E-03
0.35	-2.55	NA	+	NA	NA	NA	7	-561.61	1137.33	12.84	8.55E-04
0.48	-2.55	-0.26	+	NA	NA	NA	8	-561.16	1138.46	13.97	4.88E-04
0.55	-2.69	-0.40	+	0.28	NA	NA	9	-560.74	1139.64	15.15	2.70E-04
0.67	-2.55	-0.66	+	NA	NA	+	12	-560.27	1144.83	20.34	2.02E-05
0.72	-2.70	-0.75	+	0.29	NA	+	13	-559.88	1146.09	21.60	1.07E-05
1.10	-2.30	NA	NA	NA	NA	NA	3	-604.07	1214.16	89.67	1.77E-20
1.22	-2.30	-0.25	NA	NA	NA	NA	4	-603.59	1215.22	90.73	1.04E-20
1.29	-2.42	-0.37	NA	0.25	NA	NA	5	-603.22	1216.50	92.01	5.52E-21
-0.69	NA	NA	+	NA	NA	NA	6	-715.71	1443.50	319.01	2.81E-70
-0.60	NA	-0.19	+	NA	NA	NA	7	-715.26	1444.63	320.14	1.60E-70
-0.48	NA	-0.45	+	NA	NA	+	11	-714.59	1451.42	326.93	5.36E-72
-0.04	NA	NA	NA	NA	NA	NA	2	-745.89	1495.79	371.30	1.24E-81
0.05	NA	-0.1846	NA	NA	NA	NA	3	-745.41	1496.84	372.35	7.34E-82

Appendix Table B.3. Dredge results for model of annual survival (September 2023-November 2024). The global model included competition treatment (Comp), rainfall treatment (Dr), species identity (Spp), and all two-way interactions among these predictors, with plot identity (Plot) included as a random effect and a binomial error distribution. Germination controls and seed-addition subplots were excluded. All subsets of the global model were evaluated using AICc. For each candidate model, the table provides the degrees of freedom (df), the log likelihood (logLik), the corrected Akaike Information Criterion (AICc), the difference between each model's AICc and that of the best-fitting model (delta), and the Akaike weight (weight), indicating the relative support for that model.

Intercept	*Comp*	*Dr*	*Spp*	*Comp:Dr*	*Comp:Spp*	*Dr:Spp*	*df*	*logLik*	*AICc*	*delta*	*weight*
-0.03	-0.63	-0.53	+	NA	NA	NA	8	-346.29	708.86	0	3.57E-01
-0.08	-0.42	-0.43	+	-0.45	NA	NA	9	-345.77	709.89	1.03	2.13E-01
-0.29	-0.64	NA	+	NA	NA	NA	7	-348.00	710.20	1.34	1.83E-01
-0.43	-0.63	0.49	+	NA	NA	+	12	-343.72	712.04	3.18	7.29E-02
-0.51	-0.40	0.67	+	-0.53	NA	+	13	-343.03	712.76	3.90	5.08E-02
-0.28	0.07	-0.54	+	NA	+	NA	12	-344.34	713.28	4.41	3.93E-02
-0.31	0.22	-0.44	+	-0.41	+	NA	13	-343.90	714.51	5.64	2.12E-02
-0.55	0.09	NA	+	NA	+	NA	11	-346.03	714.57	5.71	2.06E-02
-0.24	NA	-0.52	+	NA	NA	NA	7	-350.34	714.90	6.04	1.75E-02
-0.50	NA	NA	+	NA	NA	NA	6	-352.11	716.38	7.51	8.34E-03
-0.69	0.09	0.49	+	NA	+	+	16	-341.73	716.51	7.65	7.78E-03
-0.77	0.30	0.68	+	-0.52	+	+	17	-341.07	717.33	8.47	5.18E-03
-0.63	NA	0.46	+	NA	NA	+	11	-347.80	718.11	9.25	3.50E-03
0.51	-0.56	-0.50	NA	NA	NA	NA	4	-358.70	725.48	16.62	8.77E-05

0.46	-0.37	-0.40	NA	-0.43	NA	NA	5	-358.20	726.52	17.65	5.24E-05
0.26	-0.57	NA	NA	NA	NA	NA	3	-360.52	727.08	18.22	3.94E-05
0.36	NA	-0.49	NA	NA	NA	NA	3	-362.28	730.60	21.74	6.79E-06
0.12	NA	NA	NA	NA	NA	NA	2	-364.15	732.33	23.47	2.86E-06

Appendix Table B.4. Dredge results for model of corrected germinant counts. Corrected germinant counts were obtained by subtracting species-specific background germination from observed germination in seed-addition subplots. The global model included competition treatment (Comp), rainfall treatment (Dr), species identity (Spp), and all two-way interactions among these predictors, with plot identity (Plot) included as a random effect and a negative binomial distribution. Data for ANGE, SCSC, and SONU were excluded due to extremely low corrected germinant counts that prevented model convergence. All subsets of the global model were compared using AICc. The table reports, for each candidate model, the degrees of freedom (df), the log likelihood (logLik), the corrected Akaike Information Criterion (AICc), the difference between each model's AICc and the top-ranked model (delta), and the Akaike weight (weight), which represents the relative support for each model.

Intercept	*Comp*	*Dr*	*Spp*	*Comp:Dr*	*Comp:Spp*	*Dr:Spp*	*df*	*logLik*	*AICc*	*delta*	*weight*
0.06	0.11	0.82	NA	-1.5163477	NA	NA	6	-195.71	404.07	0	1.50E-01
0.41	-0.13	NA	+	NA	+	NA	6	-195.77	404.20	0.13	1.40E-01
-0.14	0.55	0.85	+	-1.28	+	NA	8	-193.63	404.39	0.32	1.28E-01
0.55	-0.68	NA	NA	NA	NA	NA	4	-198.28	404.87	0.80	1.00E-01
0.20	0.00	0.31	+	NA	+	NA	7	-195.39	405.65	1.59	6.78E-02
0.05	0.45	0.54	+	-1.23	+	+	9	-193.22	405.86	1.79	6.11E-02
0.19	0.02	0.81	+	-1.44	NA	NA	7	-195.50	405.87	1.81	6.07E-02
0.75	-0.76	NA	+	NA	NA	NA	5	-197.80	406.07	2.00	5.52E-02

0.27	NA	NA	NA	NA	NA	NA	3	-200.22	406.62	2.55	4.18E-02
0.45	-0.15	-0.06	+	NA	+	+	8	-194.84	406.81	2.74	3.80E-02
0.47	-0.64	0.12	NA	NA	NA	NA	5	-198.23	406.92	2.85	3.61E-02
0.43	-0.13	0.40	+	-1.28	NA	+	8	-195.02	407.17	3.10	3.18E-02
0.11	NA	0.29	NA	NA	NA	NA	4	-199.85	408.01	3.94	2.09E-02
0.66	-0.72	0.16	+	NA	NA	NA	6	-197.70	408.06	3.99	2.04E-02
0.96	-0.84	-0.35	+	NA	NA	+	7	-196.65	408.18	4.11	1.92E-02
0.34	NA	NA	+	NA	NA	NA	4	-200.11	408.53	4.46	1.61E-02
0.19	NA	0.32	+	NA	NA	NA	5	-199.69	409.83	5.76	8.39E-03
0.34	NA	1.94E-07	+	NA	NA	+	6	-199.23	411.10	7.03	4.45E-03

Appendix Table B.5. Dredge results for model of early life success. Early life success was calculated as the product of corrected germination rates, growing-season survival, and annual survival. The global model included competition treatment (Comp), rainfall treatment (Dr), species identity (Spp), and all two-way interactions among these predictors, and was fit using a zero-inflated beta distribution with plot identity (Plot) included as a random effect. All subsets of the global model were ranked using AICc. For each candidate model, the table lists the degrees of freedom (df), the log likelihood (logLik), the small-sample corrected Akaike Information Criterion (AICc), the difference between each model's AICc and that of the best model (delta), and the Akaike weight (weight), indicating the relative support for that model.

Intercept	*Zi Intercept*	*Comp*	*Dr*	*Spp*	*Comp:Dr*	*Comp:Spp*	*Dr:Spp*	*df*	*logLik*	*AICc*	*delta*	*weight*
-6.00	1.34	-1.34	-1.37	+	-1.19	+	+	19	702.78	-1366.84	0.00	1
-7.67	1.34	0.36	0.80	+	-1.21	+	NA	15	669.45	-1308.44	58.40	2.08E-13
-6.00	1.34	-1.32	-1.39	+	NA	+	+	18	654.85	-1273.06	93.79	4.31E-21
-6.04	1.34	-1.04	-1.16	+	-0.33	NA	+	15	632.26	-1234.08	132.76	1.48E-29
-5.97	1.34	-1.23	-1.21	+	NA	NA	+	14	628.35	-1228.31	138.54	8.26E-31
-7.49	1.34	-0.13	0.67	+	NA	+	NA	14	614.83	-1201.27	165.57	1.11E-36
-7.20	1.34	-0.15	NA	+	NA	+	NA	13	592.85	-1159.36	207.48	8.83E-46
-7.24	1.34	-0.76	0.76	+	-0.68	NA	NA	11	562.51	-1102.78	264.07	4.56E-58
-7.13	1.34	-1.14	0.68	+	NA	NA	NA	10	550.11	-1080.02	286.82	5.22E-63
-6.69	1.34	-1.03	NA	+	NA	NA	NA	9	507.46	-996.76	370.08	4.34E-81
-6.33	1.34	NA	-0.54	+	NA	NA	+	13	477.32	-928.31	438.53	5.94E-96
-6.85	1.34	NA	0.52	+	NA	NA	NA	9	450.94	-883.72	483.13	1.23E-105
-6.56	1.34	NA	NA	+	NA	NA	NA	8	438.93	-861.72	505.12	2.06E-110
-4.65	1.34	-0.67	-0.19	NA	NA	NA	NA	6	333.48	-654.87	711.97	2.50E-155
-4.63	1.34	-0.78	-0.25	NA	0.30	NA	NA	7	334.13	-654.16	712.68	1.75E-155
-4.74	1.34	-0.64	NA	NA	NA	NA	NA	5	331.85	-653.65	713.19	1.36E-155
-4.87	1.34	NA	NA	NA	NA	NA	NA	4	318.21	-628.39	738.45	4.43E-161
-4.83	1.34	NA	-0.10	NA	NA	NA	NA	5	318.63	-627.20	739.64	2.45E-161

Appendix Table B.6. Coefficients of best-fit model describing smooth brome percent cover change (2023-2024) in seed addition subplots. *Effect* indicates if a term was fixed or random. *Term* indicates the predictor variable. *Estimate* gives the regression coefficient. *Std. Error* is the standard error. *T-value* measures the effect size. *Lower CI* and *Upper CI* show the 95% confidence interval bounds. The *Variance* and *Std. Dev* columns show the variance and standard deviation for random effects. The low competition treatment was the reference condition for the competition effect.

Effect	*Term*	*Estimate*	*Std. Error*	*t-value*	*Lower CI*	*Upper CI*	*Variance*	*Std. Dev*
Fixed	Intercept	-48.04	5.03	-9.55	-57.89	-38.17	-	-
Fixed	High competition	30.64	4.03	7.61	22.74	38.53	-	-
random	Plot (intercept)	-	-	-	-	-	687.34	26.22
random	Residual	-	-	-	-	-	324.45	18.01

Appendix Table B.7. Coefficients of best-fit model for first growing season plug survival (June 2023-September 2023). We list coefficients in the best fit model; *Effect* indicates if a term was fixed or random, *Term* indicates the coefficient name, *Estimate* gives the estimated coefficient, *Std. Error* is the standard error, *z-value* measures the effect size, and *Lower CI* and *Upper CI* show the 95% confidence interval on the coefficient estimates. The *Variance* and *Std. Dev* columns show the variance and standard deviation for random effects. Native grass species included in the Species term are big bluestem (*Andropogon gerardii*, ANGE; here, ANGE is the reference condition for the species effect, such that the estimate for Species (ANGE) = 0), sideoats grama (*Bouteloua curtipendula*, BOCU), blue grama (*Bouteloua gracilis*, BOGR), little bluestem (*Schizachyrium scoparium*, SCSC), and Indiangrass (*Sorghastrum nutans*, SONU). Low competition treatment was the reference condition for the competition effect. The AICc weight of this best-fit model was 0.53.

Effect	*Term*	*Estimate*	*Std. Error*	*z-value*	*Lower CI*	*Upper CI*	*Variance*	*Std. Dev*
Fixed	Intercept	-0.24	0.29	-0.84	-0.80	0.32	-	-
Fixed	High competition	-1.03	0.40	-2.61	-1.81	-0.26	-	-
Fixed	Species (BOCU)	2.72	0.55	4.96	1.64	3.79	-	-
Fixed	Species (BOGR)	2.33	0.40	5.84	1.55	3.11	-	-
Fixed	Species (SCSC)	0.72	0.31	2.30	0.11	1.33	-	-
Fixed	Species (SONU)	2.06	0.36	5.77	1.36	2.76	-	-
Fixed	High competition:Species (BOCU)	-2.93	0.71	-4.14	-4.32	-1.54	-	-

Effect	*Term*	*Estimate*	*Std. Error*	*z-value*	*Lower CI*	*Upper CI*	*Variance*	*Std. Dev*
Fixed	High competition:Species (BOGR)	-1.59	0.54	-2.95	-2.65	-0.53	-	-
Fixed	High competition:Species (SCSC)	-1.66	0.50	-3.32	-2.64	-0.68	-	-
Fixed	High competition:Species (SONU)	-1.63	0.49	-3.30	-2.60	-0.66	-	-
Random	Plot (intercept)	-	-	-	-	-	0.46	0.68

Appendix Table B.8. Coefficients for the best-fit model for annual survival (September 2023-November 2024). We list only coefficients present in the best fit model. *Effect* indicates if a term was fixed or random, *Term* indicates the coefficient name, *Estimate* gives the estimated coefficient, *Std. Error* is the standard error, *z-value* measures the effect size, and *Lower CI* and *Upper CI* show the 95% confidence interval on the coefficient estimates. The *Variance* and *Std. Dev* columns show the variance and standard deviation for random effects. Native grass species included in the Species term are big bluestem (*Andropogon gerardii*, ANGE; here, ANGE is the reference condition for the species effect, such that the estimate for Species (ANGE) = 0), sideoats grama (*Bouteloua curtipendula*, BOCU), blue grama (*Bouteloua gracilis*, BOGR), little bluestem (*Schizachyrium scoparium*, SCSC), and Indiangrass (*Sorghastrum nutans*, SONU). For this analysis, N=1088 and the number of plots= 34. The low competition and ambient rainfall treatments were the reference conditions for the competition and rainfall effects respectively. The AICc weight of the best fit model was 0.36.

Effect	*Term*	*Estimate*	*Std. Error*	*z-value*	*Lower CI*	*Upper CI*	*Variance*	*Std. Dev*
Fixed	Intercept	-0.028	0.37	-0.075	-0.75	0.70	-	-
Fixed	High competition	-0.63	0.22	-2.82	-1.07	-0.19	-	-
Fixed	Drought	-0.53	0.28	-1.90	-1.08	0.017	-	-
Fixed	Species (BOCU)	1.02	0.43	2.39	0.18	1.86	-	-

Effect	*Term*	*Estimate*	*Std. Error*	*z-value*	*Lower CI*	*Upper CI*	*Variance*	*Std. Dev*
Fixed	Species (BOGR)	1.27	0.39	3.29	0.51	2.02	-	-
Fixed	Species (SCSC)	0.22	0.38	0.57	-0.53	0.96	-	-
Fixed	Species (SONU)	0.28	0.36	0.77	-0.43	0.99	-	-
Random	Plot (Intercept)	-	-	-	-	-	0.36	0.60

Appendix Table B.9. Coefficients of the best-fit model for corrected germinant counts. We list only coefficients present in the best fit model. *Effect* indicates if a term was fixed or random, *Term* indicates the coefficient name, *Estimate* gives the estimated coefficient, *Std. Error* is the standard error, *z-value* measures the effect size, and *Lower CI* and *Upper CI* show the 95% confidence interval on the coefficient estimates. The *Variance* and *Std. Dev* columns show the variance and standard deviation for random effects. The low competition and ambient rainfall treatments were the reference conditions for the competition and rainfall effects respectively. The best-fit model weight=0.15.

Effect	*Term*	*Estimate*	*Std. Error*	*z-value*	*Lower CI*	*Upper CI*	*Variance*	*Std. Dev*
Fixed	Intercept	0.06	0.33	0.17	-0.59	0.70	-	-
Fixed	High competition	0.11	0.46	0.23	-0.8	1.01	-	-
Fixed	Reduced rainfall	0.82	0.45	1.83	-0.06	1.70	-	-
Fixed	High competition :Reduced rainfall	-1.52	0.66	-2.29	-2.82	-0.22	-	-
Random	Plot (intercept)	-	-	-	-	-	5.22e-09	7.22 e-05

Appendix Table B.10. Coefficients of best-fit model for early life success. We show only coefficients present in the best-fit model. *Effect* indicates if a term was fixed or random, *Term* indicates the coefficient name, *Estimate* gives the estimated coefficient, *Std. Error* is the standard error, *z-value* measures the effect size, and *Lower CI* and *Upper CI* show the 95% confidence interval on the coefficient estimates. The *Variance* and *Std. Dev* columns show the variance and standard deviation for random effects. Native grass species included in this analysis are sideoats grama (*Bouteloua curtipendula*, BOCU), blue grama (*Bouteloua gracilis*, BOGR), Big bluestem (*Andropogon gerardii*, ANGE), little bluestem (*Schizachyrium scoparium*, SCSC), and Indiangrass (*Sorghastrum nutans*, SONU). For this analysis, N=1088 and the number of plots=34. The low competition treatment the reference condition for the competition effect, ambient rainfall was the reference condition for the rainfall effect, and ANGE was the reference condition for species effect. The AICc weight of the best fit model was 1.

Effect	Term	Estimate	Std. Error	z-value	Lower CI	Upper CI	Variance	Std. Dev
Fixed	(Intercept—Conditional)	-6.00	0.13	-47.70	-6.24	-5.75	-	-
Fixed	High competition	-1.34	0.25	-5.43	-1.83	-0.86	-	-
Fixed	Drought	-1.37	0.23	-6.11	-1.82	-0.93	-	-
Fixed	Species (BOCU)	1.08	0.13	8.34	0.83	1.33	-	-
Fixed	Species (BOGR)	1.36	0.127	10.70	1.11	1.61	-	-
Fixed	Species (SCSC)	0.63	0.13	4.82	0.38	0.89	-	-
Fixed	Species (SONU)	-2.26	0.30	-7.62	-2.84	-1.68	-	-

Effect	Term	Estimate	Std. Error	z-value	Lower CI	Upper CI	Variance	Std. Dev
Fixed	High competition:Drought	-1.19	0.15	-8.00	-1.48	-0.90	-	-
Fixed	High competition:Species (BOCU)	1.87	0.26	7.14	1.36	2.39	-	-
Fixed	High competition:Species (BOGR)	0.37	0.25	1.46	-0.13	0.87	-	-
Fixed	High competition:Species (SCSC)	-0.15	0.31	-0.50	-0.76	0.45	-	-
Fixed	High competition:Species (SONU)	3.13	0.35	8.91	2.44	3.82	-	-
Fixed	Drought:Species (BOCU)	2.25	0.23	9.91	1.81	2.70	-	-
Fixed	Drought:Species (BOGR)	2.15	0.23	9.55	1.71	2.60	-	-
Fixed	Drought:Species (SCSC)	2.39	0.38	6.25	1.64	3.14	-	-
Fixed	Drought:Species (SONU)	2.19	0.33	6.66	1.55	2.84	-	-
Fixed	(Intercept—Zero infl.)	1.34	0.075	18.00	1.20	1.49	-	-
Random	Plot (Intercept)	-	-	-	-	-	0.0033	0.057

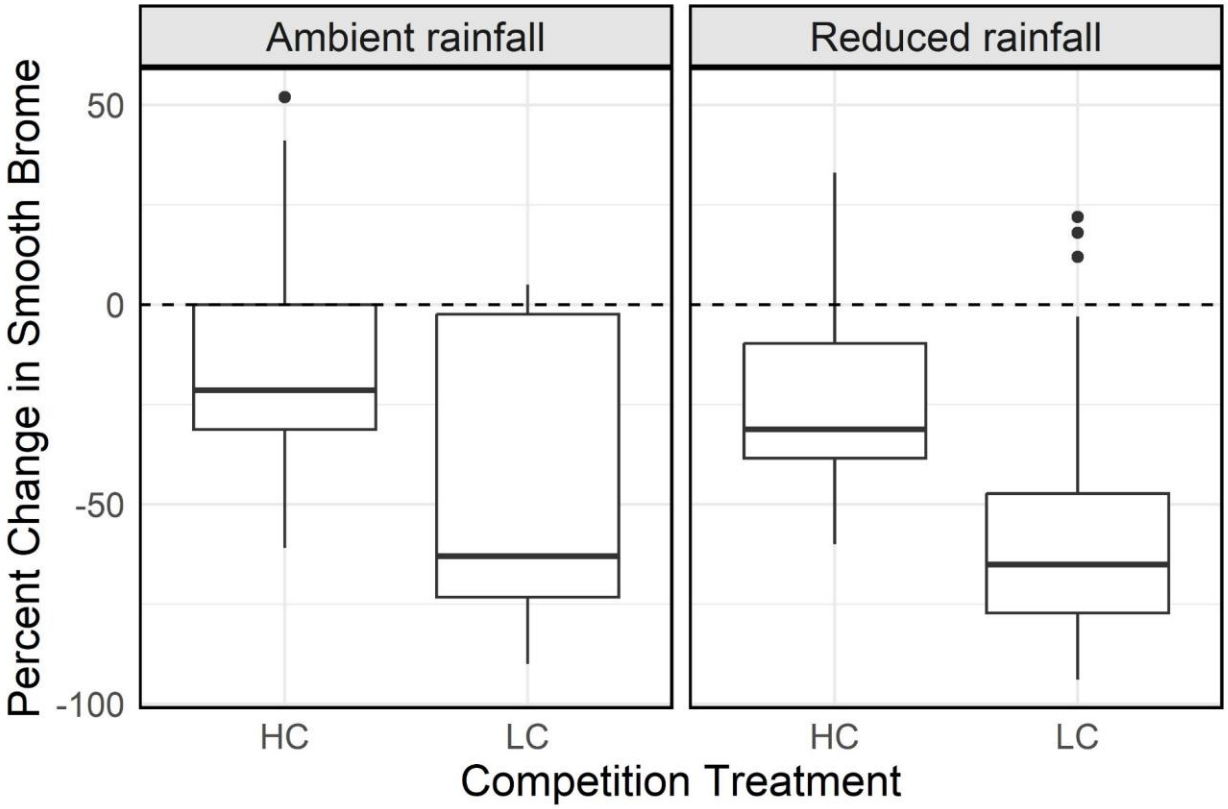

Appendix Figure B.1. Percent change in brome (*Bromus inermis*) percent cover from 2023-2024 across rainfall and competition treatments. Here, we show a boxplot of percent change in brome cover from April 2023 to March 2024 in “Low competition” (LC) treatments, where aboveground brome cover was reduced via cutting and herbicide, and “High competition” (HC) treatments, where brome cover was not reduced. “Ambient rainfall” indicates plots which were not subject to treatment with rainout shelters, and “Reduced rainfall” indicates plots which were subject to rainout shelters. Dark lines indicate sample medians, lower and upper box edges indicate the 25^{th} and 75^{th} quartiles respectively, lines represent the spread (maxima and minima of Q1 and Q3), and dots indicate outliers. Dotted lines represent 0% change in brome cover.

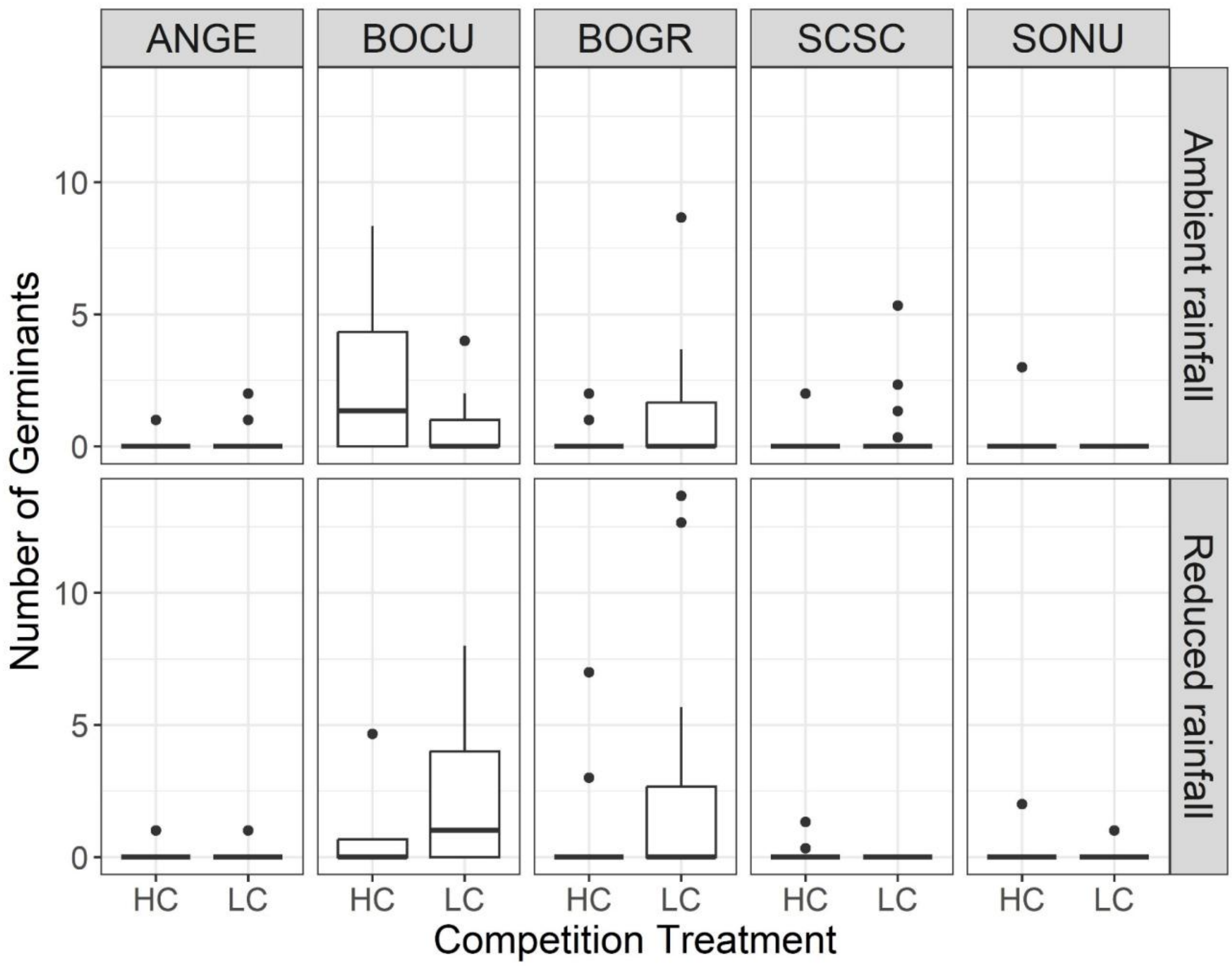

Appendix Figure B.2. Effect of competition and rainfall treatments on corrected germinant count. "Low competition" (LC) indicates that aboveground brome cover was reduced via cutting and herbicide, and "High competition" (HC) treatments indicates ambient brome cover. "Reduced rainfall" indicates plots that were under rainout shelters that reduced ~66% of ambient rainfall, and "Ambient rainfall" indicates plots that receieved ambient rainfall. Dark lines indicate sample medians, lower and upper box edges indicate the 25th and 75th quartiles respectively, lines represent the spread (maxima and minima of Q1 and Q3), and dots indicate outliers.

Appendix C - Chapter 4 Appendices

Appendix Table C.1 Sites where data on eastern redcedar (ERC) were collected. *Location* describes the name of an area, which is based on the park/refuge/preserve/research station where data collection occurred. Each site is assigned a unique code corresponding to its location and the number of unique sites at that location (*Site*). Latitude (*Lat*) and longitude (*Long*) are reported in decimal degrees. *Temperature type* and *Precipitation type* are based on mean annual temperature data and mean annual precipitation data from WorldClim for 1970–2000. For temperature types, sites which are, on average, < 9ºC annually are cold, 9-13 ºC are moderate, and >13 ºC are hot. For precipitation types, sites receiving <500 mm of annual rainfall are classified as “dry,” sites with 500–700 mm as “moderate,” and sites with >700 mm as “wet.” *Burn years* indicate years with known large-scale fires that affected the entire data collection area, based on site burn records or communications with land managers. Sites with no known large-scale fires in the past 50 years are fire-suppressed, with “≥50 years” indicating no recorded fires within that time frame (though older burns may have occurred). Sites with both known recent burns and an earlier period of fire suppression list burn years followed by “≥50 years.” *Cattle presence* reflects site grazing history: “none” indicates no cattle throughout the recorded history, “constant” indicates long-term uninterrupted cattle presence, and “variable” indicates mixed use over time (periods with and without cattle).

Location	Site	Lat	Long	Temperature Type	Precipitation type	Burn years	Cattle presence
Alabaster Caverns State Park	ALA1	36.69872	-99.14997	Hot	Moderate	≥50 years	None
Bessey Recreational Area	BESS1	41.88472	-100.3602	Cold	Moderate	≥50 years	Constant

Bessey Recreational Area	BESS2	41.88472	-100.3602	Cold	Moderate	2022, ≥50 years	Variable
Bessey Recreational Area	BESS3	41.88472	-100.3602	Cold	Moderate	2022, ≥50 years	Constant
Bessey Recreational Area	BESS4	41.88472	-100.3602	Cold	Moderate	2017, 1965, ≥50 years	Constant
Cedar Bluff State Park	CB1	38.77533	-99.78108	Moderate	Moderate	≥50 years	None
Cedar Bluff State Park	CB2	38.77533	-99.78108	Moderate	Moderate	1995, ≥50 years	Variable
Konza Prairie Biological Station	KPBS1	39.07472	-96.57758	Moderate	Wet	2017, 1991, 1973, ≥50 years	None
Konza Prairie Biological Station	KPBS2	39.07472	-96.57758	Moderate	Wet	2012, 1991, 1973, ≥50 years	None
Lonsinger Sustainability Farm	LS1	39.51097	-99.0015	Moderate	Moderate	≥50 years	Constant
McKelvie National Forest	MCK1	42.77738	-101.07982	Cold	Dry	≥50 years	Constant
Fort Niobrara National Wildlife Refuge	NIO1	42.90486	-100.48471	Cold	Dry	≥50 years	None
Tallgrass Prairie National Preserve	TAPR1	38.43404	-96.56014	Moderate	Wet	≥50 years	None

Appendix Table C.2. **Site-specific chronology metrics for *Juniperus virginiana* (eastern red cedar).** Here, we show the number of cores used to build site-specific chronologies, as well as mean sensitivity and mean interseries correlation (± SD). Mean sensitivity reflects the relative year-to-year variability in ring-width indices (RWI), while interseries correlation represents the degree of common growth signal among trees within each site. Finally, we show the mean number of recorded false rings across core samples.

Site	Number of cores	Mean Sensitivity	Interseries Correlation (mean ± SD)	Mean # false rings per sample
Konza Prairie Biological Station	27	0.84	0.39 ± 0.11	11.5
McKelvie National Forest	10	0.78	0.35 ± 0.15	4.5
Cedar Bluff	10	0.78	0.37 ± 0.11	4.75
Tallgrass Prairie National Preserve	8	0.73	0.35 ± 0.14	9.5
Alabaster Caverns State Park	11	0.73	0.38 ± 0.10	15.5
Bessey Recreational Area	31	0.71	0.36 ± 0.16	2.5
Fort Niobrara National Wildlife Refuge	24	0.69	0.55 ± 0.19	16.5
Lonsinger Sustainability Farm	22	0.68	0.41 ± 0.15	5.67

Appendix Table C.3. Comparison of generalized linear models (gamma, log link) predicting tree age (*Age*) as a function of log-scaled height (*Height*) and diameter (*Diameter*) in *Juniperus virginiana* (eastern red cedar), where both variables were originally measured in centimeters. The models in this table explore different polynomial structures for height and diameter (linear, quadratic, cubic) to identify the functional forms best supported by the data. Degrees of freedom (df) and corrected Akaike's Information Criterion (AICc) are reported for each model, with lower AICc values indicating stronger support. Site is included as a fixed effect in all models.

Model	df	AICc
Age ~ Height + I($Height^2$) + I($Height^3$) + Diameter + I($Diameter^2$) + I($Diameter^3$) + Site	15	1770.276
Age ~ Height + I($Height^2$) + Diameter + I($Diameter^2$) + I($Diameter^3$) + Site	14	1772.703
Age ~ Height + I($Height^2$) + I($Height^3$) + Diameter + Site	13	1773.197
Age ~ Height + I($Height^2$) + I($Height^3$) + Diameter + I($Diameter^2$) + Site	14	1775.051
Age ~ Height + Diameter + I($Diameter^2$) + I($Diameter^3$) + Site	13	1778.733
Age ~ Height + Diameter + I($Diameter^2$) + Site	12	1786.47
Age ~ Height + I($Height^2$) + Diameter + Site	12	1787.221
Age ~ Height + I($Height^2$) + Diameter + I($Diameter^2$) + Site	13	1787.358
Age ~ Diameter + Site	10	1789.38
Age ~ Height + Diameter + Site	11	1790.199
Age ~ Height + Site	10	1834.251

Appendix Table C.4. Table describing size-age relationship fit using sizes and dendrochronological data across sites. This function was used to predict the ages for remaining trees at sites which lacked dendrochronological ages. The model was fit using a generalized linear model with a Gamma distribution and a log link response, including first, second, and third order polynomial terms for scaled height and diameter values (originally measured in cm) and site as a categorical predictor. Columns report the model term ("Term"), estimated coefficient ("Estimate"), standard error ("Std. Error), t-value, p value, and 95% confidence intervals ("Lower 95% CI" and "Upper 95% CI"). The model was selected as the most parsimonious model (i.e., lowest AICc) from a set of models comparing various combinations of polynomial terms.

Term	Estimate	Std. Error	t-value	p value	Lower 95% CI	Upper 95% CI
Height	3.937	2.402	1.639	0.102	-0.871	8.672
I(Height^2)	-0.929	0.510	-1.821	0.070	-1.934	0.089
I(Height^3)	0.071	0.035	2.056	0.041	0.002	0.140
Diameter	1.453	0.443	3.282	0.001	0.587	2.321
I(Diameter^2)	-0.551	0.211	-2.607	0.010	-0.978	-0.128
I(Diameter^3)	0.081	0.032	2.560	0.011	0.017	0.146
site (ALA)	-3.427	3.639	-0.942	0.347	-10.593	3.871
site (BESS)	-4.168	3.637	-1.146	0.253	-11.330	3.126
site (CB)	-4.083	3.638	-1.122	0.263	-11.248	3.215
site (KNZ)	-3.854	3.653	-1.055	0.292	-11.047	3.470
site (LS)	-3.806	3.639	-1.046	0.297	-10.977	3.497
site (MCK)	-3.836	3.634	-1.056	0.292	-10.990	3.451
site (NIO)	-4.011	3.635	-1.103	0.271	-11.164	3.274

Term	Estimate	Std. Error	t-value	p value	Lower 95% CI	Upper 95% CI
site (TAPR)	-3.864	3.657	-1.057	0.292	-11.069	3.475

Appendix Table C.5. Model selection results for generalized linear models (binomial) describing the probability of fruiting in *Juniperus virginiana* (eastern red cedar). The global model included tree age (“Age”), site-specific cattle presence (“Cattle”), mean annual temperature (“MAT”, °C), mean annual precipitation (“MAP”, cm), all two-way interactions among MAT, MAP, and age, and the age × cattle interaction. Models were ranked using Akaike’s Information Criterion corrected for small sample size (AICc); ΔAICc and AICc weights indicate relative support for each model. Climate data represent 1970–2000 averages obtained from WorldClim (Fick and Hijmans 2017). The best-supported model was used in subsequent analyses.

(Intercept)	Age	Cattle	MAT	MAP	Age:Cattle	Age:MAT	Age:MAP	MAT:MAP	df	logLik	AICc	delta	weight
-50.00	0.25	-	4.18	7.74	-	-0.02	0.02	-0.71	7.00	-197.00	407.00	0.00	5.62E-01
-58.40	0.25	-0.38	4.92	9.34	-	-0.02	0.02	-0.85	8.00	-196.00	409.00	1.43	2.74E-01
-58.40	0.26	-0.31	4.91	9.32	0.00	-0.02	0.02	-0.85	9.00	-196.00	411.00	3.43	1.01E-01
-51.50	0.34	-	4.01	8.20	-	-0.02	-	-0.71	6.00	-201.00	413.00	5.62	3.37E-02
-59.20	0.35	-0.35	4.68	9.67	-	-0.02	-	-0.83	7.00	-200.00	415.00	7.17	1.56E-02
-59.70	0.42	0.35	4.72	9.45	-0.03	-0.02	-	-0.82	8.00	-200.00	415.00	7.76	1.16E-02
-3.90	0.25	1.03	0.21	-0.71	-	-0.02	0.02	-	7.00	-204.00	421.00	13.80	5.66E-04
-56.90	0.03	-1.38	4.67	10.10	0.05	-	0.01	-0.89	8.00	-203.00	423.00	15.10	2.97E-04
-46.40	0.15	-	3.53	8.04	-	-	-	-0.69	5.00	-207.00	423.00	15.60	2.29E-04
-4.35	0.27	1.22	0.23	-0.70	-0.01	-0.02	0.02	-	8.00	-204.00	423.00	15.70	2.22E-04
-45.80	0.10	-	3.59	7.91	-	-	0.01	-0.70	6.00	-206.00	424.00	16.40	1.51E-04

-53.50	0.15	-0.32	4.15	9.40	-	-	-	-0.81	6.00	-206.00	425.00	17.30	9.97E-05
-55.60	0.14	-0.91	4.34	9.85	0.03	-	-	-0.84	7.00	-205.00	425.00	17.40	9.29E-05
-53.20	0.10	-0.33	4.23	9.32	-	-	0.01	-0.81	7.00	-206.00	426.00	18.10	6.66E-05
-5.38	0.33	1.04	0.08	-0.28	-	-0.02	-	-	6.00	-207.00	426.00	18.40	5.79E-05
-6.98	0.40	1.76	0.21	-0.29	-0.04	-0.02	-	-	7.00	-206.00	426.00	18.50	5.30E-05
-5.74	0.31	1.25	-0.06	-	-	-0.01	-	-	5.00	-209.00	428.00	20.30	2.22E-05
-7.46	0.38	1.95	0.06	-	-0.03	-0.02	-	-	6.00	-208.00	428.00	20.80	1.75E-05
-2.67	0.27	-	0.15	-0.74	-	-0.02	0.02	-	6.00	-209.00	430.00	22.30	8.27E-06
-3.89	0.34	-	0.04	-0.37	-	-0.02	-	-	5.00	-212.00	434.00	26.30	1.09E-06
-2.31	0.15	1.21	-0.37	-	-	-	-	-	4.00	-213.00	435.00	27.20	6.91E-07
-0.25	0.05	0.35	-0.23	-0.48	0.04	-	0.01	-	7.00	-210.00	435.00	27.40	6.45E-07
-1.88	0.15	1.09	-0.28	-0.20	-	-	-	-	5.00	-212.00	435.00	27.50	6.11E-07
-2.11	0.14	0.81	-0.37	-	0.02	-	-	-	5.00	-213.00	436.00	28.10	4.42E-07
-1.71	0.14	0.69	-0.28	-0.20	0.02	-	-	-	6.00	-212.00	436.00	28.30	4.00E-07
-1.23	0.11	1.10	-0.26	-0.33	-	-	0.01	-	6.00	-212.00	436.00	28.70	3.32E-07
-0.99	0.01	0.43	-	-0.74	0.05	-	0.02	-	6.00	-213.00	438.00	30.40	1.43E-07
-3.57	0.31	-	-0.22	-	-	-0.01	-	-	4.00	-216.00	440.00	32.60	4.75E-08
-2.24	0.08	1.31	-	-0.61	-	-	0.01	-	5.00	-215.00	440.00	32.90	4.08E-08
-3.58	0.14	1.32	-	-0.40	-	-	-	-	4.00	-216.00	441.00	33.10	3.72E-08
-3.43	0.13	0.93	-	-0.40	0.02	-	-	-	5.00	-216.00	441.00	34.00	2.31E-08

-0.08	0.15	-	-0.35	-0.28	-	-	-	-	4.00	-218.00	445.00	37.50	4.13E-09
0.33	0.12	-	-0.34	-0.36	-	-	0.00	-	5.00	-218.00	447.00	39.10	1.85E-09
-0.26	0.15	-	-0.51	-	-	-	-	-	3.00	-220.00	447.00	39.50	1.48E-09
-6.51	0.14	1.92	-	-	-	-	-	-	3.00	-221.00	448.00	41.00	7.14E-10
-6.39	0.13	1.62	-	-	0.02	-	-	-	4.00	-221.00	450.00	42.30	3.64E-10
-1.76	0.14	-	-	-0.58	-	-	-	-	3.00	-226.00	457.00	49.80	8.51E-12
-0.70	0.08	-	-	-0.74	-	-	0.01	-	4.00	-225.00	457.00	50.00	7.90E-12
-5.73	0.14	-	-	-	-	-	-	-	2.00	-244.00	492.00	84.30	2.75E-19
-31.00	-	-	2.69	4.85	-	-	-	-0.46	4.00	-390.00	788.00	380.00	1.64E-83
-2.06	-	1.03	0.16	-0.57	-	-	-	-	4.00	-390.00	788.00	380.00	1.48E-83
-18.20	-	0.58	1.56	2.41	-	-	-	-0.25	5.00	-389.00	788.00	380.00	1.39E-83
-0.91	-	0.83	-	-0.47	-	-	-	-	3.00	-392.00	791.00	383.00	3.17E-84
0.18	-	-	-	-0.58	-	-	-	-	2.00	-398.00	800.00	393.00	2.72E-86
-0.18	-	-	0.07	-0.64	-	-	-	-	3.00	-398.00	801.00	394.00	1.77E-86
-4.51	-	1.76	-	-	-	-	-	-	2.00	-406.00	816.00	408.00	1.38E-89
-4.37	-	1.73	-0.01	-	-	-	-	-	3.00	-406.00	818.00	410.00	5.10E-90
-0.32	-	-	-0.32	-	-	-	-	-	2.00	-423.00	850.00	442.00	5.55E-97
-3.95	-	-	-	-	-	-	-	-	1.00	-436.00	874.00	467.00	2.52E-102

Appendix Table C.6. Results from the best-fit generalized linear model (binomial distribution) describing the probability of cone production as a function of tree age, mean annual temperature, and total precipitation. The model included all two-way interactions among predictors. Parameter estimates (± SE), z-values, and associated p-values are shown., where *** indicates significance.

Term	Estimate	Std. Error	z value	Pr(>|z|)
Intercept	-48.63	10.52	-4.62	3.8×10^{-6} ***
Age	0.27	0.06	4.45	8.5×10^{-6} ***
Precipitation	7.55	1.85	4.08	4.5×10^{-5} ***
Temperature	3.98	0.88	4.53	5.8×10^{-6} ***
Age × Temperature	-0.0186	0.0043	-4.35	1.4×10^{-5} ***
Age × Precipitation	0.0129	0.0067	1.93	0.054 .
Precipitation × Temperature	-0.682	0.152	-4.47	7.7×10^{-6} ***

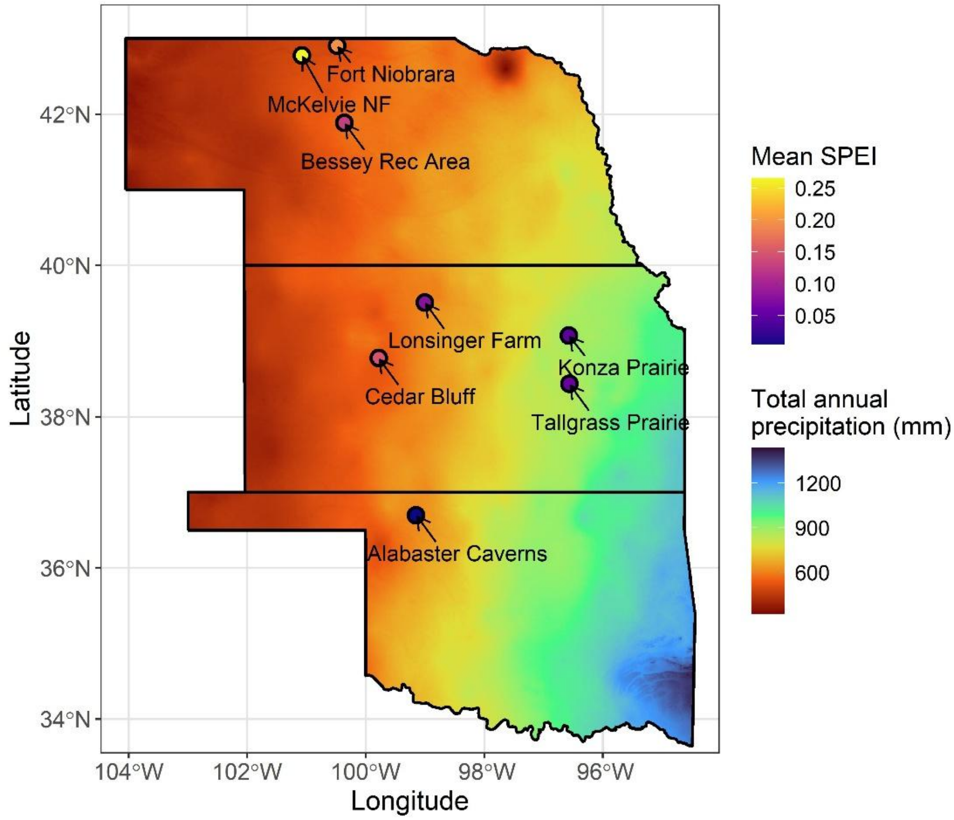

Appendix Figure C.1. Map of study locations. Study locations include Fort Niobrara (NIO), McKelvie National Forest (MCK), Bessey Recreational Area (BESS), Lonsinger Farm (LF), Konza Prairie Biological Station (KNZ), Cedar Bluff State Park (CB), Tallgrass Prairie National Preserve (TAPR), and Alabaster Caverns State Park (ALA). Location points are colored by the mean of annual SPEI (Standardized Precipitation-Evapotranspiration Index; Beguería et al. 2010) values calculated over the chronology period of each location. Lower SPEI values reflect either a greater frequency and/or intensity of drought. The background map is shaded according to total annual precipitation (mm) for the period 1970–2000 (Fick and Hijmans 2017).

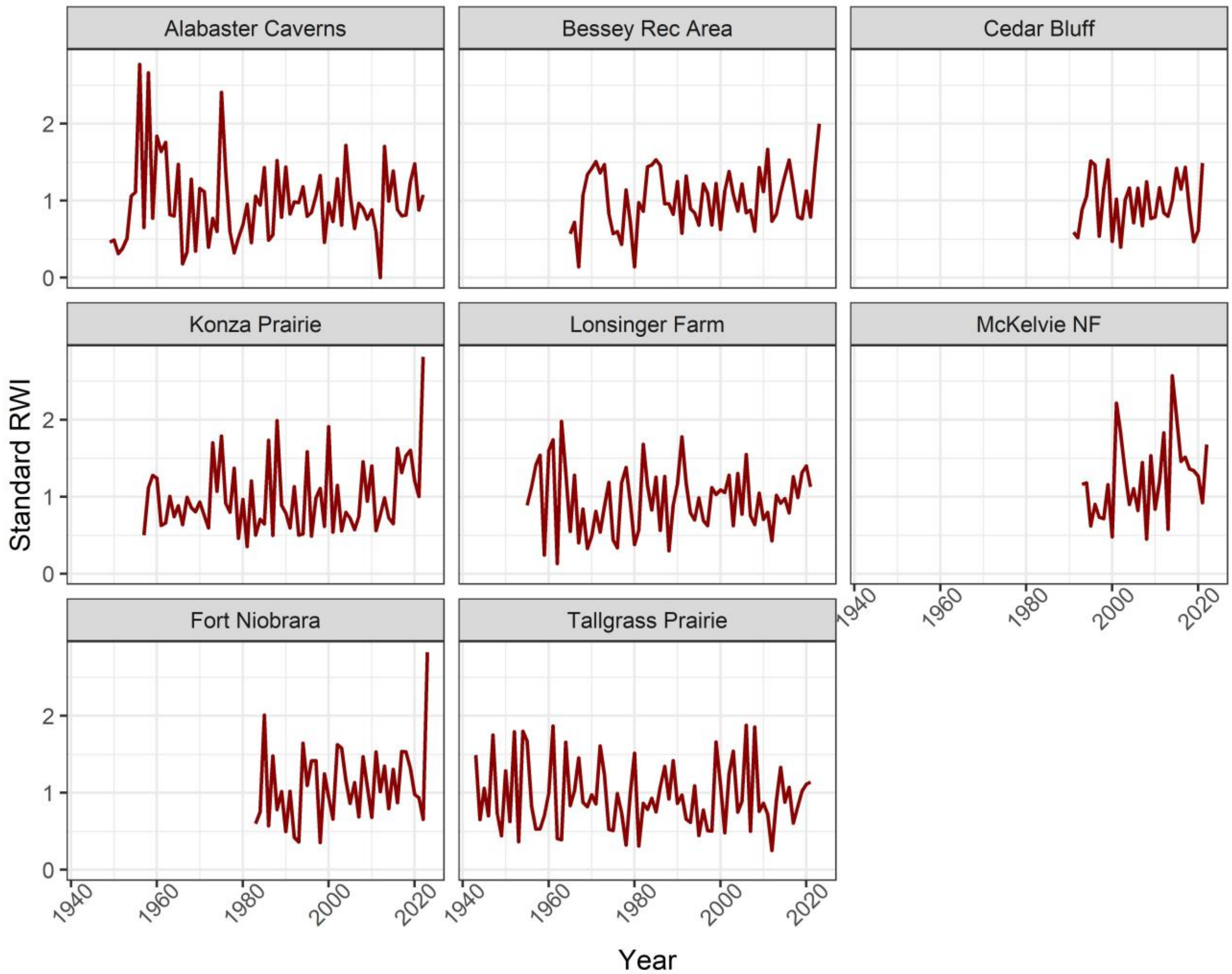

Appendix Figure C.2. Mean chronologies of eastern redcedar across multiple sites across years. Each panel shows a single site, with standard ring width indices (detrended to remove age related trends) plotted in dark red. Lower SPEI values in a year indicate greater frequency and/or intensity of drought across the months in that year.

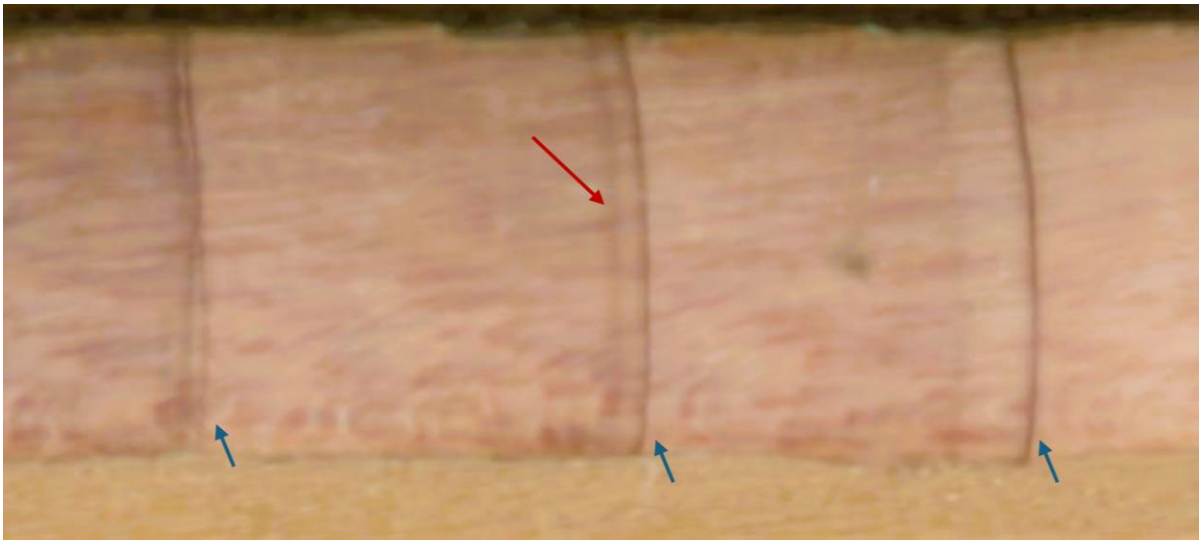

Appendix Figure C.3. Example of a false ring in eastern red cedar. Here, the false ring is labeled with a red arrow, and true rings are labeled with blue arrows.

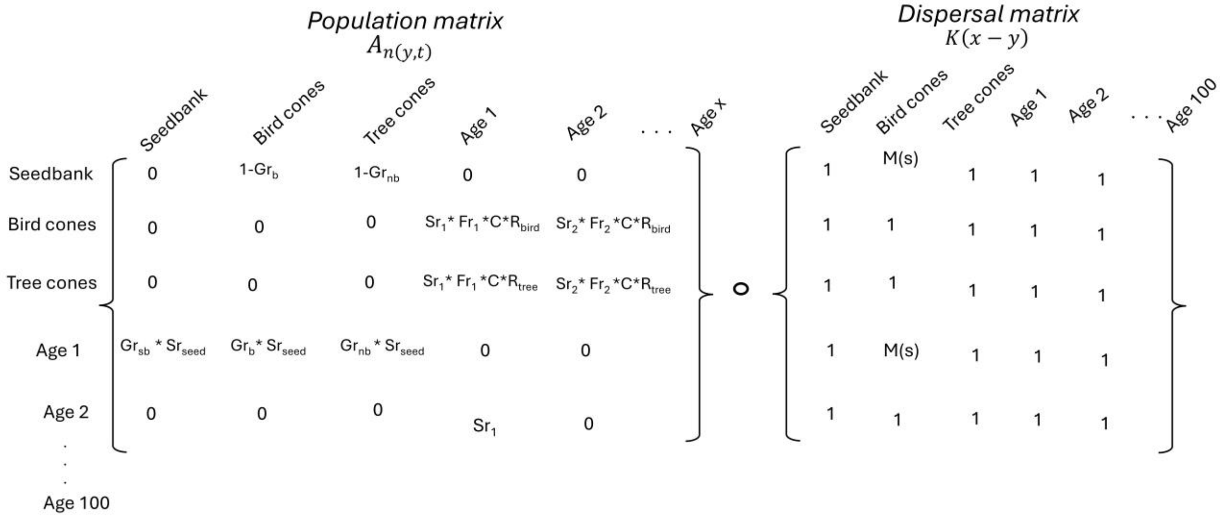

Appendix Figure C.4. Population projection and dispersal matrices used to model spatial population dynamics. The population projection matrix $\boldsymbol{A_{n(y,t)}}$describes transitions of individuals among stages from time $\boldsymbol{t}$ to $\boldsymbol{t+1}$at location $\boldsymbol{y}$. Stages include the seedbank, bird-dispersed cones, tree-dispersed cones, and age classes (1–100). Stage transitions depend on survival ($\boldsymbol{S_r}$), fruiting rate ($\boldsymbol{F_r}$), cone production ($\boldsymbol{C}$), and the proportion of cones dispersed by birds ($\boldsymbol{R}_{\text{bird}}$) or dropped near the tree ($\boldsymbol{R}_{\text{tree}}$); these proportions do not sum to 1 because some cones are predated. Germination rates ($\boldsymbol{G_r}$) differ by seed source ($\boldsymbol{G_{r_{sb}}}$, $\boldsymbol{G_{r_b}}$, and $\boldsymbol{G_{r_{nb}}}$for seedbank, bird-dispersed, and tree-dispersed seeds, respectively). The dispersal matrix $\boldsymbol{K(x-y)}$ describes spatial redistribution between locations. The moment-generating function $\boldsymbol{M(s)}$ represents the Laplace dispersal kernel, which integrates to $\boldsymbol{1/(1-(s^2b^2))}$ for parameter $\boldsymbol{b}$, corresponding to a mean dispersal distance of 106.56 m. $\boldsymbol{M(s)}$ is applied to stages that disperse spatially (bird-dispersed cones which either germinate and transition to age 1 or enter the seedbank), whereas all other entries are set to 1, representing the Dirac delta function for stationary stages that do not disperse.